

Methods of Exploration

3.1 WELL DRILLING AND COMPLETION

In the earliest days of oil exploration, oil was collected from surface seepages. Herodotus, writing in about 450 BC, described oil seeps in Carthage (Tunisia) and the Greek island Zachynthus. He gave details of oil extraction from wells near Ardericca in modern Iran, although, as mentioned in Chapter 1, the wells could not have been very deep, because fluid was extracted in a wineskin on the end of a long pole mounted on a fulcrum. Oil, salt, and bitumen were produced simultaneously from these wells. In China, Burma, and Romania, mine shafts were dug to produce shallow oil. Access was gained by ladders or a hoist, and air was pumped down to the mines through pipes. Oil seeped into the shaft and was lifted to the surface in buckets. This type of technology was not conducive to a healthy life and long retirement for the miners.

Oil has also been mined successfully in several parts of the world by driving horizontal adits into reservoirs. Oil dribbles down the walls onto the floor and flows down to the mine entrance. This technique has been used in the North Tisdale field of Wyoming (Dobson and Seelye, 1981). Conventionally, however, oil and gas are located and produced by drilling boreholes. Before exploration for oil began, cable-tool drilling was an established technique in many parts of the world in the quest for water and brine (Fig. 3.1). The first well to produce oil intentionally in the Western World was drilled at Oil Creek, Pennsylvania, by Colonel Drake in 1859 (Owen, 1975). Previously, water wells in the Appalachians and elsewhere produced oil as a contaminant. The technology for drilling Drake's well was derived from Chinese artisans who had traveled to the United States to work on the railroads. Cable-tool drilling had been used in China since at least the first century b.c., the drilling tools being suspended from bamboo towers up to 60 m high. In China, however, this drilling technology had developed to produce artesian brines, not petroleum (Messadie, 1995). The two methods, cable-tool and rotary-tool drilling, are briefly described in the following sections.

3.1.1 Cable-Tool Drilling

Cable-tool drilling seems to have developed spontaneously in several parts of the world. In the early nineteenth century, the Chinese were sinking shafts to depths of some 700 m using an 1800-kg bit suspended from a rattan cord. Hole diameters were of the order of 10–15 cm, and the rate of penetration was about 60–70 cm/day. The wells were cased with bamboo or

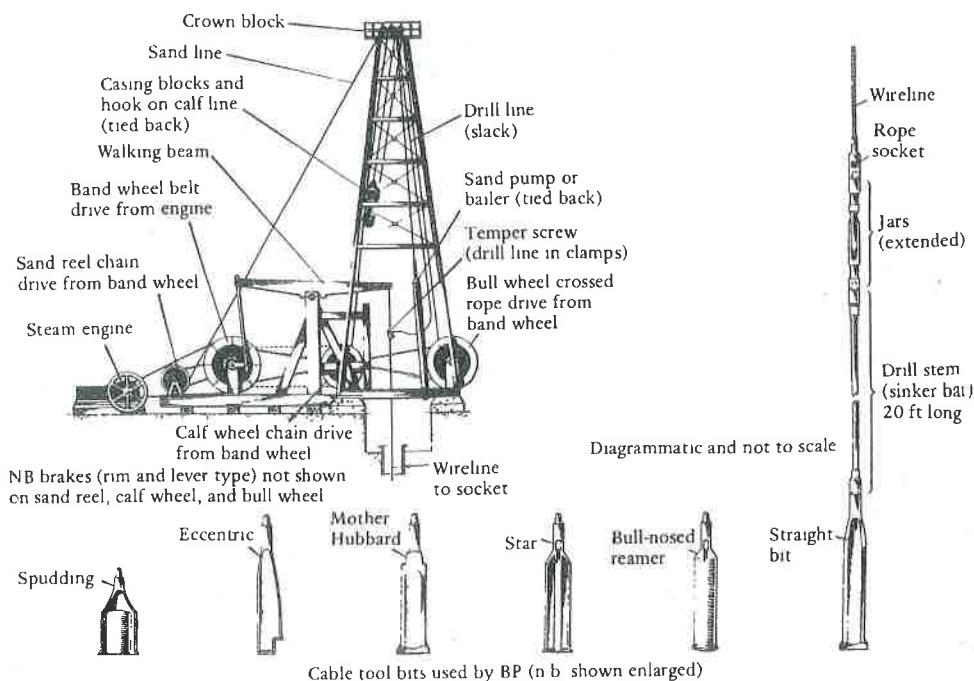


FIGURE 3.1 A steam-driven cable-tool rig and equipment. *Courtesy of British Petroleum.*

hollow cypress trunks (Imbert, 1828; Coldre, 1891). These wells were sunk in the search for freshwater and for brines from which salt could be extracted. In modern cable-tool drilling, a heavy piece of metal, termed the *bit*, is banged up and down at the end of a cable on the bottom of the hole. The bit is generally chisel shaped. This repeated percussion gradually chips away the rock on the bottom of the hole. Every now and then, the bit is withdrawn to the surface, and a bailer is fitted to the end of the cable. This bailer is a steel cylinder with a one-way flap at the bottom. As the bailer is dropped on the floor of the hole, chips of rock are forced into it through the trap flap. When the bailer is lifted prior to the next drop, the rock cuttings are retained in the trap (Fig. 3.1). When the cuttings have been removed from the borehole, the bailer is drawn out and emptied. The bit is then put back on the end of the cable, and percussion recommences. As the hole is gradually deepened, the sides have a natural tendency to cave in. This tendency is counteracted by lining the hole with steel casing.

In the early days of oil exploration, the percussive power of the cable tool was provided by a man or men pulling on the rope or, later, aided by a spring-pole. In more recent times, however, motive power was provided by a steam or internal combustion engine.

The mechanical cable-tool drilling method evolved toward the end of the eighteenth century. It was then used primarily for the sinking of water wells. Occasionally, such wells would find water contaminated with oil, to the displeasure of the driller. When the economic

uses of oil were discovered in the mid-nineteenth century, however, the cable-tool rig became the prime method of sinking oil wells, and it remained so for some 80 years.

Cable-tool drilling has several major mechanical constraints. First, the depth to which one may drill is severely limited. The deeper the hole, the heavier the cable. There comes a point, therefore, when the cable at the well head is not strong enough to take the combined weight of the bit and the downhole cable. Although cable-tool rigs have drilled to >3000 m, the average capability is about 1000 m. This capability is adequate for most water wells, but too shallow for the increased depths required for oil exploration. A further limitation of the cable-tool method is that it can only work in an open hole. The cable must be free to move, so it is not possible to keep the hole full of fluid. The bailer removes water that oozes into the hole. Thus, when the bit breaks through into a high-pressure formation, the oil or gas shoots up to the surface as a gusher. Because of these limitations of penetration depth and safety, cable-tool drilling is of limited use in petroleum exploration.

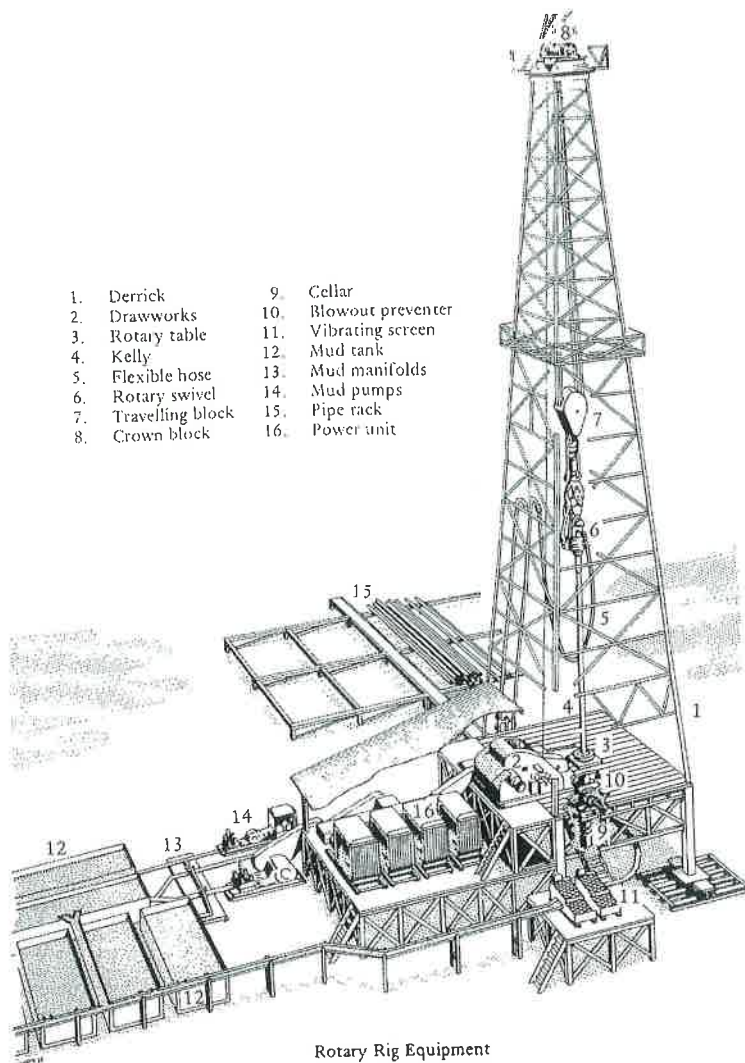
3.1.2 Rotary Drilling

Because of the greater safety and depth penetration of rotary drilling, it has largely superseded the cable-tool method for deep drilling in the oil industry (Fig. 3.2). In this technique, the bit is rotated at the end of a hollow steel tube called the *drill string*. Many types of bit are used, but the most common consists of three rotating cones set with teeth (Fig. 3.3). The bit is rotated, and the teeth gouge or chip away the rock at the bottom of the borehole. Simultaneously, mud or water is pumped down the drill string, squirting out through nozzles in the bit and flowing up to the surface between the drill string and the wall of the hole. This circulation of the drilling mud has many functions: It removes the rock cuttings from the bit; it removes cavings from the borehole wall; it keeps the bit cool; and, most importantly, it keeps the hole safe. The hydrostatic pressure of the mud generally prevents fluid from moving into the hole, and if the bit penetrates a formation with a high-pore pressure, the weight of the mud may prevent a gusher. A gusher can also be prevented by sealing the well head with a series of valves termed the *blowout preventers*.

As the bit deepens the hole, new joints of drill pipe are screwed on to the drill string at the surface. The last length of drill pipe is screwed to a square-section steel member called the kelly, which is suspended vertically in the kelly bushing, a square hole in the center of the rotary table. Thus, rotation of the table by the rig motors imparts a rotary movement down the drill string to the bit at the bottom of the hole. As the hole deepens, the kelly slides down through the rotary table until it is time to attach another length of drill pipe (Fig. 3.4). When the bit is worn out, which depends on the type of bit and the hardness of the rock, the drill pipe is drawn out of the hole and stacked in the derrick. When the bit is brought to the surface, it is removed and a new one is fitted.

After drilling for some depth, the borehole is lined with steel casing, and cement is set between the casing and the borehole wall. Drilling may then recommence with a narrower gauge of bit. The diameters of bits and casing are internationally standardized. Depending on the final depth of the hole, several diameters of bit will be used with the appropriate casing (Fig. 3.5). The average depth of an oil well is between 1 and 3 km, but depths of up to 11.5 km can be penetrated.

FIGURE 3.2 Simplified sketch of an onshore derrick for rotary drilling. *Courtesy of British Petroleum.*



When drilling into a reservoir, an ordinary bit may be removed and replaced by a core barrel. A core barrel is a hollow steel tube with teeth, commonly diamonds, at the downhole end. As the core barrel rotates, it cuts a cylinder of rock and descends over it as the hole deepens. When the core barrel is withdrawn to the surface, the core of rock is retained in the core barrel by upward-pointing steel springs. Coring is slower than drilling with an ordinary bit and is thus more expensive. It is only used sparingly in hydrocarbon exploration to collect large, intact rock samples for geological and engineering information.

Geologists are involved to varying degrees in drilling wells. In routine oil field development wells, where the depth and characteristics of the reservoir are already well known,

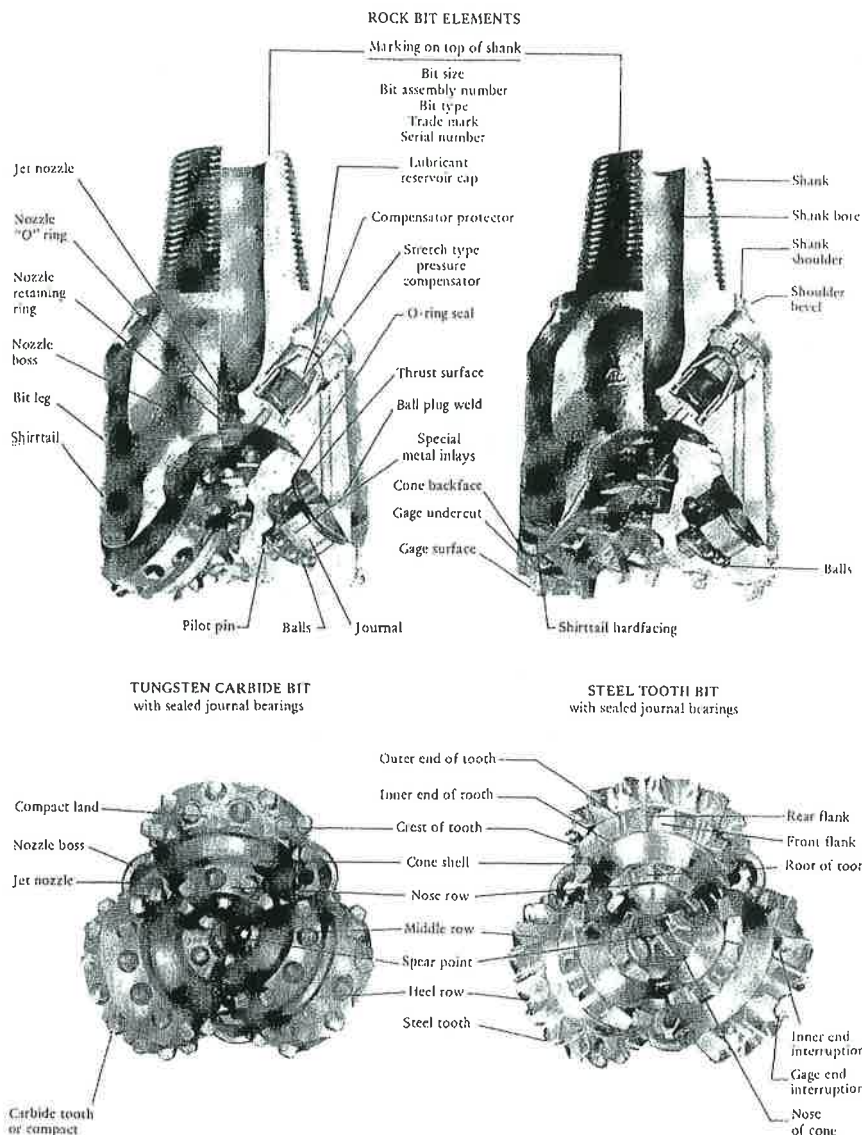


FIGURE 3.3 Two types of tricone bit used for rotary drilling. *Courtesy of Hughes Tool Co.*

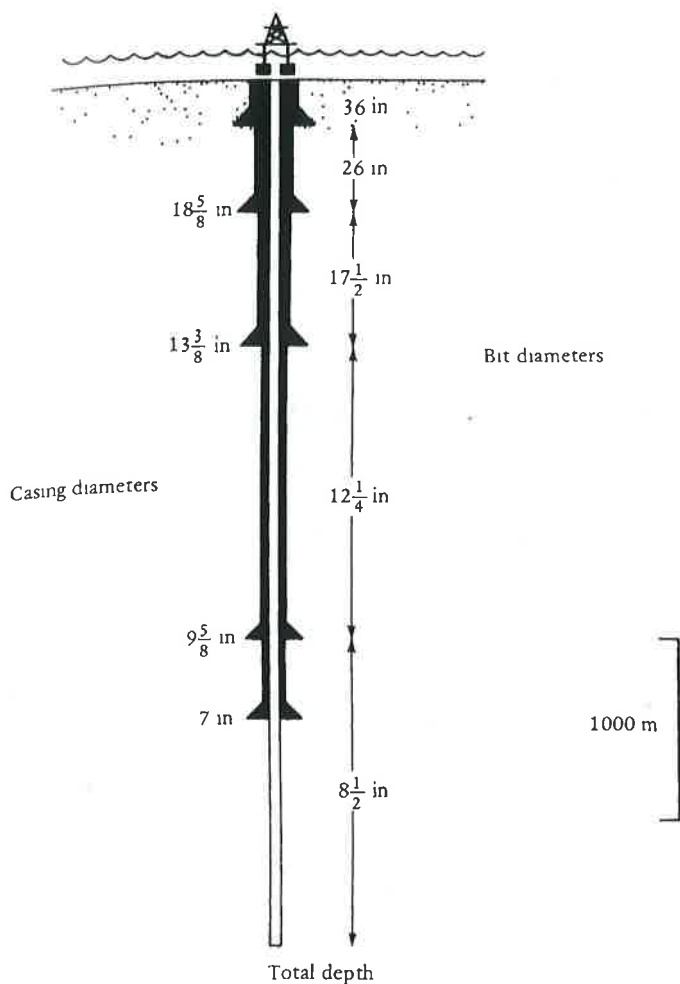
geologists may not be present at the well site, although they will monitor the progress of the well from the office. On an offshore wildcat well, however, there may be five or more geologists. The oil company for whom the well is being drilled will have one of their own well site geologists on board. His or her duties include advising both the driller and the operational headquarters on the formations, fluids, and pressures to be anticipated; picking casing and coring points; deciding when to run wireline logs; supervising logging and interpreting the end result; and, most importantly, identifying and evaluating hydrocarbon shows in the well.

FIGURE 3.4 Applying the tong to make up the drill pipe on the rig floor of British Petroleum's rig, Sea Conquest. *Courtesy of British Petroleum.*



The other geologists are mudloggers, working in pairs on 12-h shifts. The mudlogging company is contracted by the oil company to carry out a complex and continuous evaluation of the well as it is drilled. This evaluation is done from a mudlogging unit, which is a cabin or caravan trailer packed with computers and electronic monitors (Fig. 3.6). The mudloggers record many drilling variables, including the rate of penetration, mud temperature, pore pressure, and shale density. Gas chromatographs monitor the presence of hydrocarbon gases in the mud. Samples of the well cuttings are collected at specified depth intervals, checked with ultraviolet light and other tests for the presence of oil, identified, and described. These data are continuously plotted on a mud log (Fig. 3.7). A useful account of the geological aspects of mudlogging and associated rig activities is given by Dickey (1979). Nowadays, however, it is also possible to run a series of geophysical logs while the well is actually being drilled, the sondes being lowered inside the drill pipe. Geophysical logs are described in more detail later in the chapter; for now, note that MWD (measurement while drilling) is an important aspect of formation evaluation, providing early warnings of rock type, hydrocarbon saturation, and potentially perilous zones of high pressure.

FIGURE 3.5 The casing and bit diameters of a typical well.



3.1.3 Various Types of Drilling Units

The derrick for rotary drilling may be used on land or at sea. On land, prefabricated rigs are used; they can be transported by skidding, by vehicle, or, in the case of light rigs, by helicopter. Once a well has been drilled, the derrick is dismantled and moved to the next location, whether the well is productive or barren of hydrocarbons (colloquially termed a *dry hole* or *duster*). Thus, modern oil fields are not marked by a forest of derricks as shown in old photographs and films.

In offshore drilling, the derrick can be mounted in various ways. For sheltered inland waterways, it may be rigged on a flat-bottomed barge. This technique has been employed, for example, in the bayous of the Mississippi delta for >60 years. In water depths of up to about 100 m, jack-up rigs are used. In jack-up rigs, the derrick is mounted on a flat-bottomed barge

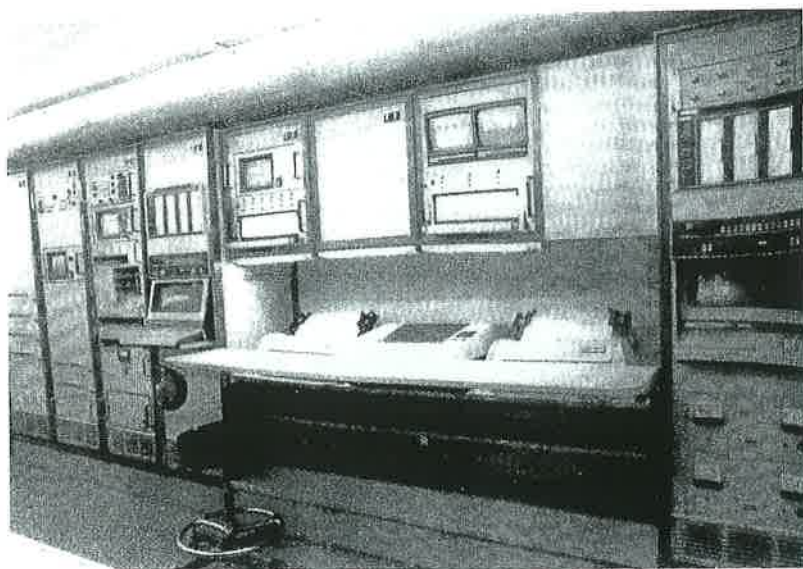


FIGURE 3.6 The inside of a mudlogging unit. *Courtesy of Exploration Logging Services, Ltd.*

fitted with legs that can be raised or lowered. When the rig is to be moved, the legs are raised (i.e., the barge is lowered) until the barge is floating. Some barges are self-propelled, but the majority are moved by tugs. On reaching the new location, the legs are lowered, thus raising the barge clear of all but the highest waves (Fig. 3.8).

Submersible units are platforms mounted on hollow caissons, which can be flooded with seawater. The platform supports can be sunk onto the seabed, leaving a sufficient clearance between the sea surface and the underside of the platform. Like jack-ups, submersible rigs are only suitable for shallow water. For deeper waters, drill ships or semisubmersible units are used. On drill ships, the derrick is mounted amidships, and the ship is kept on location either by anchors or by a specially designed system of propellers that automatically keeps the ship in the same position regardless of wind, waves, and currents. Semisubmersibles are floating platforms having three or more floodable caisson legs (Fig. 3.9). With the aid of anchors and judicious flooding of the legs, the unit can be stabilized, although still floating, with the rotary table 30 m or so above the sea. Some semisubmersibles are self-propelled, but the majority are towed by tugs from one location to another (Fig. 3.10). In shallow water Arctic conditions, where there is extensive pack ice, drill ships, jack-ups, and semisubmersibles are unsuitable. In very shallow water, artificial islands are made from gravel and ice. Monopod rigs are also used, which, as their name implies, balance on one leg around which the pack ice can move with minimum obstruction.

3.1.4 Vertical, Directional, and Horizontal Drilling

Most wells drilled in the United States for oil and natural gas historically have been vertical wells (Fig. 3.11). A dramatic change started in 2004 when a switch occurred to horizontal

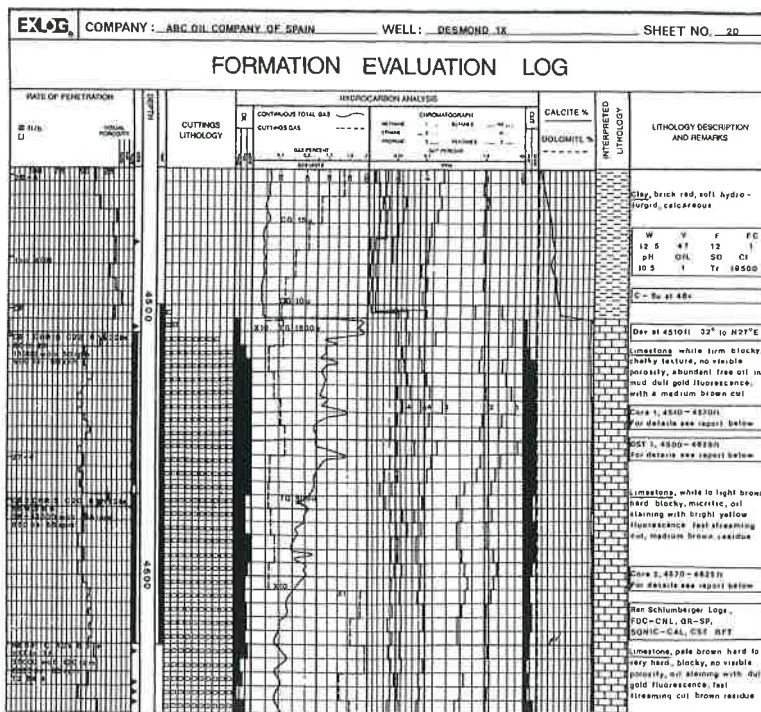


FIGURE 3.7 Example of part of a typical mud log, showing the range of drilling and geological data recorded. *Courtesy of Exploration Logging Services, Ltd.*



FIGURE 3.8 Jack-up drilling rig, Key Gibraltar (on charter to British Petroleum) in British Petroleum's West Sole gas field. *Courtesy of British Petroleum.*

wells. The 2014 percentage of wells drilled in the United States is as follows: vertical 20%, horizontal 67%, and directional 12%.

Drilling wells directionally or horizontally has several advantages over vertical wells:

1. target areas under cities or lakes where surface occupancy is impossible;
2. drain a large area with pad drilling (several wells from one pad to reduce surface footprint);

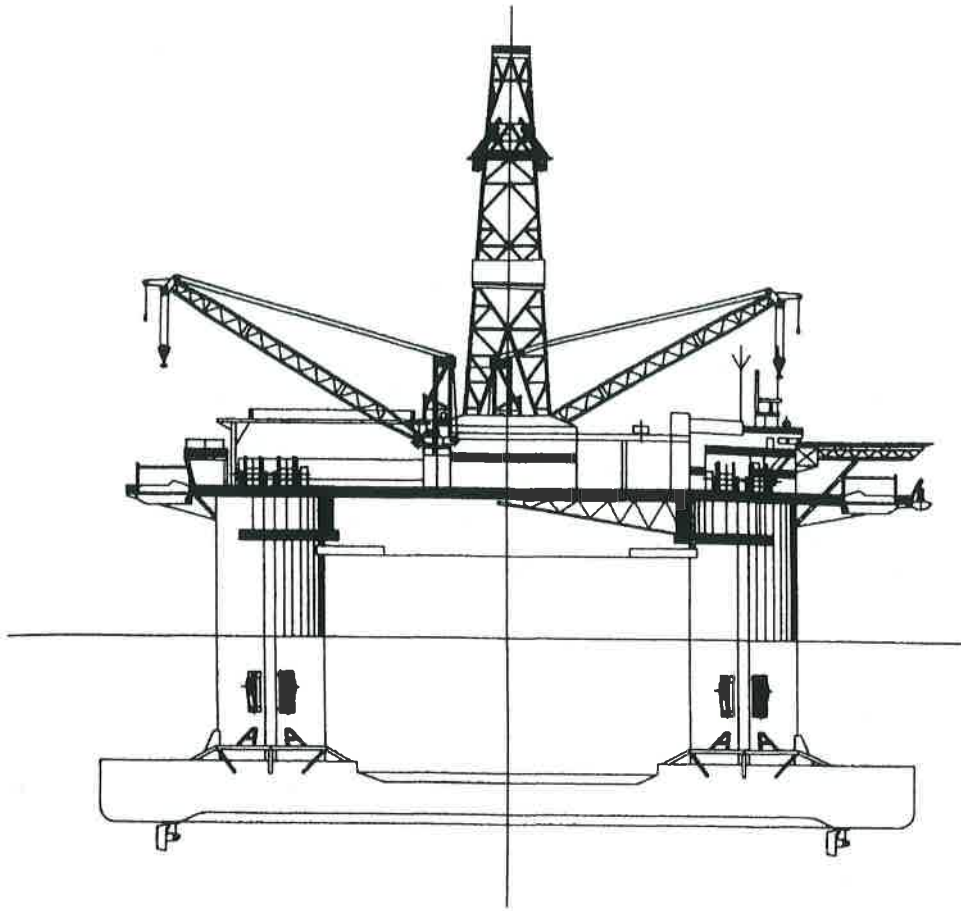


FIGURE 3.9 Diagram of a modern semisubmersible drilling rig, the GVA 8400. *Courtesy of GVA Consultants.*

3. increase the contact area of the pay zone with the well bore;
4. improve productivity in fractured reservoirs by contacting more fractures;
5. relieve pressure or seal "out-of-control wells."

Figure 3.12 illustrates vertical, slant-hole, and horizontal wells. Slant holes in this example target a combination of lenticular (e.g., channel sandstones) and blanket deposits (e.g., shore-line sandstones). Horizontal wells target a single horizon and are generally drilled in a direction to maximize natural fracture intersections or selected reservoir compartments.

3.1.5 Horizontal Drilling and Multistage Hydraulic Fracture Stimulation

Most tight reservoirs (e.g., shale gas, tight gas, tight oil, and coal seam gas) require hydraulic fracture stimulation in order for them to produce. The fracture stimulation process involves injecting water, chemicals, and proppant (sand or ceramics) at high pressures into



FIGURE 3.10 British Petroleum's semisubmersible drilling rig, Sea Conquest. *Courtesy of British Petroleum.*

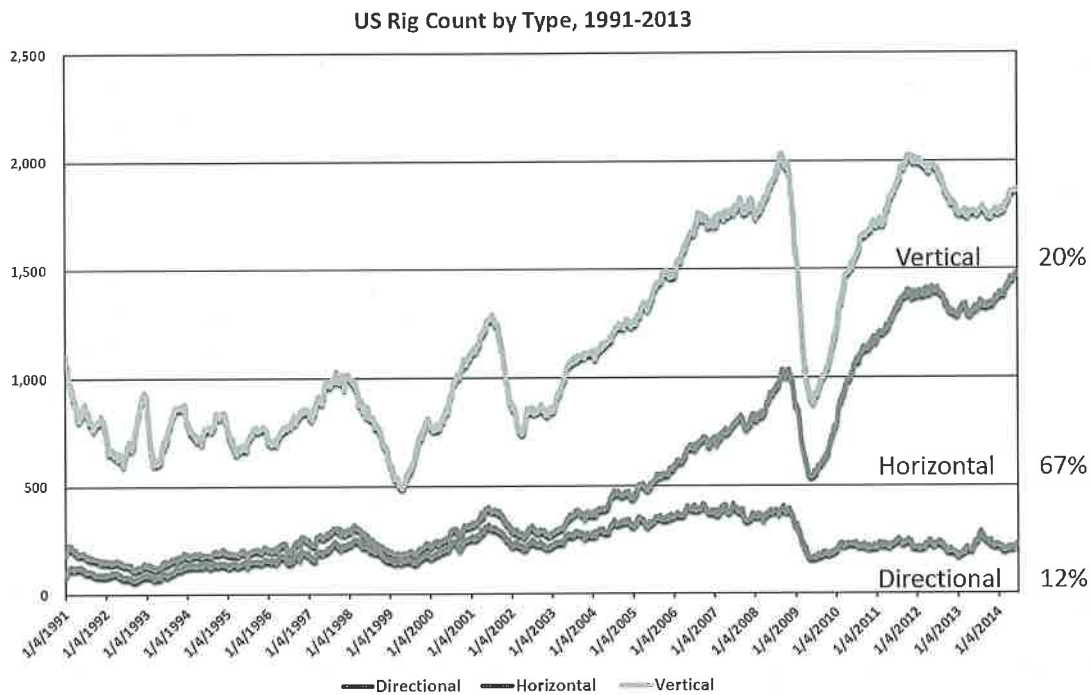


FIGURE 3.11 US rig count by type, 1991–2013. *Data from Baker-Hughes.*

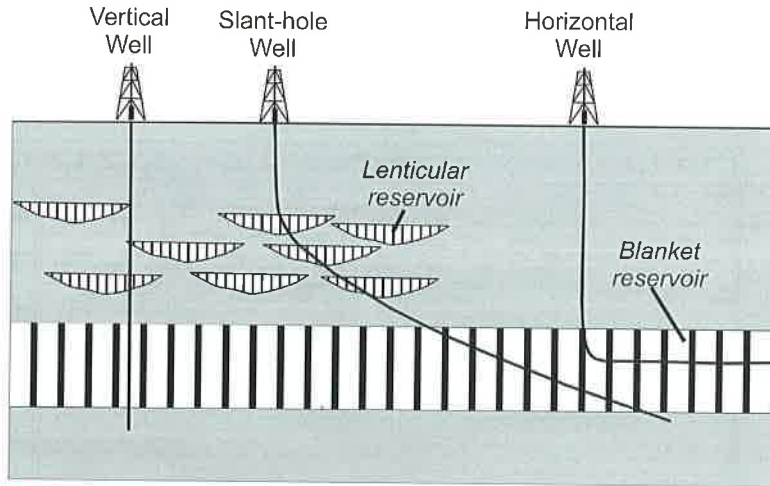


FIGURE 3.12 Diagrammatic sketch illustrating vertical, slant-hole, and horizontal wells. Fractures are the vertical lines in the sketch.

a formation, which creates small fractures in the surrounding rock and allows natural gas or oil to flow from the rock fractures to the production well. Chemicals used in this process generally include gelling agents, crosslinkers, friction reducers, corrosion inhibitors, scale inhibitors, biocide, and even diesel fuel. Proppants are used to keep the fractures open. Hydraulic fracture stimulation of wells has occurred since the 1940s but increased dramatically in 2003, when energy companies began drilling shale formations horizontally and completing the wells with multistage fracturing. Hydraulic fracturing is applied to tight formations to enhance well performance, minimize drilling, and recover otherwise inaccessible resources.

Figure 3.13 illustrates horizontal and vertical wells completed with hydraulic fracture stimulation. The advantage of horizontal drilling with multistage hydraulic fracturing over vertical wells with hydraulic fracturing is dramatically increasing the contact area of the formation with the well bore. Hydraulic fractures lengths are described by Davies et al. (2012) and Fisher and Warpinski (2011).

3.1.6 Various Types of Production Units

As previously noted, when a well has been drilled, the derrick is moved to the next location. Oil and gas are produced from wells in several ways. Details of the various drive mechanisms of reservoirs are outlined in Chapter 6. Actual production is achieved in one of two ways, depending on whether or not the oil flows to the surface without the use of a pump.

In most cases, the reservoir has sufficient pressure for oil or gas to flow to the surface. In this situation, casing is generally run below the producing zone, and perforations are shot through it by explosive charges opposite the hydrocarbon pay interval. Steel tubing is hung from the well head to the producing zone, and the annulus between tubing and casing

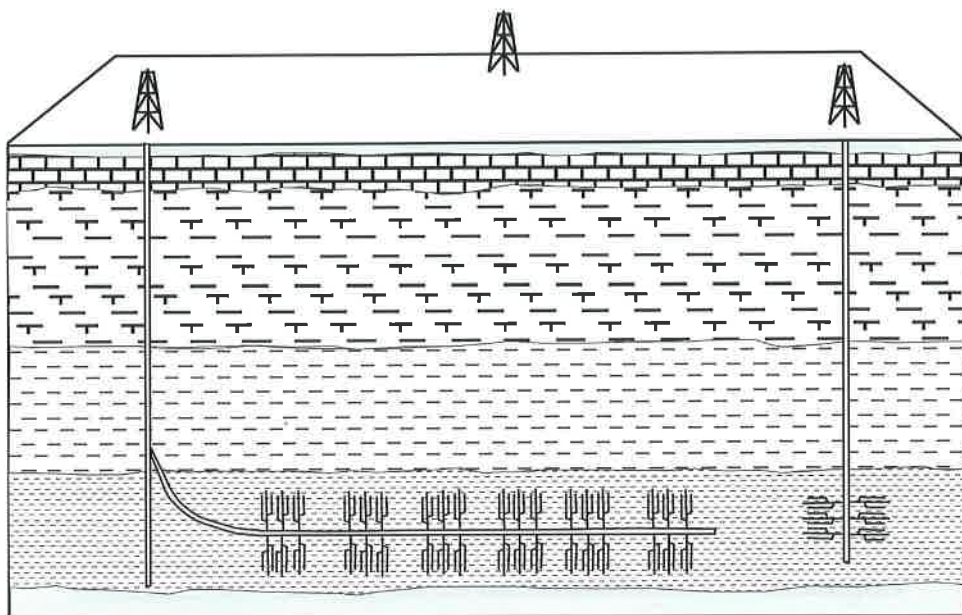


FIGURE 3.13 Sketch illustrating horizontal and vertical wells completed with hydraulic fracture stimulation.

sealed off with a packer (Fig. 3.14). The productivity of many wells may be stimulated, either initially or worked over later during their life. Typical stimulation techniques involve fracturing the formation, generally by high-pressure pumping of metallic or plastic shrapnel into fractures to wedge them open. For a finale, hydrochloric or some other acid may then be injected to enlarge the fractures and hence increase permeability and productivity. These techniques are largely, but not exclusively, applied to carbonate reservoirs.

At the well head, a system of valves, termed the Christmas tree, is installed from which a flowline leads to a tank in which produced oil and gas are separated at atmospheric pressure.

If the reservoir pressure is too low for oil to flow to the surface, a pumping device is used: either a nodding donkey at the well head, or a downhole pump installation. Figure 3.15 illustrates a well-head pump. A diesel or electrically powered beam engine raises and lowers a connected string of sucker rods, which are connected to a piston at the base of the borehole. Alternatively, an electrically driven centrifugal pump may be installed at the bottom of the hole. This device is more effective than the nodding donkey and less ecologically shocking. Maintenance costs may be higher because of difficulties of access, and reliability may be lower.

Onshore development wells are drilled on various types of geometric arrangements at spacings determined by the permeability of the reservoir and radius of drainage anticipated for each well. Offshore, however, this procedure is not feasible. Various types of production facilities are now used. These include floating buoys, ships, floating production platforms (Fig. 3.16), and fixed production platforms (Figs 3.17 and 3.18). Fixed platforms have been used for water depths of up to some 450 m; below that floating production facilities are

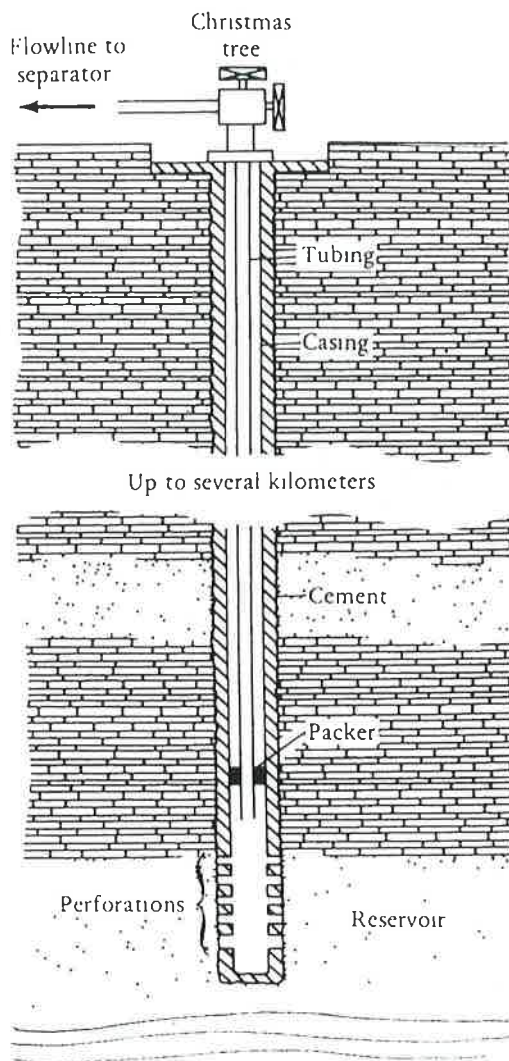


FIGURE 3.14 A typical well completion through perforated casing. Details of the various casing strings are omitted (Fig. 3.5).

used. The offshore Gulf of Mexico is a major source of oil and gas for the United States. Sixty-five discoveries have been made in water depths >1500 m. The greatest water depth in which a discovery has been made is 3040 m. Notable major oil and gas fields include Mensa, Eugene Island 330, Atlantis, and Tiber. Tiber is a BP operated field located in the Keathley Canyon Block 102. The field is reported to have four to six billion barrels in place and an estimated ultimate recovery of 600–900 million barrels of oil. The deepest well in the field was drilled to 10,685 m under 1260 m of water.



FIGURE 3.15 Nodding donkey well-head pump at British Petroleum's Kimmeridge Bay field, Dorset.

Offshore petroleum production requires the ability to drill a multitude of wells that radiate out from a single platform. In the old days, wells could be deviated from vertical by dropping a steel wedge or "whipstock" down the borehole. Nowadays, with motorized drill bits and sophisticated navigation systems, it is possible to steer a well in any orientation that is required. Although this technology was largely developed to facilitate drilling many wells off a single offshore platform, it has now been reintroduced onshore and applied to drilling horizontal wells. Such wells can be drilled to penetrate individual channel reservoir sands or to crosscut fault systems that may serve as natural conduits for petroleum production. Horizontal drilling has been widely applied, for example, to the Austin Chalk of Texas, where petroleum is produced from fault-related fracture systems in a rock that has porosity, but normally lacks permeability (Koen, 1996). Wells of up to 12.3 km extended-reach have now been drilled in the Sakhalin-1 project on Sakhalin Island. Wells on Sakhalin Island target three offshore fields: Chayvo, Odoptu, and Arkutun-Dagi. In 2012, Exxon Neftegas Ltd. completed the Z-44 Chayvo extended-reach well after it had reached a measure depth of 12,376 m. The extended-reach drilling technology enables onshore-based drilling to reach petroleum reservoirs far offshore.

3.2 FORMATION EVALUATION

Boreholes yield much geological and engineering information, particularly when extensive lengths of core are recovered. Because coring is so expensive, holes are usually drilled with an ordinary rotary bit. Further information is gained about the penetrated formations by measuring their geophysical properties with the aid of wireline logs. Formerly, geophysical logs were run after drilling a section of the well and before setting casing, so several log runs are necessary during the drilling of a single well. Nowadays, however, it is possible

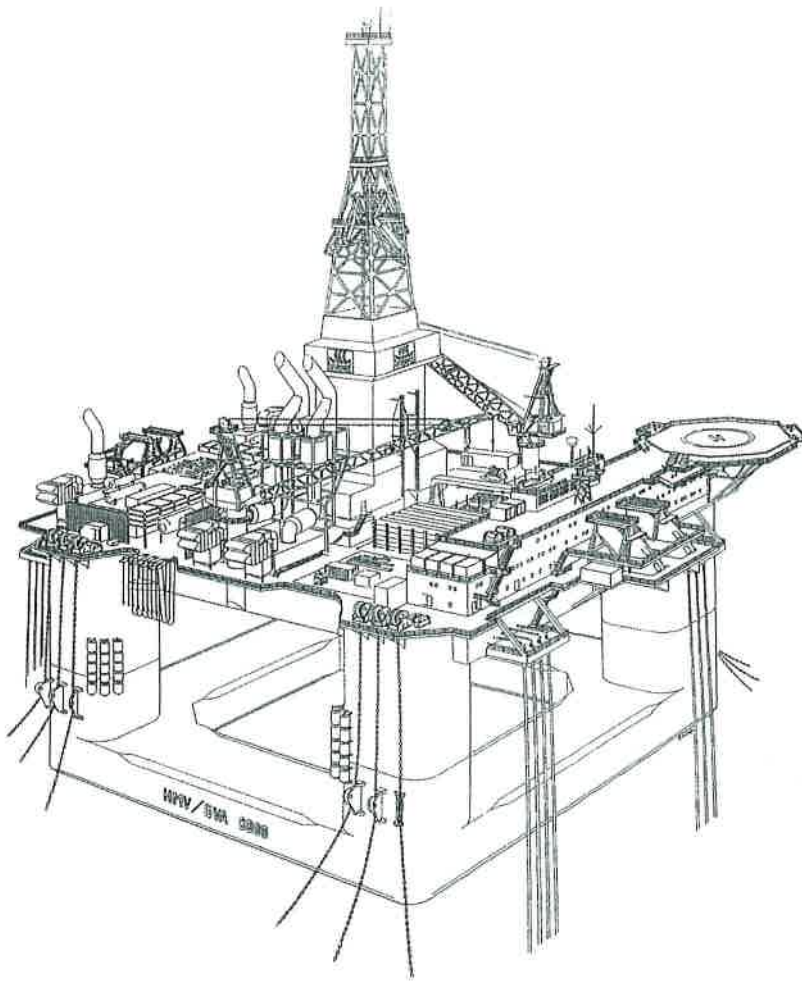


FIGURE 3.16 A typical modern floating production platform, the HMV/GVA 8000. *Courtesy of GVA Consultants.*

to run some geophysical logs within the drill pipe while the well is actually being drilled. MWD is an important advance in formation evaluation, providing early warnings of rock type, hydrocarbon saturation, and potentially perilous zones of high pressure.

The equipment that measures the geophysical properties of the penetrated rocks is housed in a cylindrical sonde, which is lowered down the borehole on a multiconductor electric cable (Fig. 3.19). On reaching the bottom of the hole, the recording circuits are switched on and the various properties measured as the sonde is drawn to the surface. The measurements are transmitted up the cable and recorded on film or magnetic tape in the logging unit. In onshore operations, the recorders are generally mounted on a truck (Fig. 3.20).

Many different parameters of the rock can be recorded, such as formation resistivity, sonic velocity, density, and radioactivity. The recorded data can then be interpreted to determine

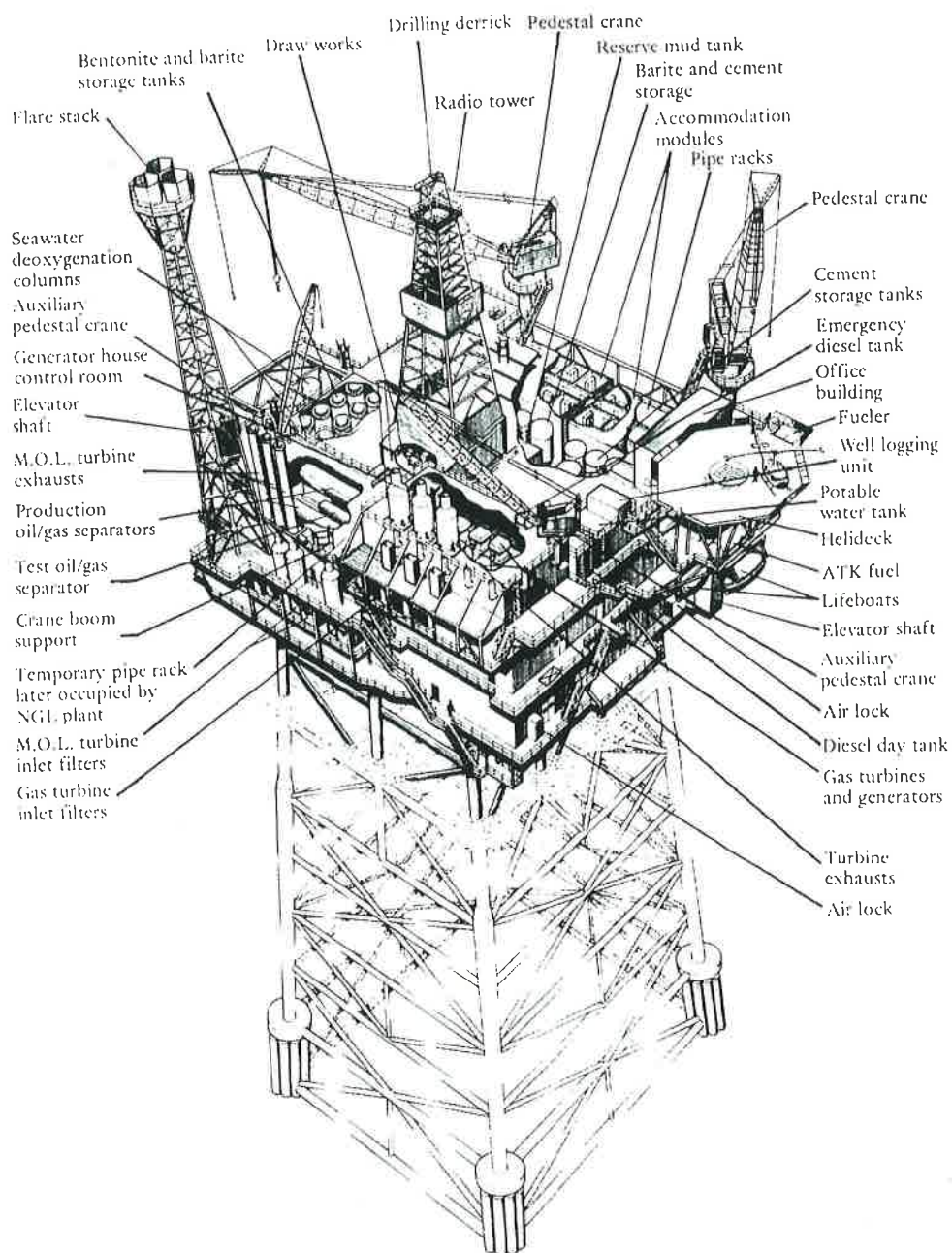


FIGURE 3.17 One of British Petroleum's Forties field production platforms in the North Sea. *Courtesy of British Petroleum.*

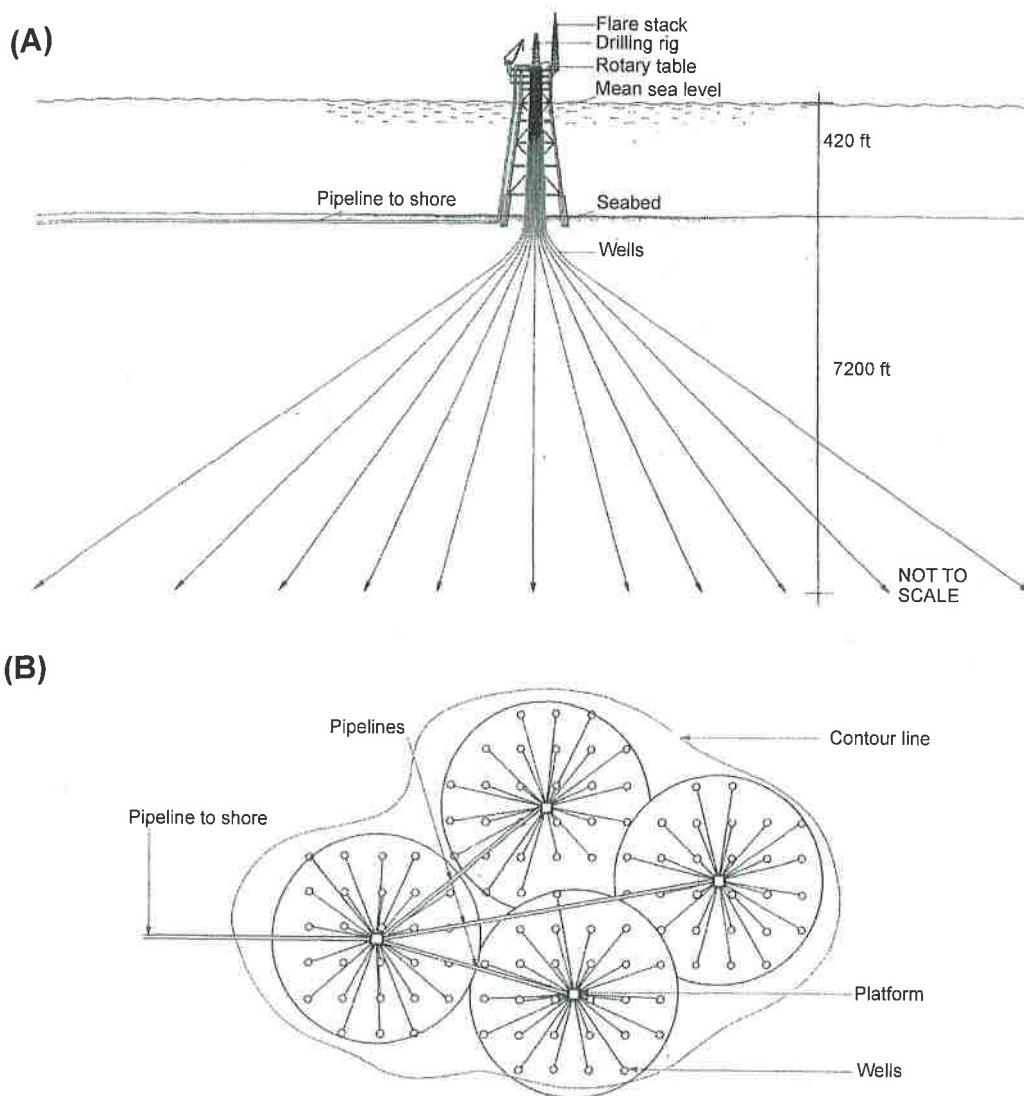


FIGURE 3.18 (A) Cross-section showing how deviated wells are drilled from a platform to penetrate the reservoir at the required depth (B). *Courtesy of British Petroleum.*

the lithology and porosity of the penetrated formations and also the type and quantity of fluids (oil, gas, or water) within the pores.

Formation evaluation is a large and complex topic. Many oil companies employ full-time log analysts. The following account is only intended as an introduction to the topic. The various types of logs are now described, and the principles of log analysis are reviewed. Petroleum geoscientists generally attend courses on log analysis early in their professional career. These courses provide up-to-date and detailed information on new tools and

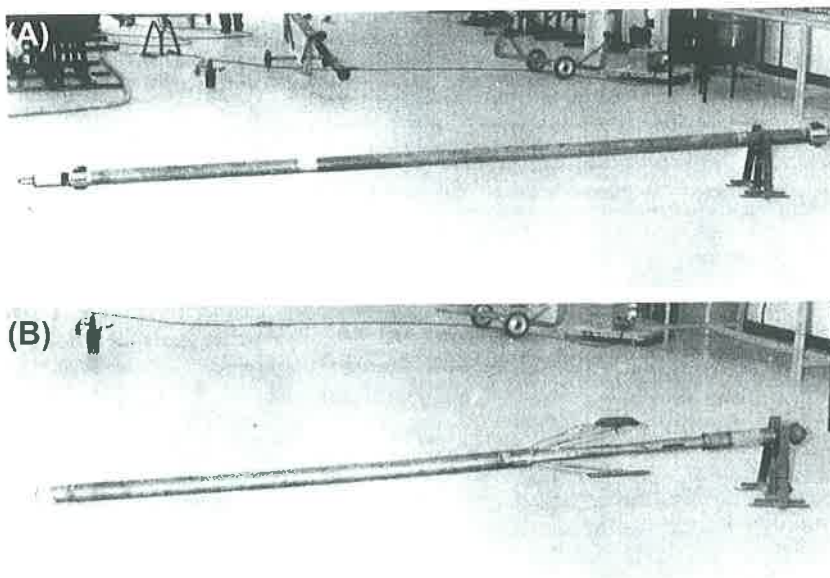


FIGURE 3.19 Two sondes for measuring electric properties of formations: (A) Induction resistivity tool, which combines the spontaneous potential (SP), a 16-in normal to measure R_{xo} , and a deep induction log to measure R_t . (B) A microfocused log, which records SP, R_{xo} , and hole diameter. *Courtesy of Tesel Services, Ltd.*

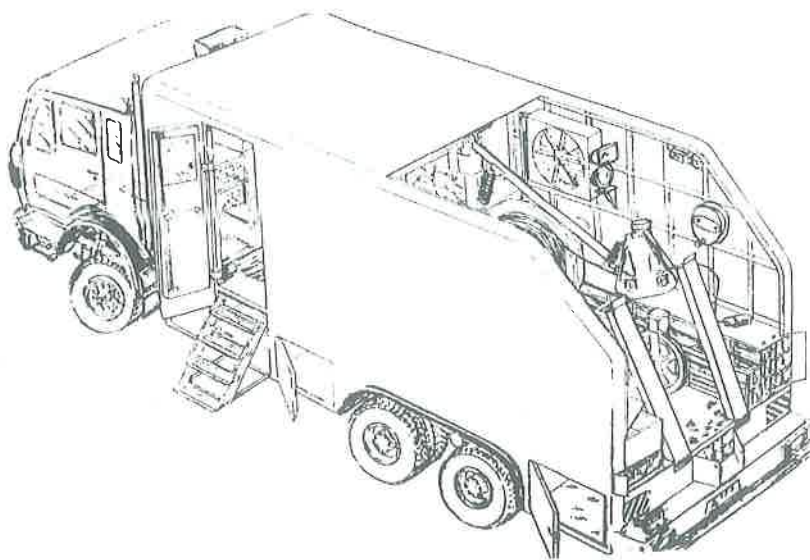


FIGURE 3.20 A typical truck for onshore well-logging operations. *Courtesy of Tesel Services Ltd.*

analytical methods and software programs. When the author attended his first logging course some 30 years ago, calculations were done by slide rules, aided by curious graphs and nomograms. Nowadays, of course, it is all done by computer. Even so, it is important to understand the fundamental principles that underlie the complex calculations, statistical gymnastics, and brightly colored displays that are an integral part of modern formation evaluation.

3.2.1 Electric Logs

3.2.1.1 The Spontaneous Potential, Self-Potential, or SP Log

The spontaneous potential, or self-potential, log is the oldest type of geophysical log in use. The first one was run in 1927. The spontaneous log records the electric potential set up between an electrode in a sonde drawn up the borehole and a fixed electrode at the earth's surface (Fig. 3.21). It can only be used in open (i.e., uncased) holes filled with conductive mud. Provided that there is a minimum amount of permeability, the SP response is dependent primarily on the difference in salinity between drilling mud and the formation water.

The electric charge of the SP is caused by the flow of ions (largely Na^+ and Cl^-) from concentrated to more dilute solutions. Generally, this flow is from salty formation water to fresher drilling mud (Fig. 3.22). This naturally occurring electric potential (measured in millivolts) is basically related to the permeability of the formation. Deflection of the log from an arbitrarily determined shale baseline indicates permeable and therefore porous sandstones or carbonates. In most cases, this deflection, termed a *normal* or *negative* SP deflection, is to the left of the baseline. Deflection to the right of the baseline, termed *reversed* or *positive* SP, occurs when formation waters are fresher than the mud filtrate. A poorly defined or absent SP deflection occurs in uniformly impermeable formations or where the salinities of mud and formation water are comparable (Fig. 3.23). In most cases, with a normal SP, the curve can

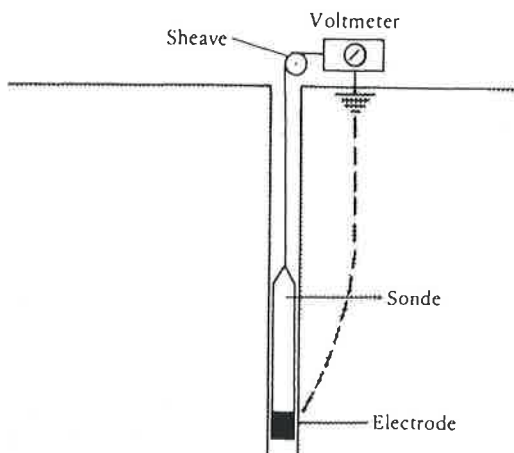


FIGURE 3.21 Basic arrangement for the SP log.

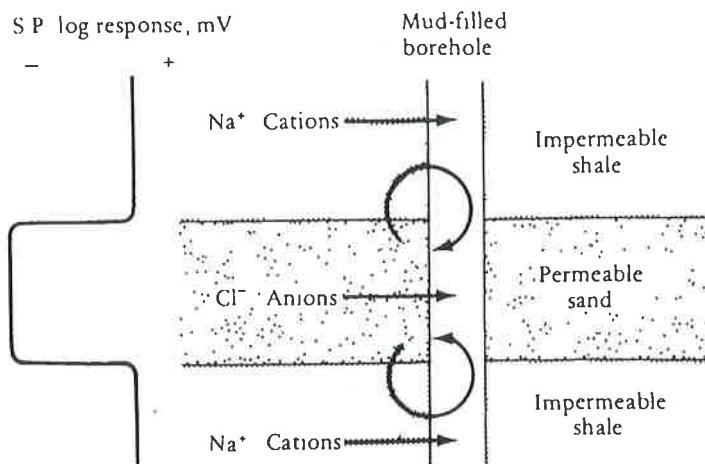


FIGURE 3.22 Diagram showing how ionic diffusion causes the spontaneous potential effect. Looped arrows show the direction of a positive current flow. Log response is for the situation in which the salinity of the formation water is greater than that of the drilling mud.

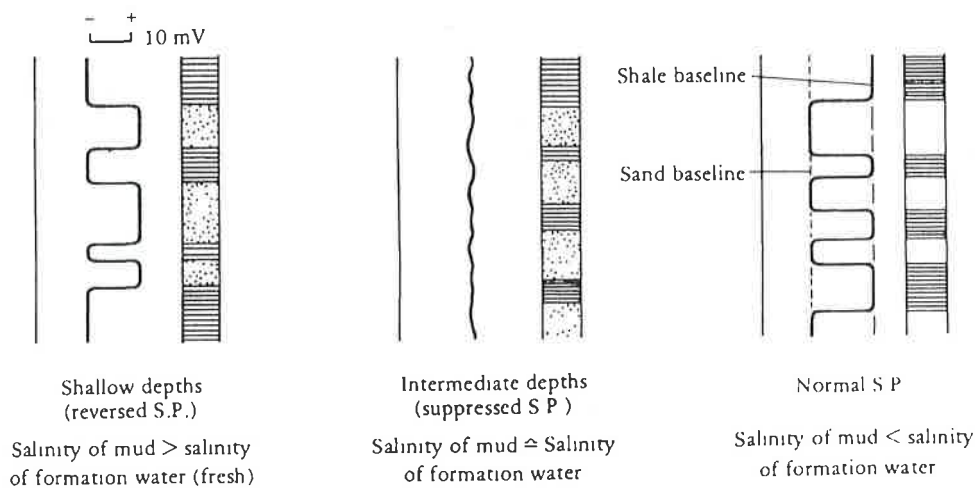


FIGURE 3.23 Schematic SP logs for different salinity contrasts of mud and formation water. Reversed SP logs are very rare. Suppressed SP logs occur where salt muds are used. The usual response, in which the salinity of the drilling mud is less than the salinity of the formation water, is shown in the right-hand log.

be used to differentiate between interbedded impermeable shales and permeable sandstones or carbonates.

Note that the millivolt scale on the SP curve has no absolute value. The logging engineer shifts the baseline as the curve gradually drifts across the scale during the log run. The SP

deflections of adjacent wells are not comparable. Similarly, although local deflections on the curve are caused by vertical variations in permeability, no actual millidarcy values can be measured.

The amount of the current and, hence the amplitude of deflection on the SP curve, is related not only to permeability but also to the contrast between the salinity of the drilling mud and the formation water. Specifically, it is the contrast between the resistivity of the two fluids. Empirically, it has been found that

$$E = K \log \frac{R_{mf}}{R_w}$$

where E is the SP charge (millivolts); K is a constant, which is generally taken as $65 + 0.24T$ (degrees centigrade) or $61 + 0.133T$ (degrees Fahrenheit); R_{mf} is the resistivity of mud filtrate (ohms per meter); and R_w is the resistivity of formation water (ohms per meter).

Details of this relationship are found in Wyllie (1963) and the various wireline-logging service company manuals. Note that since the resistivity of salty water varies with temperature, it is necessary to allow for that factor when solving the equation. The resistivity of the filtrate of the drilling mud may be measured at the surface and, if the bottom hole temperature is known, it can be recalculated for the depth of the zone at which the SP charge is measured. The equation may then be solved, and R_w , the resistivity, and hence the salinity of the formation water can be determined.

In summary, the SP log may be used to delineate permeable zones, and hence, it aids lithological identification and well-to-well correlation. The SP log can also be used to calculate R_w , the resistivity of the formation water. The SP is limited by the fact that it cannot be run in cased holes and is ineffective when R_{mf} is approximately equal to R_w . This situation occurs with many offshore wells drilled using saltwater-based drilling muds.

3.2.1.2 Resistivity Logs

The three main ways of measuring the electrical resistivity of formations penetrated by boreholes are the *normal log*, *laterolog*, and *induction log* techniques. With the normal, or conventional resistivity, log an electric potential and flow of current is set up between an electrode on the sonde and an electrode at the surface. A pair of electrodes on the sonde is used to measure the variation in formation resistivity as the sonde is raised to the surface. The spacing between the current electrode and the recording electrode can be varied, as shown in Fig. 3.24(A). The three electrode spacings usually employed are 16 in (short normal), 64 in (long normal), and 8 ft 8 in (long lateral). They can generally be run simultaneously with an SP log.

Normal resistivity devices, although largely superseded by more sophisticated types, may be encountered on old well logs. For low-resistivity salty muds, laterologs, or guard logs, are now generally used (Fig. 3.24(B)). In these systems, single electrodes cause focused current to flow horizontally into the formation. This horizontal flow is achieved by placing two guard electrodes above and below the current electrode. By balancing the guard electrode current with that of the central generating electrode, a sheet of current penetrates the formation. The potential of the guard and central electrodes is measured as the sonde is raised. As with conventional resistivity logs, various types of laterologs can be used to measure

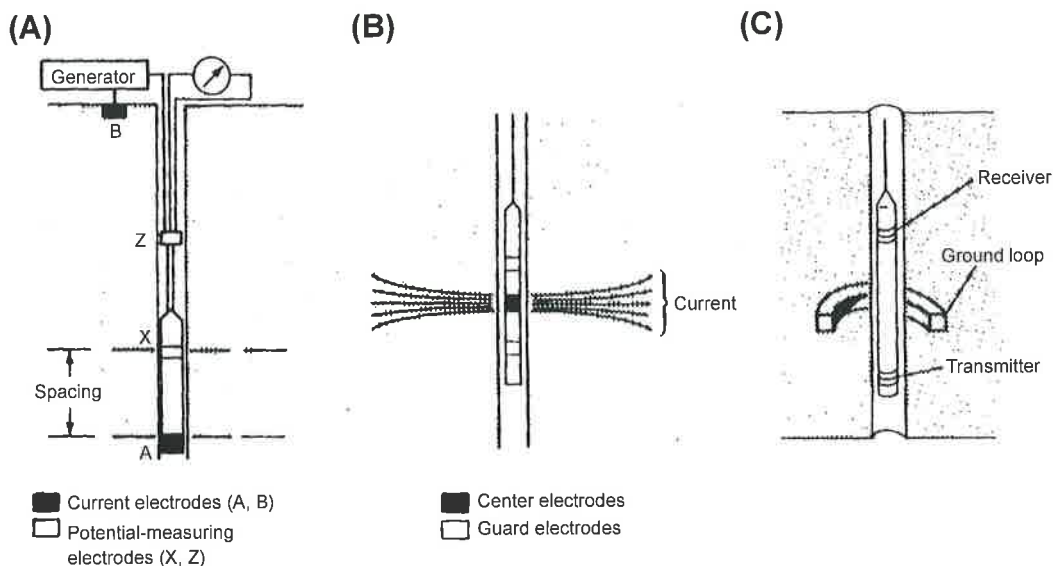


FIGURE 3.24 Illustrations of the three types of resistivity logging devices. (A) The normal resistivity logging device. Variation of the spacing between A and X determines the distance away from the borehole at which the resistivity is measured. (B) Diagram of the laterolog method. (C) Diagram of the induction principle. For explanations see the text.

resistivity at different distances from the borehole. This measurement is achieved by changing the geometry of the focusing electrodes.

For freshwater or oil-based muds, which have a low resistivity, a third type of device is used. This device is the induction log, in which transmitter and receiver coils are placed at two ends of a sonde and are used to transmit a high-frequency alternating current. This current creates a magnetic field, which, in turn, generates currents in the formation. These currents fluctuate according to the formation resistivity and are measured at the receiver coil, as shown in Fig. 3.24(C).

The electrical resistivity of formations varies greatly. Solid rock is highly resistive, as is porous rock saturated in freshwater, oil, or gas. Shale, on the other hand, and porous formations saturated with salty water or brine have very low resistivities. When run simultaneously, SP and resistivity logs enable qualitative interpretations of lithology and the nature of pore fluids to be made (Fig. 3.25). One of the functions of drilling mud is to prevent fluids from flowing into the borehole from permeable formations. At such intervals, a cake of mud builds up around the borehole wall, and mud filtrate is squeezed into the formation. Thus, the original pore fluid is displaced, be it connate water, oil, or gas. So a circular invaded, or flushed, zone is created around the borehole with a resistivity (referred to as R_{xo}) that may be very different from the resistivity of the uninvaded zone (R_t). A transition zone separates the two. This arrangement is shown in Fig. 3.26. As already noted, various types of resistivity logs are not only adapted for different types of mud but also for measuring resistivity of both the uninvaded zone (R_t) and the flushed zone (R_{xo}). The latter

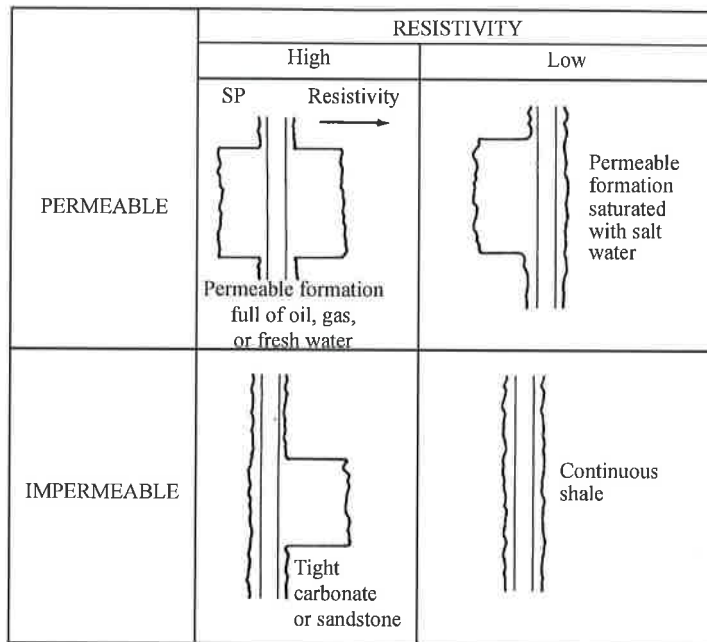


FIGURE 3.25 The four basic responses for SP and resistivity logs for a bed between impermeable formations.

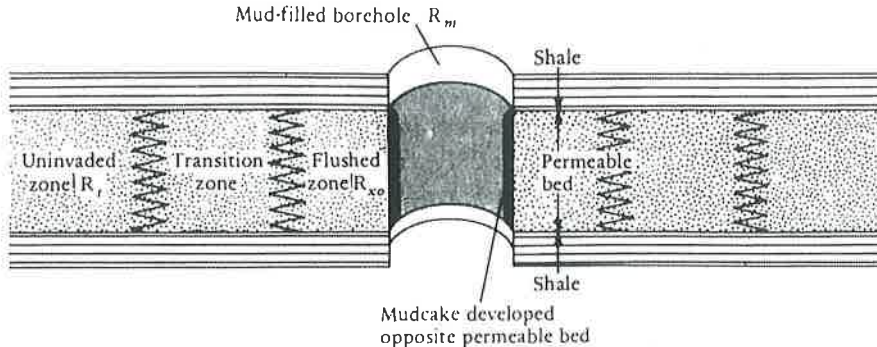


FIGURE 3.26 The situation around a borehole adjacent to a permeable bed. Resistivity of flushed zone, R_{xo} ; resistivity of uninvaded zone, R_i ; resistivity of mud filtrate, R_{mf} ; and resistivity of formation water, R_w .

are generally referred to as *microresistivity logs*, of which there are many different types with different trade names. Figure 3.24 shows the responses of R_t and R_{xo} (deep and shallow) resistivity logs in various water-bearing reservoirs. Note the convention that the deep-penetrating log is shown by a dashed curve and the shallow log by a continuous line. Where formations are impermeable, there is no separation between the two logs, since there is no flushed zone. A single sonde can simultaneously record the SP and more than one resistivity curve (Fig. 3.19).

The identification of hydrocarbon zones from a single resistivity log has already been discussed. Where two resistivity logs are run together, the response is as shown in Fig. 3.27. This figure is, however, only a qualitative interpretation. No absolute resistivity cut-off reading can be used to determine oil saturation.

3.2.2 Quantitative Calculation of Hydrocarbon Saturation

Having reviewed the various resistivity logs and their qualitative interpretation, it is appropriate to discuss the quantitative calculation of the hydrocarbon content of a reservoir. Generally, this calculation is approached in reverse, by first calculating the water saturation (S_w). A reservoir whose pores are totally filled by oil or gas has an S_w of 0% or 0.00; a reservoir devoid of hydrocarbons has an S_w of 100% or 1.0. Consider now a block of rock whose resistivity is measured as shown in Fig. 3.28. Then,

$$\text{Resistance } [\Omega] = R \times \frac{L}{A} [\Omega/(\text{m})(\text{m}^2)],$$

where R is the resistivity (ohms per meter), L is the length of conductive specimen, and A is the cross-sectional area. Note also that

$$\text{Resistivity} = \frac{1}{\text{conductivity (mhos)}}.$$

Most reservoirs consist of mineral grains that are themselves highly resistive, but between them are pores saturated with fluids whose conductivity varies with composition and

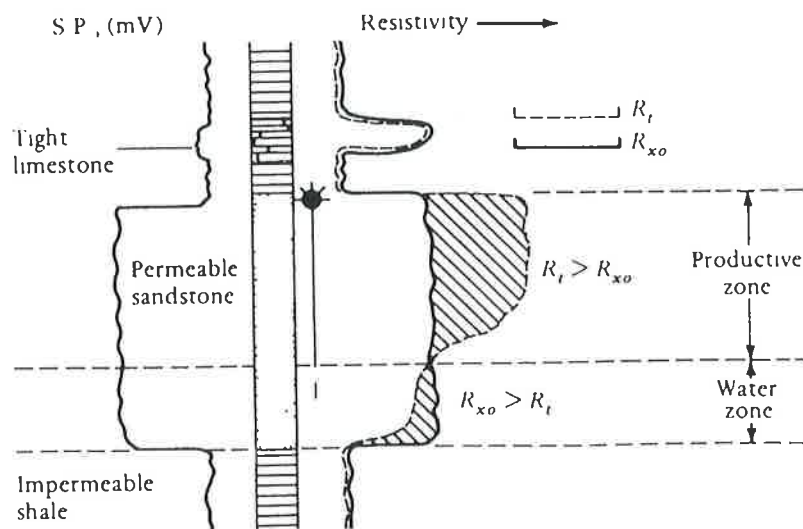


FIGURE 3.27 SP and resistivity logs through a hydrocarbon reservoir showing typical responses for the situation where $R_{mf} > R_w$.

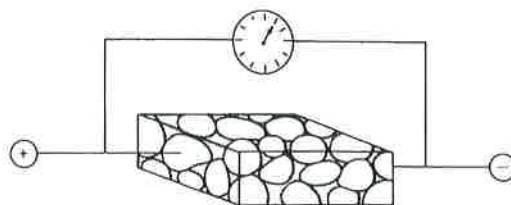


FIGURE 3.28 Sketch showing how the resistivity of a rock is measured.

temperature. An important number in log interpretation therefore is the particular formation resistivity factor (F), defined as

$$\text{Formation resistivity factor (F)} = \frac{R_o}{R_w}$$

where R_o is the resistivity of rock 100% saturated with water of resistivity R_w . Note that R_w decreases with increasing salinity and temperature, as, therefore, does R_o . The value of F increases with decreasing porosity. Archie (1942) empirically derived what is now termed the Archie formula:

$$F = \frac{a}{\phi^m},$$

where a is a constant, ϕ is the porosity, and m is the cementation factor. The values of a and m depend on formation parameters that are difficult to measure, being influenced by the tortuosities among interconnected pores.

Several values for a and m have been found that empirically match various reservoirs. For sands,

$$F = \frac{0.81}{\phi^2}.$$

For compacted formations, notably carbonates,

$$F = \frac{1}{\phi^2}.$$

The Shell formula for low-porosity nonfractured carbonates is

$$F = \frac{1}{\phi^m},$$

where

$$m = 1.87 + \frac{0.019}{\phi}.$$

The Humble formula (suitable for soft formations) is

$$F = \frac{0.62}{\phi^{2.15}}.$$

Again, it has been found empirically that in clean clay-free formations, water saturation can be calculated from the following equation:

$$S_w^n = \frac{FR_w}{R_t},$$

where n is the saturation exponent (generally taken as 2). But, by definition,

$$F = \frac{R_o}{R_w}$$

or

$$R_o = FR_w.$$

Thus,

$$S_w^2 = \frac{R_o}{R_t}$$

or

$$S_w = \sqrt{\frac{R_o}{R_t}}.$$

Using a log reading deep resistivity, R_t can be measured in the suspected oil zone and R_o in one that can be reasonably assumed to be 100% water saturated. Thus, S_w may be calculated throughout a suspected reservoir. This is the simplest method and is only valid for clean (i.e., clay-free) reservoirs. If a clay matrix is present, the resistivity of the reservoir is reduced, and oil-saturated shaley sands may be missed. This method also assumes that the value for F is the same in the oil and water zones, which is seldom true because oil inhibits cementation, which may continue in the underlying water zone. To overcome some of these problems, the ratio method may be used. This method is based on the assumption that

$$S_{xo} = S_w^0{}^2.$$

From this equation, the following relationship may be derived:

$$S_w = \frac{(R_{xo}/R_t)^{5/8}}{R_{mt}/R_w},$$

where R_{xo} can be measured from a microlog; R_t from a deep resistivity log; R_{mt} from the drilling mud at the surface (corrected for temperature at the zone of interest); and R_w from the SP log, as shown in Fig. 3.29.

3.2.3 Radioactivity Logs

3.2.3.1 The Gamma-Ray Log (and Caliper)

Three types of logs that measure radioactivity are commonly used: the gamma-ray, neutron, and density logs. The gamma-ray log, or gamma log, uses a scintillation counter

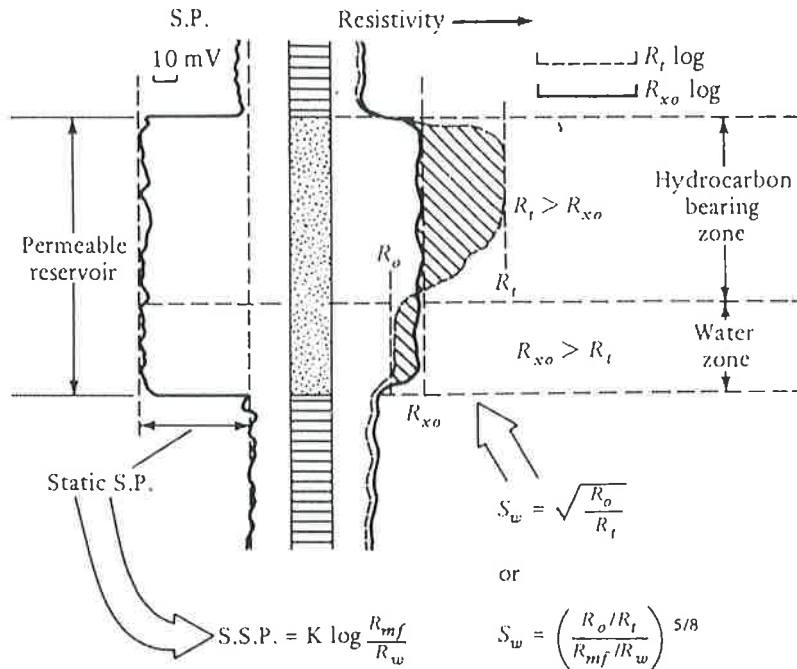


FIGURE 3.29 SP and resistivity logs for a hydrocarbon zone showing where readings are taken to solve the R_w and S_w calculations. For an explanation, see the text.

to measure the natural radioactivity of formations as the sonde is drawn up the borehole. The main radioactive element in rocks is potassium, which is commonly found in illitic clays and to a lesser extent in feldspars, mica, and glauconite. Zirconium (in detrital zircon), monazite, and various phosphate minerals are also radioactive. Organic matter commonly scavenges uranium and thorium, and thus oil source rocks, oil shales, sapropelites, and algal coals are radioactive. Humic coals, on the other hand, are not radioactive. The gamma log is thus an important aid to lithological identification (Fig. 3.30). The radioactivity is measured in API (American Petroleum Institute) units and generally plotted on a scale of 0–100 or 0–120 API.

Conventionally, the natural gamma reading is presented on the left-hand column of the log in a similar manner to, and often simultaneously with, the SP log. The gamma log can be used in much the same way as an SP, with a shale baseline being drawn. Deflection to the left of this line does not indicate permeability, but rather a change from shale to clean lithology, generally sandstone or carbonate. The gamma reading is affected by hole diameter, so it is generally run together with a caliper log, a mechanical device that records the diameter of the borehole. The caliper log shows where the hole may be locally enlarged by washing out or caving and hence deviating the expected gamma-ray and other log responses. The hole may also be narrower than the gauge of the bit where *bridging* occurs. Bridging is caused by either sloughing of the side of the hole and incipient collapse or a build-up of mud cake opposite permeable zones. Although the gamma log is affected by hole diameter,

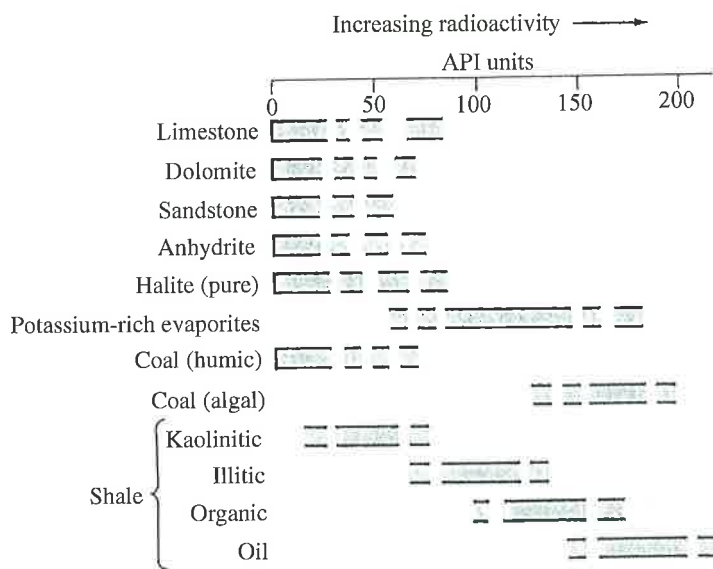


FIGURE 3.30 The approximate gamma log ranges for various rocks. Note that small quantities of radioactive clay, for example, can increase the reading of any lithology.

it has the important advantage that it can be run through casing. The gamma log is important for identifying lithology, calculating the shaliness of reservoirs, and correlating between adjacent wells.

3.2.3.2 The Natural Gamma-Ray Spectrometry Tool

One of the limitations of the standard gamma-ray log is that it is unable to differentiate among various radioactive minerals causing the gamma response. This lack of differentiation causes a severe problem when the log is used to measure the clay content of a reservoir in which either the clay is kaolin (potassium-free and nonradioactive) or other radioactive minerals are present, such as mica, glauconite, zircon, monazite, or uranium adsorbed on organic matter.

By analyzing the energy wavelength spectrum of detected gamma radiation, the refined gamma-ray spectrometry tool measures the presence of three commonly occurring radioactive decay series, whose parent elements are thorium, uranium, and potassium (Hassan et al., 1976). This information can be used for detailed mineral identification and, in particular, it allows a study of clay types to be made. An example of such an application is shown in Fig. 3.31, where the potassium–thorium ratio indicates the trend from potassic feldspar to kaolinite clays. Gamma-ray spectrometry logging is also important in source rock evaluation because it can differentiate detrital radioactive minerals containing potassium and thorium from organic matter with adsorbed uranium.

3.2.3.3 The Neutron Log

The neutron log, as its name suggests, is produced by a device that bombards the formation with neutrons from an Americium beryllium or other radioactive source. Neutron bombardment causes rocks to emit gamma rays in proportion to their hydrogen content.

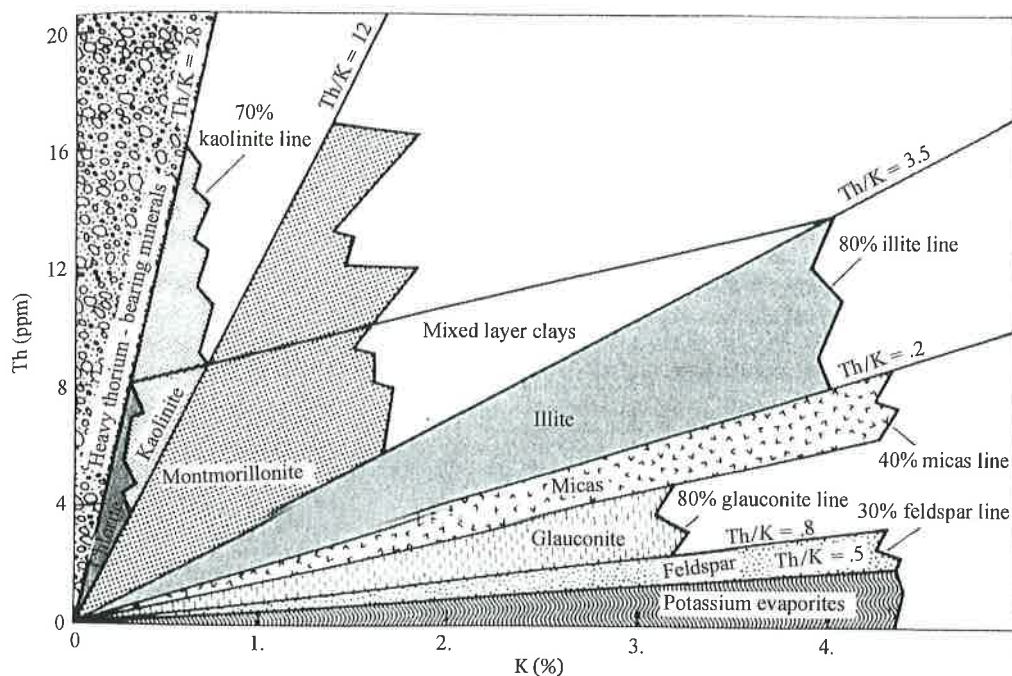


FIGURE 3.31 Crossplot of thorium and potassium showing how the different types of clays (and other minerals) can be identified by the gamma-ray spectrometry log.

This gamma radiation is recorded by the sonde. Hydrogen occurs in all formation fluids (oil, gas, or water) in reservoirs, but not in the minerals. Thus, the response of the neutron log is essentially correlative with porosity. Hole size, lithology, and hydrocarbons, however, all affect the neutron log response. The effect of variation in hole size is overcome by simultaneously running a caliper with an automatic correction for bit gauge. In the early days, the neutron log was recorded in API units. Because it is so accurate for clean reservoirs, the neutron log is now directly recorded in either limestone or sandstone porosity units (LPUs and SPUs, respectively). As with all porosity logs, the log curve is presented to the right of the depth scale, with porosity increasing to the left. Because shales always contain some bonded water, the neutron log will always give a higher apparent porosity reading in dirty reservoirs than actually exists. The hydrogen content of oil and water is about equal, but is lower than that of hydrocarbon gas. Thus, the neutron log may give too low a porosity reading in gas reservoirs. As shown in the following section, this fact can be turned into an advantage. The neutron log can be run in cased holes because its neutron bombardment penetrates steel.

3.2.3.4 The Density Log

The third type of radioactivity tool measures formation density by emitting gamma radiation from the tool and recording the amount of gamma radiation returning from the formation (Fig. 3.32). For this reason, the device is often called the gamma-gamma tool.

Corrections are automatically made within the sonde for the effects of borehole diameter and mud cake thickness. The corrected gamma radiation reading can be related to the electron density of the atoms in the formation, which is, in turn, directly related to the bulk density of the formation. Bulk density of a rock is a function of lithology and porosity. Porosity may be calculated from the following equation:

$$\text{Porosity}(\phi) = \frac{P_{ma} - P_b}{P_{ma} - P_f},$$

where P_{ma} is the density of the dry rock (grams per cubic centimeter), P_b is the bulk density recorded by the log, and P_f is the density of the fluid. Density values commonly taken for different lithologies are as follows:

Lithology	Density (g/cm ³)
Sandstone	2.65
Limestone	2.71
Dolomite	2.87

The fluid in the pores near the borehole wall is generally the mud filtrate. Because the tool has only a shallow depth of investigation and effectively "sees" only that part of the formation invaded by filtrate from the drilling mud, it reads this value for the porosity. Thus, the density of the fluid may vary from 1.0 g/cm³ for freshwater mud to 1.1 g/cm³ for salty mud.

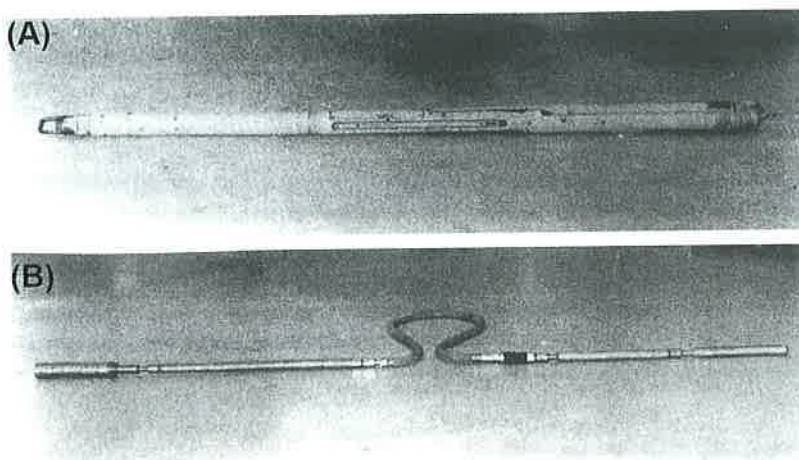


FIGURE 3.32 (A) A density tool, which records the porosity of the formation, making automatic corrections for hole diameter and mud cake thickness. (B) A sonic sonde for measuring the acoustic velocity of formations. Courtesy of Tesel Services, Ltd.

Shale also affects the accuracy of the density-derived porosity of the reservoir. Also, several minerals have anomalous densities, the log traces of which may affect porosity values. Notable among these minerals are mica, siderite, and pyrite. The presence of oil has little effect on porosity values, but gas lowers the density of a rock and thus causes the log to give too high a porosity. This effect can be turned to an advantage, however, when combined with the information derived from the neutron log.

3.2.3.5 The Lithodensity Log

Improvements in density logging techniques include the addition of a new parameter: the photoelectric cross-section, commonly denoted P_e , which is less dependent on porosity than is the formation density and is particularly useful in analyzing the effects of heavy minerals on log interpretation. The P_e records the absorption of low-energy gamma rays by a formation in units of barns per electron. The logged value is a function of mineralogy and the aggregate atomic number of the elements in the formation. Common reservoir mineral reference values are quartz 1.81; dolomite 3.14; calcite 5.08 b/electron. Coals typically are <1 , and typical shales are approximately 3 b/electron (can be distinguished from dolomite by high gamma ray log readings). Typical log scale for a P_e curve is 0–10 b/electron. The P_e curve has a finer resolution (about half a foot) than the neutron/density curves (~ 2 ft). Thus, the curve can help resolve lithology in thin bedded units.

An application that is particularly useful involves combining P_e with the thorium–potassium ratio from the gamma-ray spectrometry device, as indicated in Fig. 3.33.

3.2.4 The Sonic, or Acoustic, Log

A third way of establishing the porosity of a rock is by measuring its acoustic velocity by the sonic, or acoustic, log (Fig. 3.33(B)). In this technique, interval transit times are recorded of clicks emitted from one end of the sonde traveling to one or more receivers at the other end.

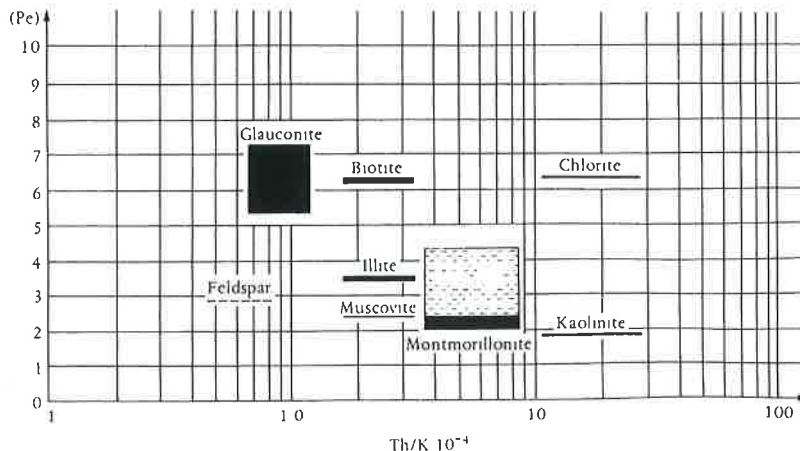


FIGURE 3.33 Crossplot showing mineral identification using the spectrometry and lithodensity logs. Courtesy of Schlumberger.

Sound waves generally travel faster through the formation than through the borehole mud. The interval transit time (Δt), which is measured in microseconds per foot, can then be used to calculate porosity according to the following equation (Wyllie et al., 1956, 1958):

$$\phi = \frac{\Delta t_{\log} - \Delta t_{ma}}{\Delta t_f - \Delta t_{ma}},$$

where Δt_{\log} is the interval transit time recorded on the log, Δt_{ma} is the velocity of the rock at $\phi = 0$, and Δt_f is the velocity of the pore fluid. Some commonly used velocities are shown in Table 3.1.

The sonic log can be used only in open, uncased holes. The circuitry associated with the receiver has to be carefully adjusted for sensitivity so that it does not trigger on spurious noise, yet picks up the first arrival from the signal sound wave. A rapid to-and-fro log trace, termed *cycle skipping*, occurs if the sensitivity is insufficient or if the returned signal is very weak. It results from triggering on a later part of the sound wave pulse, which causes an erroneously long computed transit time. Cycle skip occurs in undercompacted formations (especially if gas filled), fractured intervals, and areas where the hole is enlarged and out of gauge so that a wider than normal width of borehole mud is traversed before the signal pulse enters the formation. Advances with computer-controlled logging devices greatly reduce the problem of balancing trigger sensitivity, which previously required continuous monitoring by the logging engineer.

The sonic method is the least accurate of the three porosity logs because it is the one most affected by lithology. On the other hand, for this very reason, it is widely employed as a means of lithology identification and hence for correlation from well to well. The sonic log is also extremely useful to geophysicists because it can be used to determine the interval velocities of formations and thus relate timing of seismic reflectors to actual rocks around a borehole by means of computed time—depth conversions. For this reason, the sonic log also records the total travel time in milliseconds along its length by a process of integration, the result being recorded as a series of pips along the length of the log. The cumulative number of these constant time interval pips can be counted between formation boundaries, and hence, formation velocities can be related in time and depth.

TABLE 3.1 Some Commonly Used Velocities

Lithology (i.e., pure mineral, $\phi = 0$)	Velocity	
	ft/s	$\mu\text{s}/\text{ft}$
Sandstone (quartz)	18,000–21,000	55.5–51.3
Limestone (calcite)	21,000–23,000	47.5
Dolomite (dolomite)	23,000	43.5
Anhydrite (calcium sulfate)	20,000	50.0
Halite (sodium chloride)	15,000	67.0
Fluid (freshwater or oil)	5300	189.0

3.2.5 Porosity Logs in Combination

The three porosity logs are influenced by formation characteristics other than porosity, notably by their lithology, clay content, and the presence of gas. When used in combination rather than individually, the logs give a more accurate indication of porosity and extract much other useful information. It has already been noted that in gas zones the neutron log indicates too low a porosity and the density log, too high a porosity. These different porosity values can be turned to advantage if the two curves are calibrated so that they track each other on the log. In limestones, the curves are calibrated so that 0 LPU = 2.71 g/cm³; in sandstones, 0 SPU = 2.65 g/cm³. If this calibration is done, separation between the log traces indicates the presence of gas (Fig. 3.34). Note that this phenomenon only applies in reservoir zones. Separation will commonly be seen in the shale sections, but in the reverse direction.

Accurate identification of porosity and lithology can be determined by crossplotting the readings of two porosity logs, using the chart books provided by the particular service company that ran the logs. Figure 3.35 shows one such graph for Schlumberger's formation density and compensated neutron logs run in freshwater holes. These crossplots are satisfactory only in the presence of limestone, sandstone, or dolomite, but are inaccurate in the presence of clay or other anomalous minerals.

A more sophisticated method of lithology identification is the M - N crossplot (Burke et al., 1969). The two formulas used in this method take the readings from the three porosity logs and remove the effect of porosity, thereby leaving only the lithological effect. For example, for water-saturated formations,

$$M = \frac{\Delta t_f - \Delta t_{log}}{\rho_b - \rho_f} \times 0.01,$$

$$N = \frac{(\phi_N)f - \phi_N}{\rho_b - \rho_f}.$$

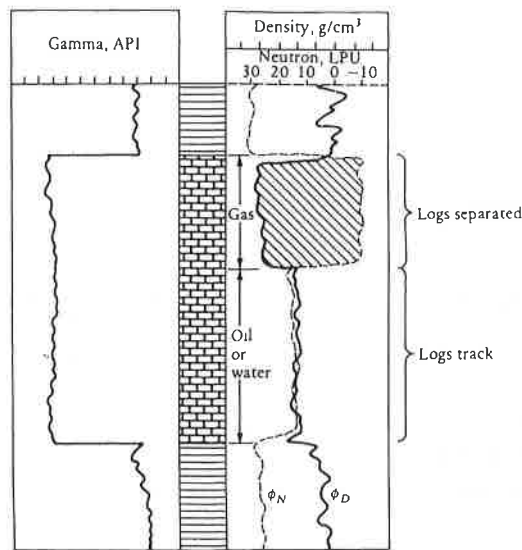


FIGURE 3.34 Log showing how separation of the density and neutron logs may indicate gas-bearing intervals.

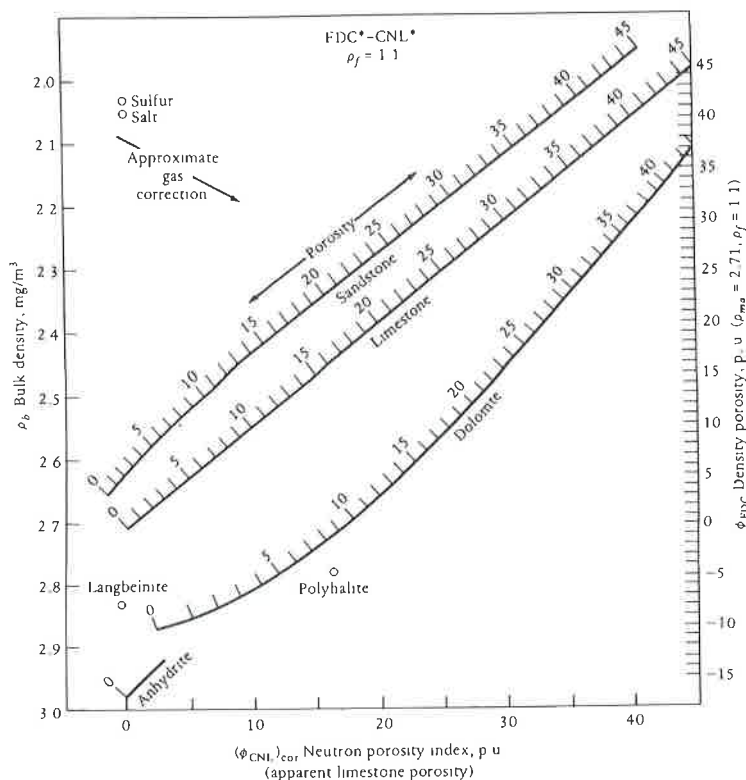


FIGURE 3.35 Density-neutron crossplot for determining porosity and lithology. For an explanation, see the text. Courtesy of Schlumberger.

For freshwater muds,

$$\begin{aligned}\Delta_t &= 189 \mu\text{s/ft}, \\ \phi_N &= 1.0, \\ \rho_b &= 1.0.\end{aligned}$$

The M and N values are then plotted on the graph in Fig. 3.36. This method has an advantage over the simple two-log crossplot in that it can differentiate the proportions of multi-mineralic rocks. Note, however, that the computation is still susceptible to the effects of gas, clay, and anomalous minerals.

3.2.6 Nuclear Magnetic Resonance Logging

The principle of nuclear magnetic resonance (NMR) has been understood for >25 years, and has been used in medicine to produce internal images of the human body. The application of NMR to borehole logging began in the 1950s (Brown and Gammon, 1960). It is only recently, however, that improvements in electronics and magnet design have made it possible for it to be applied effectively.

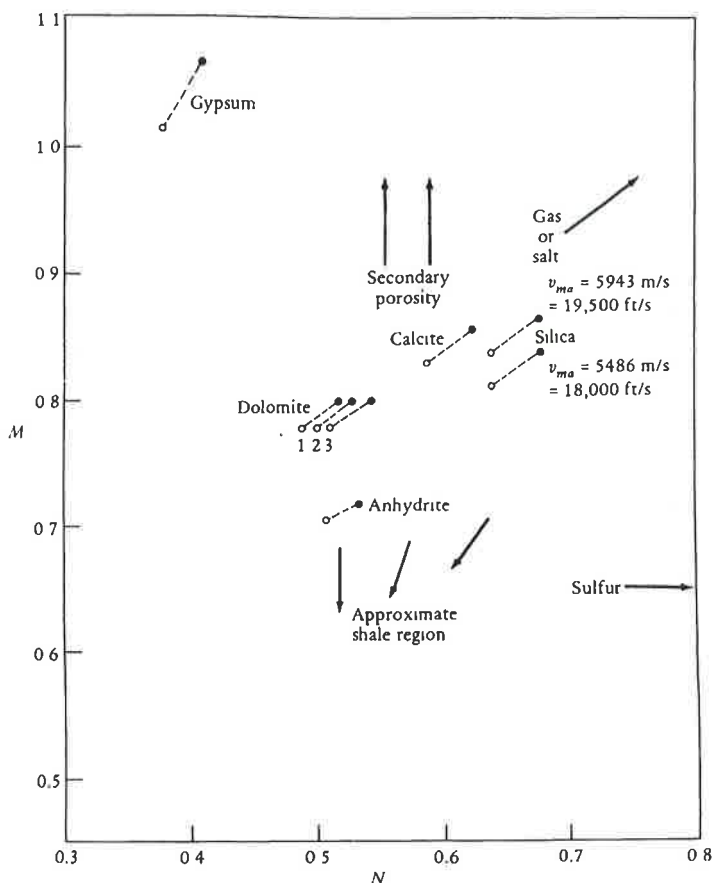


FIGURE 3.36 M-N crossplot for complex lithology identification. For an explanation, see the text. Courtesy of Schlumberger.

NMR logging is an extremely effective way of measuring porosity and permeability. It can differentiate movable from immovable water. When correctly calibrated, it can be used to identify gas reservoirs that would have been missed by conventional logging arrays (Coope, 1994). To really enjoy NMR logging, a PhD in nuclear physics is essential. For simple geologists without such a qualification, an elementary account follows based on Camden (1994).

In rocks, hydrogen occurs principally in the fluids, water, oil, and/or gas that fills pores. Hydrogen nuclei act as randomly aligned positive magnets. When they are exposed to a magnetic field, termed the B_0 field, they will become aligned to it and proceed around it at a velocity proportional to the field strength, known as the *Larmor Frequency*. The orientation of the field may be termed the Z axis, and the perpendicular plane normal to it the X-Y axis. The time taken for the hydrogen nuclei to orient themselves to the magnetic field is termed the polarization time (T_1). When the field is removed, the nuclei will return to their original random orientation. The time taken for this to happen is known as the relaxation time (T_2). The NMR is measured by exposing the hydrogen atoms to pulses of a second magnetic

field (B_1). This causes the magnetization to be rotated back from the vertical (Z) axis to the horizontal ($X-Y$) plane. The energy absorbed from the B_1 field is proportional to the density of the hydrogen nuclei, in other words, it is proportional to the porosity of the rock. When the B_1 field is switched off, the protons return to their random orientation. Thus, it is possible to measure porosity. But the ratio of T_1 to T_2 is proportional to pore size. Slow polarization and relaxation times indicate small pores, which will retain fluid. Fast polarization and relaxation times indicate large pores, which will yield fluid. Thus, this can be used to measure the permeability of the rock.

Fortuitously, the NMR signal ignores bound water and measures the effective porosity. This is the sum of the bulk volume irreducible (BVI) and the free-fluid index (FFI). Selection of the appropriate cut-off on the relaxation time curve enables these two essential parameters to be differentiated.

NMR logs can have different depths of invasion, in the same way as resistivity logs. It is also possible to vary the frequency of the B_0 and B_1 pulses. With appropriate depths of invasion and pulse frequency, it is possible to differentiate hydrogen in liquids from hydrogen in the gaseous phase. Thus, it is possible to differentiate producible gas from bound water. Figure 3.37 illustrates a suite of conventional logs beside a suite of NMR logs that identified a hydrocarbon-bearing zone missed by the former.

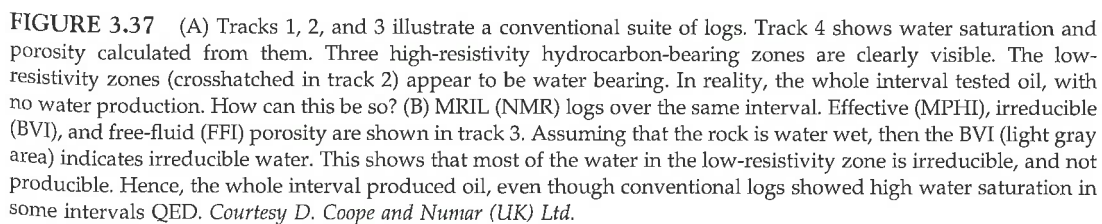
3.2.7 Dielectric Logging

In the quest for ever more accurate measurement of porosity and water saturation logging the variation of the dielectric constant of the formation has been developed (Wharton et al., 1980). The dielectric constant is a factor that controls electromagnetic wave propagation through a medium. Water has a dielectric constant that is much higher than of other fluids or rocks. It ranges from about 50 for freshwater, to 80 for saline water. Oil has a dielectric constant of about 2.2, and air and gas have 1.0. Sedimentary rocks have values of between 4 and 10. Thus, the much higher dielectric constant of water may be used, in combination with other logs, to measure porosity and S_w .

Several tools are available for measuring the dielectric constant. These include the electromagnetic propagation tool, the dielectric constant log (DCL), and the deep propagation tool. The difference between total porosity, measured by the other porosity logs, and the porosity measured by the DCL will indicate the hydrocarbon saturation of the reservoir. Dielectric logs are particularly useful in low R_w situations, and also where there are rapid vertical variations in R_w . As with all tools, there are problems with the dielectric log method. Dielectric logs respond to water, whether it is connate water, mud filtrate, or water bound to mineral grains. If the depth of investigation is shallow, it may record high readings where mud filtrate has invaded permeable hydrocarbon-bearing zones. This problem may be overcome, as with resistivity logging, by running shallow and deep investigative dielectric logs together.

3.2.8 Logging or Measurement while Drilling

The foregoing account of logging related to logs run in open or cased holes after drilling sections of a well. Since the early 1980s, however, it has been possible to run some logs within drill pipes while the well is actually being deepened. The main problem that had



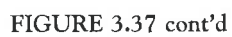


FIGURE 3.37 cont'd

to be overcome was the telemetric link between the surface and the sonde adjacent to the drill bit. Various techniques were tried, including electromagnetic, acoustic, mud pulse, and wire telemetry. Only the last two of these have proved to be effective. Running logs while drilling is variously termed *measurement while drilling* or *logging while drilling* (LWD).

In the early days, only simple resistivity and gamma logs could be run (Fontenot, 1986). Their usefulness was largely restricted to correlating the drilling well with adjacent previously drilled wells. Today, density and neutron logs can also be used, together with a range of resistivity logs (Bonner, 1992, 1996). Both laterologs and induction logs are available for dealing with a range of formation and drilling mud resistivities. MWD/LWD now has many more uses than heretofore. As mentioned earlier, offshore petroleum exploration has led to the increased need to drill lengthy directional holes. It is thus extremely important not only to know where the drill bit is underground but also to have real-time information on rock type, hydrocarbon occurrences, and signs of overpressure.

3.2.9 Dip Meter Log and Borehole Imaging

The dip meter is a device for measuring the direction of dip of beds adjacent to the borehole. It is essentially a multiarm microresistivity log (Fig. 3.38). Three or four spring-loaded arms record separate microresistivity tracks, while, within the sonde, a magnetic compass records the orientation of the tool as it is drawn up the hole. A computer correlates deviations, or kicks, on the logs and calculates the amount and direction of bedding dip and assesses dip reliability (Fig. 3.39). Many different computer programs can be applied. Some programs essentially smooth the dips over large intervals; others use statistical techniques to discriminate against minor bedding features so as to display only large-scale dip trends. Both these types are suitable for determining structural dip. Some programs calculate dips over intervals of only a few centimeters. This type of program (after removal of structural dip) can be used to discover small-scale sedimentary dips, such as crossbedding.

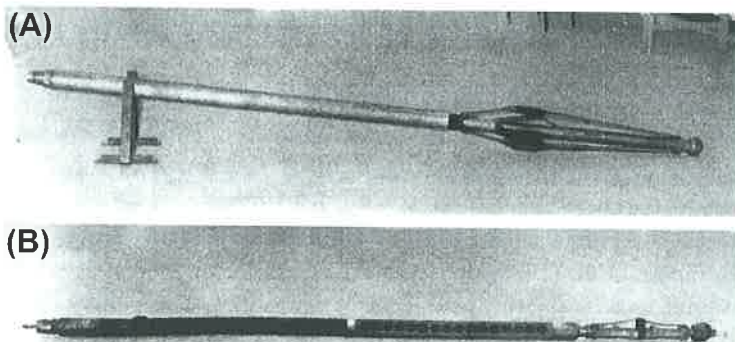


FIGURE 3.38 (A) Three-arm dip meter sonde. (B) Sidewall core gun. This device fires cylindrical steel bullets, which are attached to the gun by short cables, into the side of a borehole. Small samples of rock may thus be collected from known depths. Courtesy of Tesel Services, Ltd.

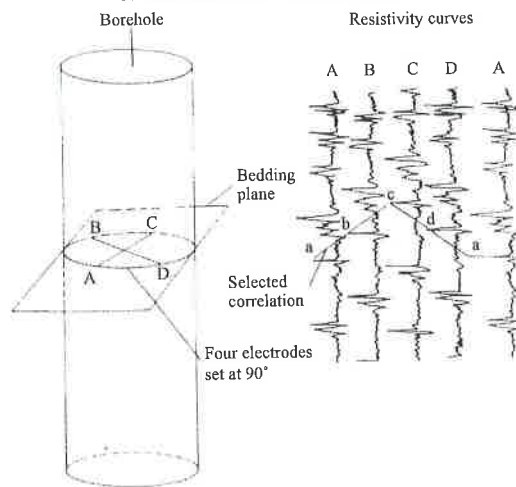


FIGURE 3.39 Sketch of an antique four-pad four-track dip meter showing how the direction of dip around a borehole may be calculated. Today, the simple dip meter shown here has been superseded by multitrack imaging tools, but the basic principle of dip calculation is still as shown here.

Calculated dips are usually presented on a tadpole plot (Fig. 3.40). Four basic types of motif are commonly identifiable:

1. Uniformly low dips (referred to as green patterns) are generally seen in shales and indicate the structural dip of the formation.
2. Upward declining dip sequences (referred to as red patterns) may be caused by the drape of shales over reefs or sandbars; by the infilling of sandstones within channels; or by the occurrence of folds, faults, or unconformities.
3. Upward increasing dip sequences (referred to as blue patterns) may be caused by sedimentary progrades in reefs, submarine fans, or delta lobes. They may also be caused by folds, faults, or unconformities.
4. Random bag o' nails motifs can reflect poor hole conditions or they might be geologically significant, indicating fractures, slumps, conglomerates, or grain flows.

The dip meter provides much valuable information, but it can only be interpreted fully in the light of other logs and geological data. For additional discussion, see the service company manuals and Gilreath and Maricelli (1964), Campbell (1968), McDaniel (1968), Jageler and Matuszak (1972), Goetz et al. (1978), Serra (1985), and Selley (1996).

The first dip meter tool had three arms 120° apart. This was replaced by the four-arm dip meter. Originally having only four micrologs, the number was eventually increased to 8, four on each pad to increase reliability. There was then a major jump to increase the number of tracks to 25, and now up to nearly 200. Simultaneously, the widths of the pads were increased so that almost the entire borehole was covered. With some cunning statistical gymnastics, it is now possible to process this multiplicity of microresistivity log data to produce incredible pseudovisual images of the borehole (Fig. 3.41). These tools, made by several companies with several trade names, can be used, both to measure the direction and amount of dip of

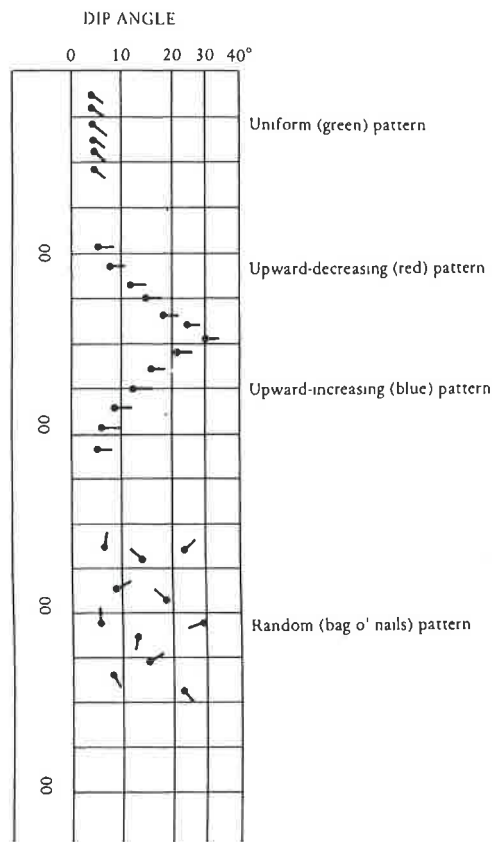


FIGURE 3.40 Conventional dip meter tadpole plot showing the four common dip motifs. Each motif can be produced by several quite different geological phenomena. The head of the tadpole shows the amount of dip. The tail of the tadpole points in the direction of dip.

strata around the borehole, and also to identify faults, fractures, unconformities, and sedimentary structures (Fig. 3.42).

Acoustic borehole imaging tools have also been developed. They are generally not as effective as resistivity-based tools. The best results are normally seen in very hard items such as basement, quartzites, and carbonates, where there is a large contrast in the acoustic velocity between the rock and open fractures and vugs.

3.2.10 Uses of Logs in Petrophysical Analysis: Summary

The previous sections provide a short, and therefore simplified, review of a major group of borehole logging techniques that are crucial to the exploration for and production of hydrocarbons. New tools and techniques are continuously being introduced, but the basic principles remain constant. Figure 3.43 provides a summary of the more common geophysical logs and their principal uses. Figures 3.44 and 3.45 provide typical examples of suites of

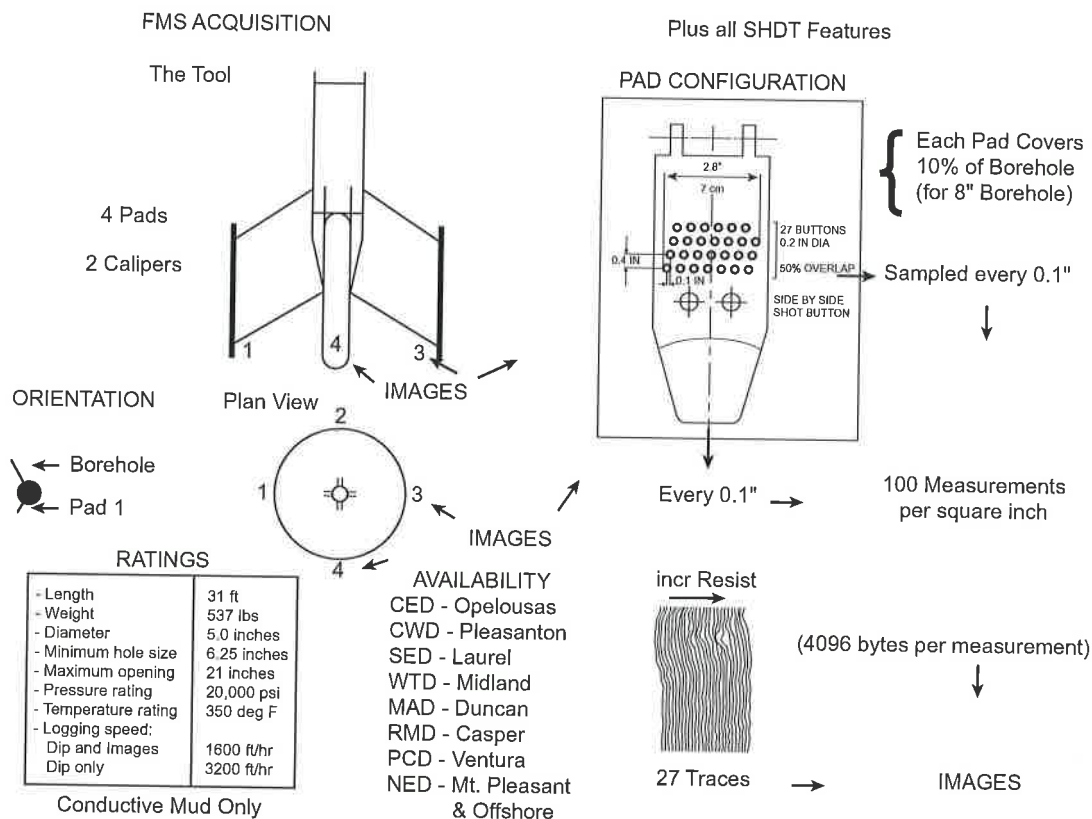


FIGURE 3.41 Diagrams to show the workings of the Schlumberger Formation MicroScanner. This was the first borehole imaging tool. It is now superseded by the Fullbore MicroImager. *Courtesy of Schlumberger.*

logs with their responses for parts of two boreholes. In the old days, the calculations of R_w , S_w , ϕ , and so forth were made using service company chart books and a calculator. Today, however, computer-processed interpretations, which give continuous readings of lithology, porosity, and the percentages of the various fluids, are preferable (Fig. 3.46). Although computer outputs look very convincing, especially when brightly colored, the old adage "rubbish in, rubbish out" must be remembered (Plate 3.1). Failure to check the quality of the original logs or failure to note the presence of an unusual or aberrant mineral will invalidate the whole procedure. For example, abundant mica flakes in a sandstone will read as "clay" on logs, giving a false value of porosity. This is because of the way in which small amounts of anomalous minerals can alter log readings that geochemical logging programs have been developed. These involve very complex algorithms to identify and measure the vertical variations of such minerals. Once this has been done, it is possible to calculate the essential reservoir parameters of porosity and hydrocarbon saturation (Wendtland and Bhuyan, 1990; Harvey and Lovell, 1992). These logs, together with conventional logs, can also be used to identify and understand diagenetic phenomena within reservoirs. Thus, it has been

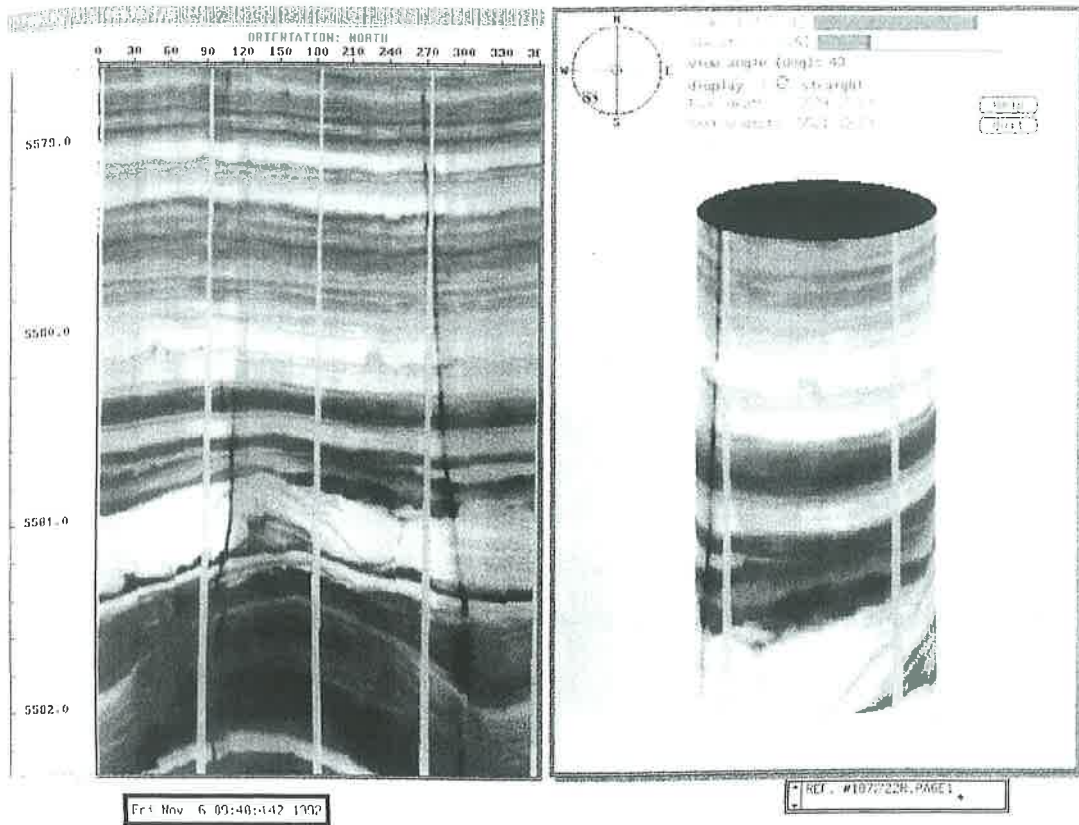


FIGURE 3.42 An example of a borehole image produced by the Formation MicroImager. Note that the borehole can be displayed in both cylindrical and unrolled formats. *Courtesy of Schlumberger.*

argued that formation evaluation is now entering its third age (Selley, 1992). The first age was the application of logs to petrophysical analysis, the second age to facies analysis (discussed later), and the third to reservoir diagenesis (discussed in Chapter 6).

3.2.11 Applications of Logs in Facies Analysis

The previous sections reviewed the various types of geophysical logs and their application in identifying lithology, porosity, and hydrocarbon saturation. Logs are also used in other ways. When the stratigraphy of a well has been worked out, whether it be the lithostratigraphy or the biostratigraphy (in which paleontological zones are introduced), adjacent wells can be stratigraphically correlated. Logs can also be used to determine the facies and depositional environment of a reservoir. From such studies, the geometry and orientation of reservoirs may be predicted. Carbonate facies are largely defined, and their depositional environments deduced, from petrography. Geophysical logs show porosity

ELECTRIC LOGS	Lithology	Hydrocarbons	Porosity	Pressure prediction	Structural and sedimentary dip	OTHER
Spontaneous potential	✓					Calculation of R_w , and bed shaliness, Qualitative identification of permeability
Resistivity	✓	✓		✓		Calculation of R_{xo} , R_t , and hence S_w
RADIOACTIVE LOGS						
Gamma	✓					Calculation of bed shaliness and organic content
Neutron		✓	Gas effect ✓			Lithology identification by cross-plots Calibration of formations with seismic data
Density		✓				
SONIC	✓	✓	✓	✓		
DIPMETER					✓	

FIGURE 3.43 Summary of the main types of wireline logs and their major applications.

distribution in carbonates, but because it is commonly of secondary origin, little correlation exists between log response and original facies. In sandstones, however, porosity is mainly of primary origin. Studies of modern depositional environments show that they deposit sediments with characteristic vertical profiles of grain size. For example, channels often fine up, from a basal conglomerate, via sand, to silt and clay. Conversely, prograding deltas and barrier islands deposit upward-coarsening grain-size profiles. Grain-size profiles may thus be of use in facies analysis. Both the SP and gamma logs may indicate grain-size profiles in sand–shale sequences. As discussed earlier, the deflection on the SP is locally controlled by permeability, with the maximum leftward deflection occurring in the most permeable interval. Permeability, however, increases with grain size. Therefore, the SP log is generally a vertical grain-size log in all but the most cemented sand–shale sections.

The gamma log may be used in a similar way, since the clay content (and hence radioactivity) of sands increases with declining grain size. Exceptions to this general statement may be caused by intraformational clay clast conglomerates and the presence of anomalous radioactive minerals, such as glauconite, mica, and zircon (Rider, 1990). Gamma and SP logs often show three basic motifs:

1. Sands that fine upward gradually from a sharp base (bell motifs)
2. Sands that coarsen up gradually toward a sharp top (funnel motifs)
3. Clean sands with sharp upper and lower boundaries (boxcar, or blocky motifs)

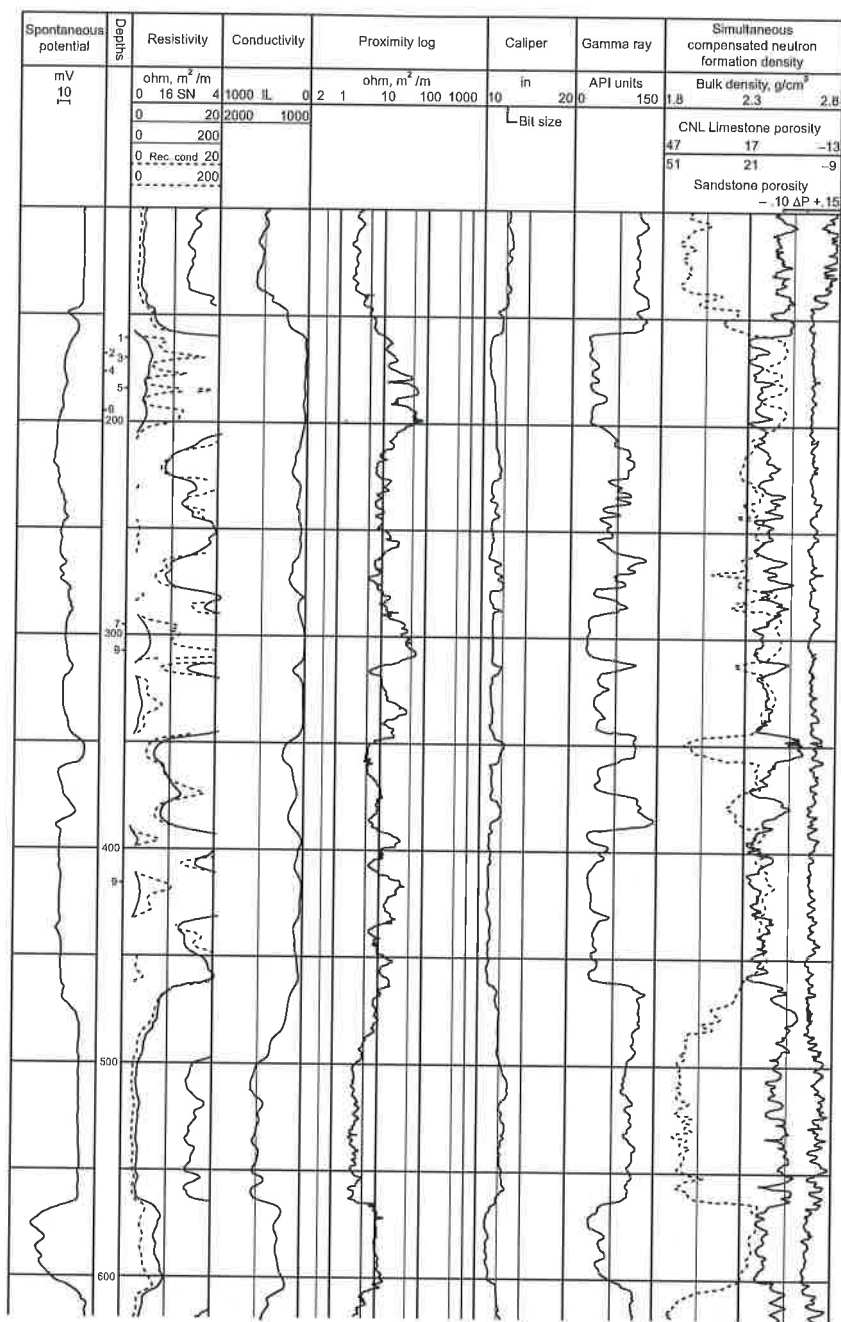


FIGURE 3.44 Typical suite of logs through a sand-shale sequence in the Niger delta. Note high-resistivity hydrocarbon-bearing zones at 160–210 ft and below. *Courtesy of Schlumberger.*

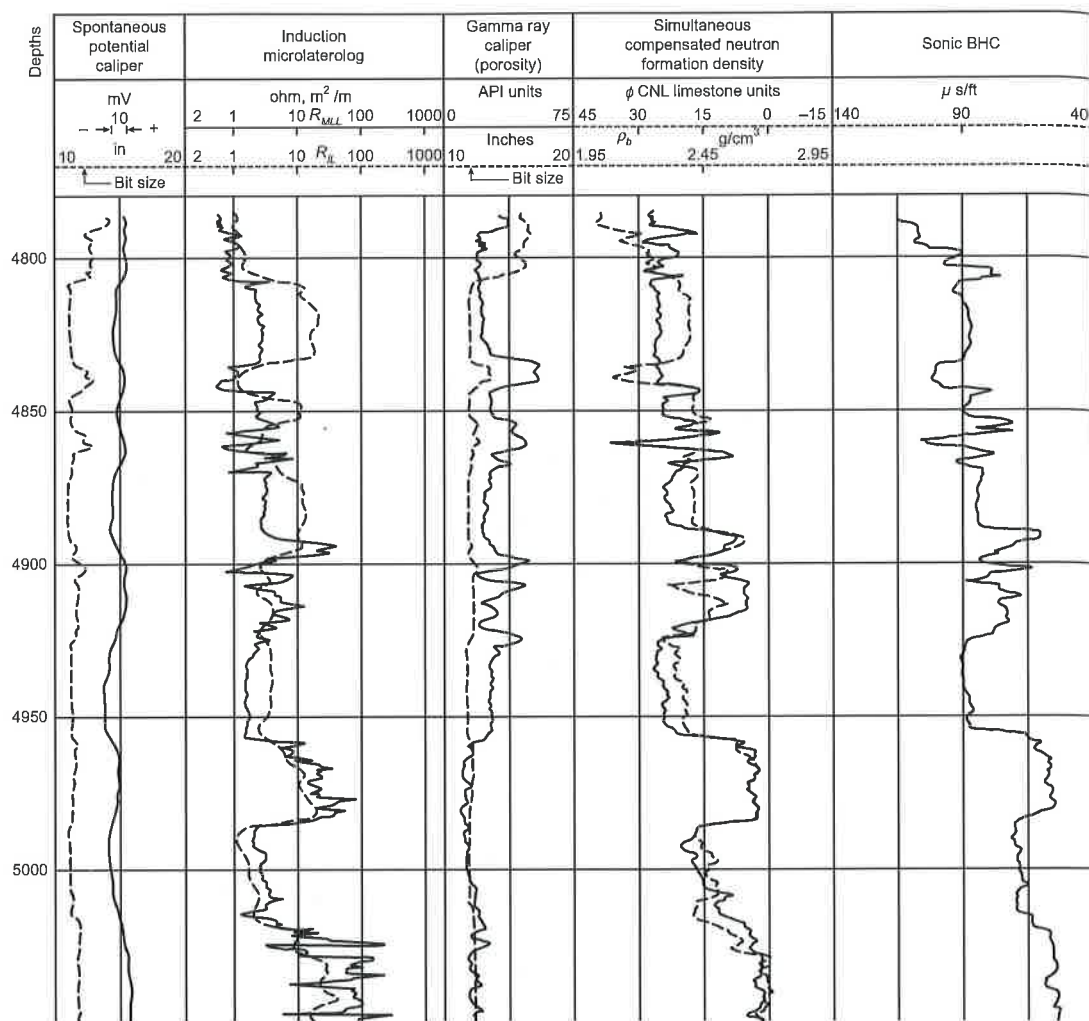


FIGURE 3.45 Typical suite of logs through the Paleocene section of the North Sea. Sands and shales in the upper part pass down into limestones. High resistivity in sands between 4805 and 4895 m suggest the presence of hydrocarbons. The separation between the neutron and density logs suggests that these may be gas. *Courtesy of Schlumberger.*

These three patterns may show variations from smooth to serrated curves when considered in detail (Fig. 3.47). No log motif is specific to a particular sedimentary environment, but by combining an analysis of log profile with the composition of well samples, an interpretation of environment can be attempted. Constituents to look for in the cuttings are glauconite, shell debris, carbonaceous detritus, and mica. Glauconite forms during the early diagenesis of shallow marine sediments. Once formed, it is stable in the marine realm, but

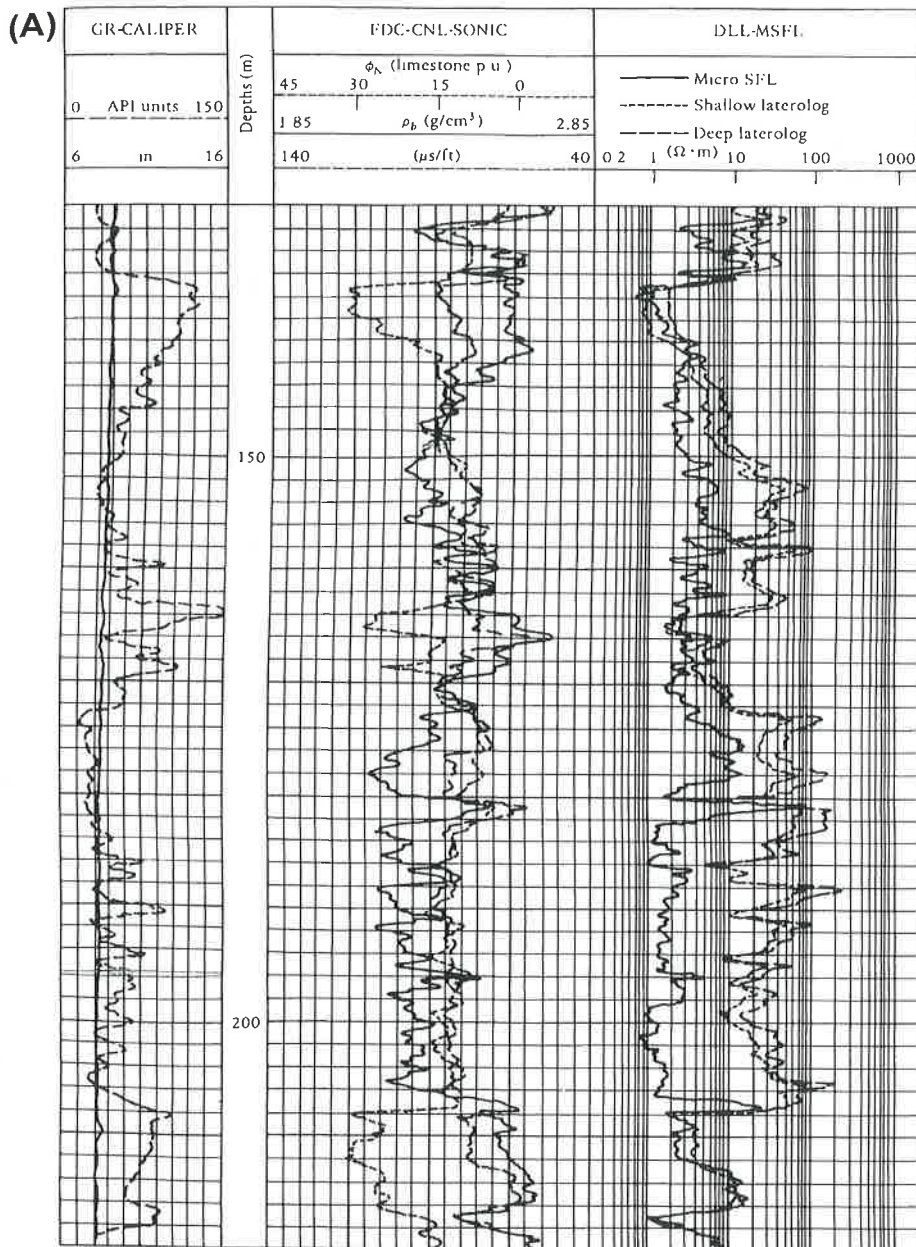


FIGURE 3.46 (A) A "raw" unprocessed suite of logs, compare with (B), a computer-calculated interpretation. This shows the percentage of porosity and hydrocarbon saturation, together with the variation in clay and matrix. Note that engineers use the term *matrix* to describe grains, not in the geological sense of the finer sediment (silt and clay) that is syndepositionally deposited along with the framework grains. Courtesy of Schlumberger.

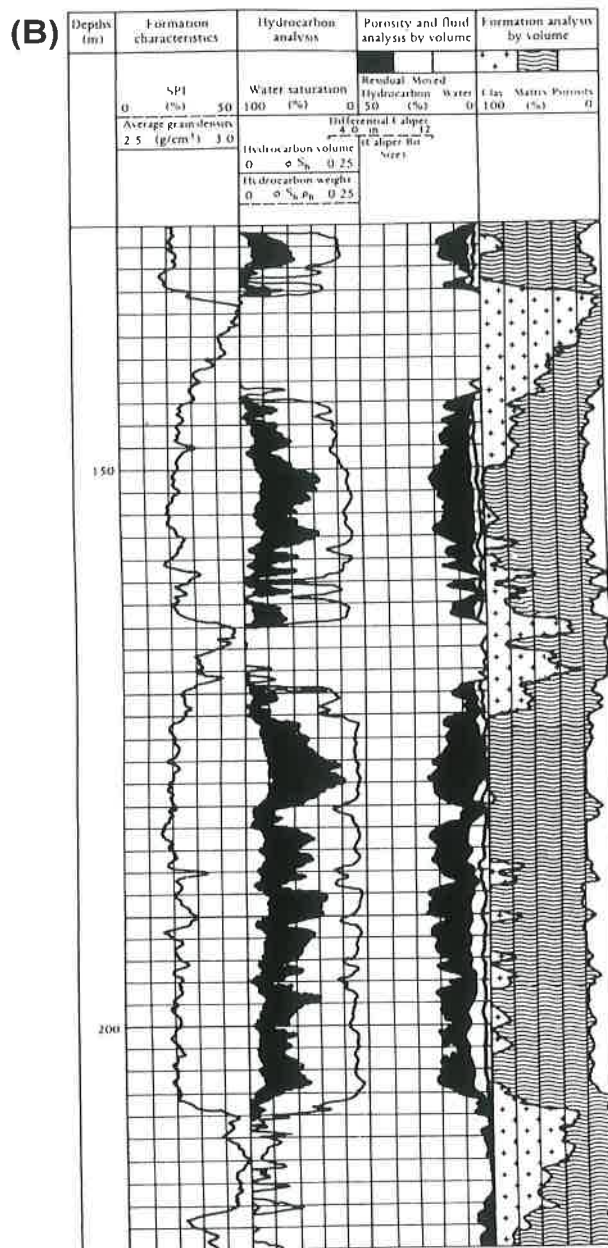
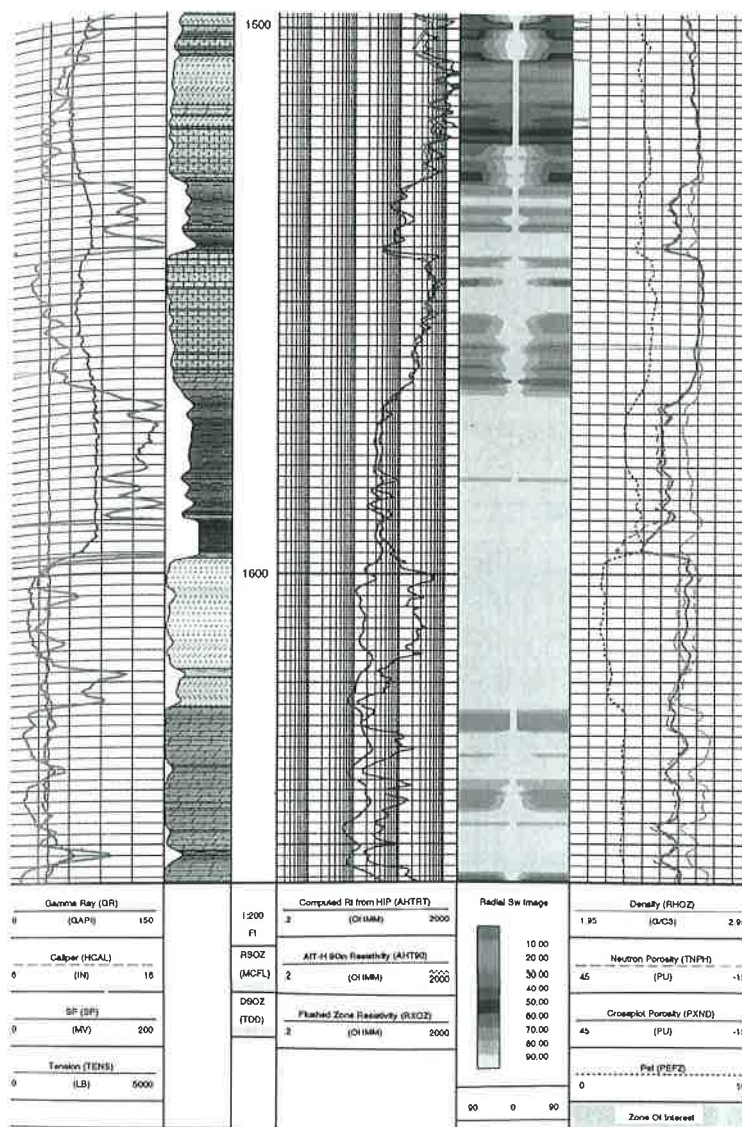


FIGURE 3.46 cont'd



LITHOLOGY with AITH Sw Processing

PLATE 3.1 An example of a suite of well logs. Gamma, self-potential, and caliper logs in left-hand column help to indicate lithology. Resistivity logs in track to immediate right of depth column calculate hydrocarbon saturation in right-hand colored column. Porosity logs in the far right column. Reservoir zone at the top of the section is highlighted by pink bar at right of radial S_w log (See the color plate). *Courtesy of Schlumberger Wireline and Testing.*

can be transported landward on to beaches or basinward on to deep sea fans. Glauconite is readily oxidized at outcrop, however, so reworked second-cycle glauconite is virtually unknown. Thus, the presence of glauconite grains in a sandstone indicates a marine environment, although its absence indicates nothing.

Shell-secreting invertebrates live in freshwater and seawater environments, but shelly sands tend to be marine rather than nonmarine. Diagnosis is obviously enhanced if fragments of specific marine fossils can be identified. Carbonaceous detritus includes coal, plant


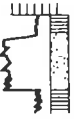
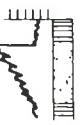
Log motif			
Glauconite and shell debris (high-energy marine)	Tidal channel	Tidal sand wave	Regressive barrier bar
Glauconite, shell debris, carbonaceous detritus, and mica (dumped marine)	Submarine channel		Prograding submarine fan
	Turbidite fill	Grain flow fill	
Carbonaceous detritus and mica (dumped)	Fluvial or deltaic channel	Delta distributary channel	Prograding delta or crevasse splay

FIGURE 3.47 Diagram showing the three common grain-size motifs seen on SP and gamma logs. Note how, by combining these with the visual petrographical analysis of well samples, environmental interpretations of sand bodies can be made.

fragments, and kerogen. These substances may be of continental or marine origin, but the preservation of organic matter generally indicates rapid deposition with minimal reworking and oxidation. Similarly, the presence of mica indicates rapid sedimentation in either marine or continental environments.

These four constituents are commonly recorded in well sample descriptions. Coupled with a study of log motifs, their presence (but not their absence) may aid the identification of the depositional environment of sand bodies and hence the prediction of reservoir geometry and trend (Fig. 3.47). This technique was first proposed by Selley (1976) and later refined (Selley, 1996). In an ideal world, facies analysis should be based on a detailed sedimentological and petrographic study of cores, but this method may be used to extend interpretation beyond cored wells or in regions where cores are not available. Figures 3.48 and 3.49 show the sort of facies synthesis that can be produced by integrating log and rock data. Real examples of some of these motifs are illustrated in this book, especially in Chapters 6 and 7.

Facies analysis becomes easier still when grain-size profiles from logs are combined with facsimiles of sedimentary structures from borehole imaging tools. Then, the orientation of sedimentary structures, notably crossbedding, may be used to predict paleocurrent direction, and hence the orientation of reservoir units. As seismic becomes ever more effective at imaging the shapes of reservoirs, however, facies analysis using these techniques becomes increasingly unnecessary.

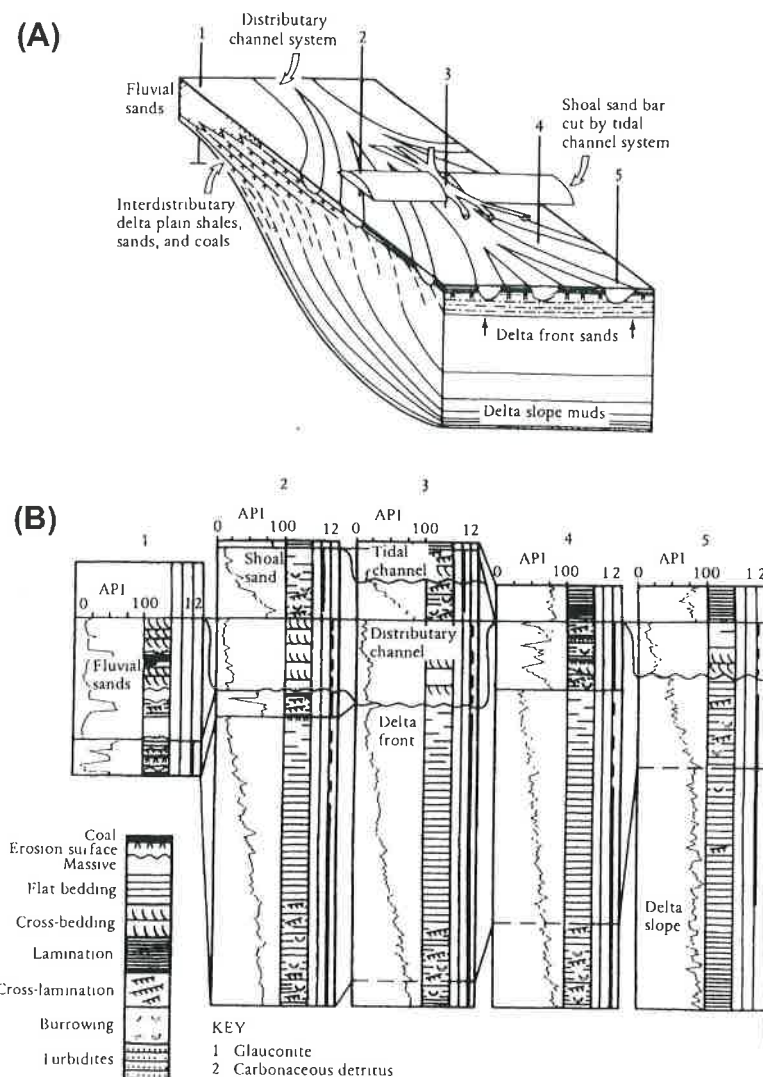


FIGURE 3.48 (A) Sand body geometry and (B) log responses for a delta system. Note how carbonaceous detritus and mica occur in the progradational phase of the delta, and are replaced by glauconite and shell debris in the transgressive sands that were deposited following delta abandonment. From Selley (1996). Reprinted with permission from Chapman & Hall.

3.3 GEOPHYSICAL METHODS OF EXPLORATION

Petroleum exploration and production are largely concerned with the geological interpretation of geophysical data, especially in offshore areas. Petroleum geologists need to be well acquainted with the methods of geophysics. For many years, a large communication barrier

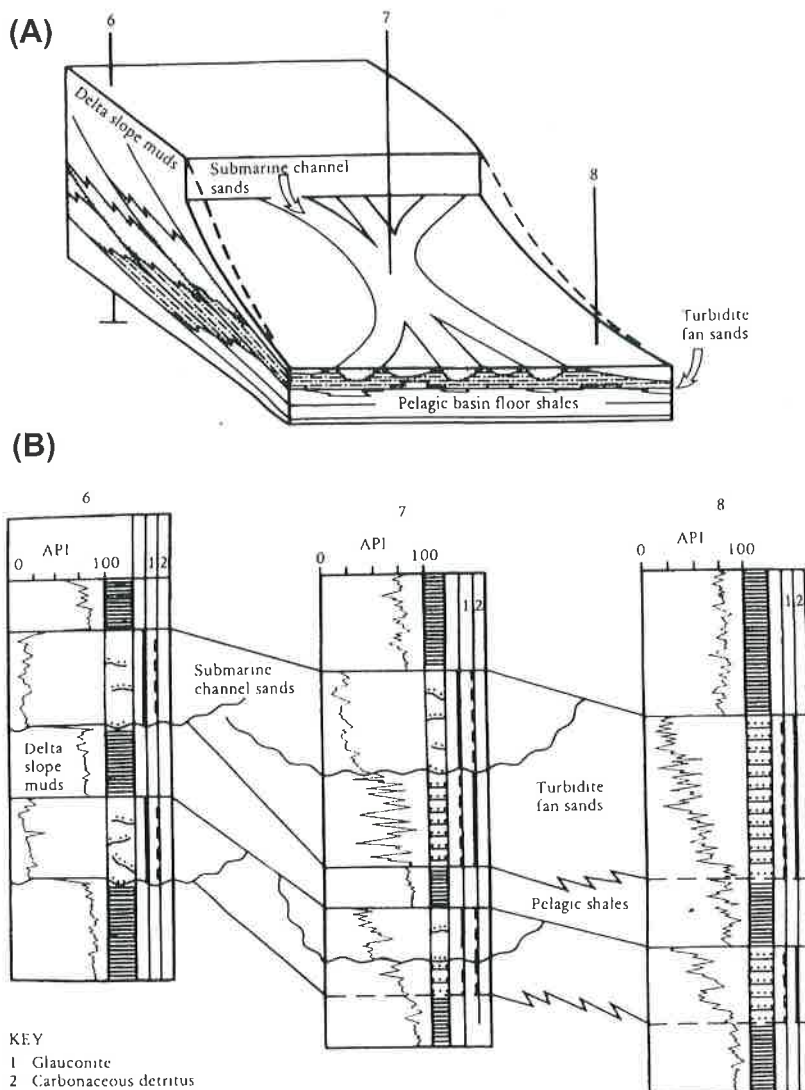


FIGURE 3.49 (A) Sand body geometry and (B) log responses for submarine channel and fan deposits. Note how deep marine sediments may be characterized by an admixture of land-derived carbonaceous detritus and mica together with shelf-derived glauconite and shell fragments. The log profiles are not dissimilar from those produced by a prograding delta, but the petrography may be used to differentiate them. *From Selley (1996). Reprinted with permission from Chapman & Hall.*

existed in many oil companies between the two groups, which were usually organized in different departments. This separation has now largely disappeared, as a new breed of petroleum geoscientist appears—half geologist and half geophysicist. Unfortunately, a new division has developed within the geophysical world between the mathematicians, physicists,

and computer programmers (who acquire and process geophysical data) and those who use geological concepts to interpret this information.

The following account of geophysical methods of petroleum exploration has two objectives. It seeks to explain the basic principles and to illustrate the wonders of modern geophysical display. What it does not pretend to do, however, is explain the arcane mathematics and statistical gymnastics that are used to get from first principles to the finished brightly colored geophysical image. This account is probably sufficient for petroleum reservoir engineers seeking to know the origins of the maps by which fields are found and reserves assessed. For petroleum geologists, however, it is only an introduction and will be followed by courses in geophysics in general and in seismic interpretation in particular.

Three main geophysical methods are used in petroleum exploration: magnetic, gravity, and seismic. The first two of these methods are used only in the predrilling exploration phase. Seismic surveying is used in both exploration and development phases and is by far the most important of the three methods (Fig. 3.50).

3.3.1 Magnetic Surveying

3.3.1.1 Methodology

The earth generates a magnetic field as if it were a dipole magnet. Lines of force radiate from one magnetic pole and converge at the other. The inclination of the magnetic field varies from vertical at the magnetic poles to horizontal at the magnetic equator. The magnetic axis of the earth moves about within a circle of some 10–15 degrees of arc from the rotational axis. The force between two magnetic poles may be expressed as follows:

$$F = \frac{AM_1M_2}{r^2},$$

where F is the force; A is the constant, generally unity; M_1 , M_2 are strengths of the respective poles; and r is the distance between the poles.

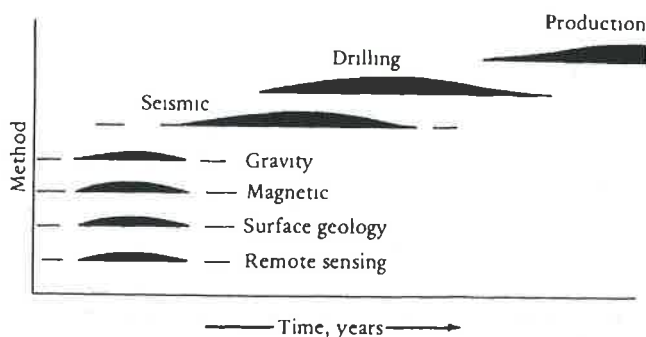


FIGURE 3.50 Sketch showing the times at which different geophysical methods are used in petroleum exploration.

Magnetic field strength is measured either in gammas or in oersteds. One oersted is the field that exerts a force of 1 dyne on a unit magnetic pole. One gamma is 10^{-5} Oe. The magnetic field of the earth varies from about 60,000 gamma (0.6 Oe) at the poles to about 35,000 gamma (0.35 Oe) at the Equator. By way of contrast, a schoolboy's horseshoe magnet has a field of about 350 Oe.

The magnetic field of the earth shows considerable time-varying fluctuations, with periods ranging from hundreds of years to about a second. Diurnal variations are the most significant for magnetic surveys and have to be corrected before interpreting the results. Less easy to allow for, however, are large amplitude fluctuations in the earth's magnetic field during magnetic storms, which last for several hours and are caused by sun spot activity.

The intensity of magnetization of a magnetic mineral will normally be related to the regional field strength according to the following relation:

$$J = kH,$$

where J is the intensity of magnetization, defined to be the magnetic moment per unit volume of the rock; k is the magnetic susceptibility of the rock; and H is the intensity of the magnetic field inducing the magnetism. The intensity of magnetization may also have increments that have been acquired and retained at earlier stages in the history of the rock and may have to be taken into account in the interpretation. The magnetic susceptibility of rocks is very variable, ranging from <10 to 4 emu/cm^3 for sedimentary rocks to between 10^{-3} and 10^{-2} emu/cm^3 for iron-rich basic igneous rocks.

At any point above the earth, the measured geomagnetic field will be the sum of the regional field and the local field produced by the magnetic rocks in the vicinity. The purpose of magnetic surveys, therefore, is to measure the field strength over the area of interest. The recorded variations of the field strength will be due to changes in the earth's magnetic field and to the volume and magnetic susceptibility of the underlying rocks. These variations can be eliminated by removing the fluctuations recorded by a fixed station in the survey area. The residual values are then directly related to the rocks beneath. Magnetic surveys can be carried out on the ground or on board ship, but taking the readings from the air is far more efficient. In aeromagnetic surveys, a plane trails a magnetometer in a sonde attached to a cable and flies in a grid pattern over the survey area. The spacing of the survey lines will vary according to the nature of the survey and the budget, but the lines may be as close as 1 km with crosstie lines on a 5-km spacing. Magnetic surveys may also be carried out from satellites. Data acquired by these various methods may be used to construct a map that contours anomalies in the earth's magnetic field in gamma units (Fig. 3.51).

3.3.1.2 Interpretation

Magnetic surveys are used in the early stages of petroleum exploration. Magnetic anomaly maps show the overall geological grain of an area, with the orientation of basement highs and lows generally apparent. Faults may show up by the close spacing or abrupt changes in orientation of contours. Sometimes, magnetic maps may be used to differentiate basement (i.e., igneous and metamorphic rocks devoid of porosity) from sedimentary cover that may be prospective. However, this differentiation is only possible where there is a sharp contrast between the magnetic susceptibility of basement and cover, and where this contrast is

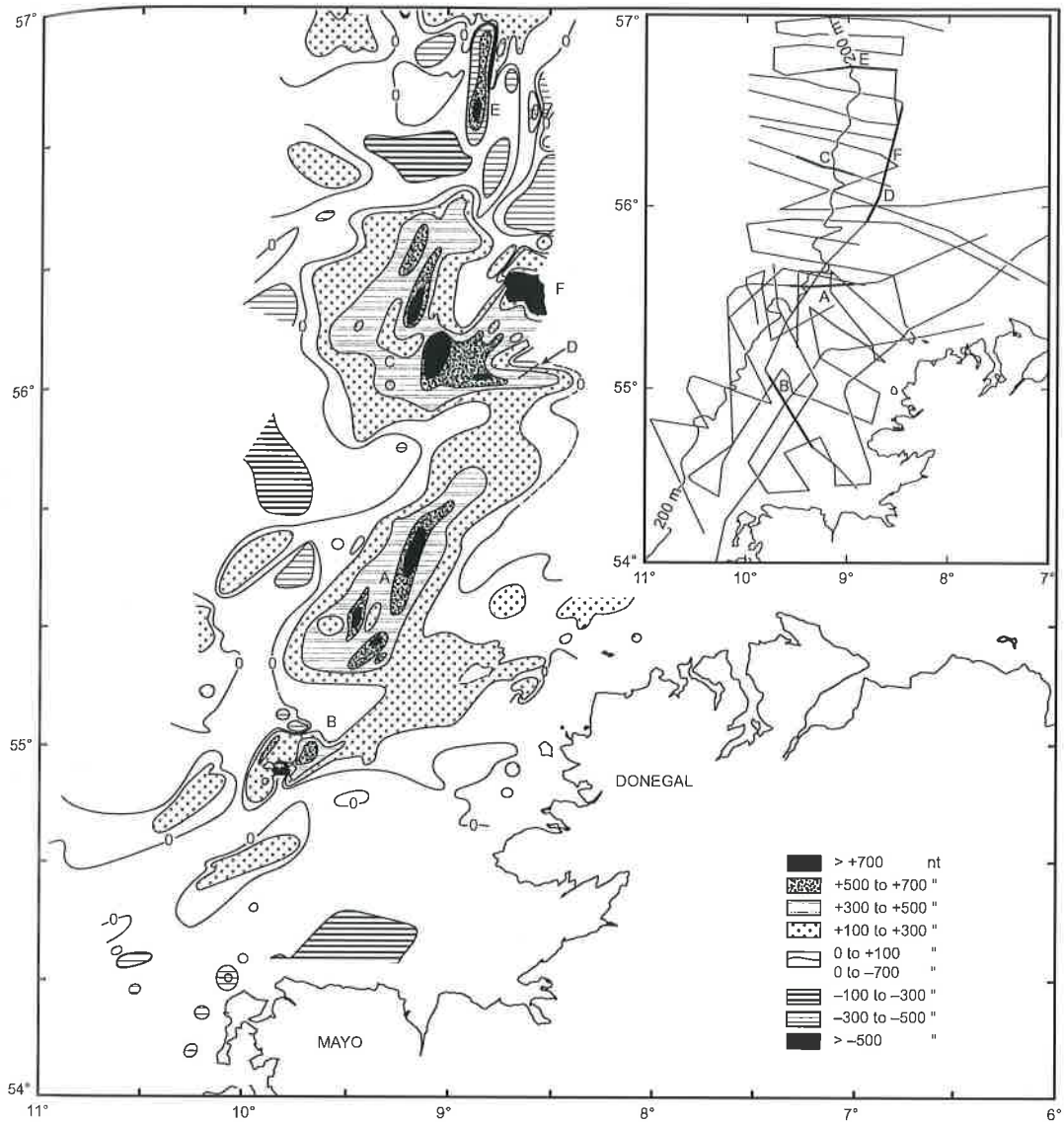


FIGURE 3.51 An example of a total magnetic intensity map of offshore northern Ireland. Location of survey lines shown in the inset map. Compare with the refined, processed version in Fig. 3.49. From Bailey *et al.* (1975).

laterally persistent. An original magnetic survey can be interpreted and presented as a depth-to-magnetic basement map (Fig. 3.52). This procedure can be done when there is some well control on the basement surface, backed by measured rock parameters, and some knowledge of the regional geology. Magnetic anomaly maps are also useful to petroleum exploration in indicating the presence of igneous plugs, intrusives, or lava flows, areas normally to be

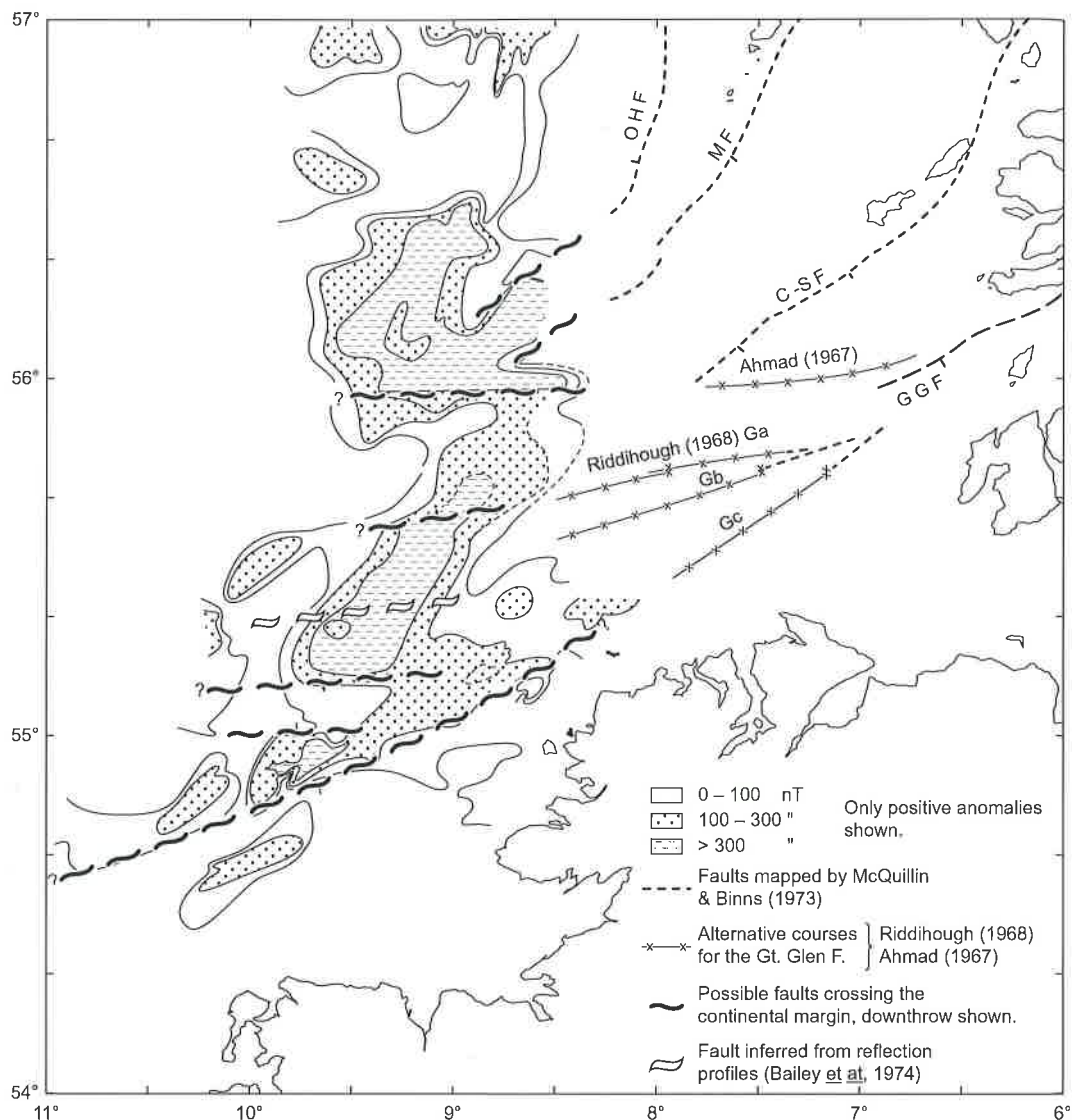


FIGURE 3.52 An interpretation of the magnetic intensity map of offshore northern Ireland shown in Fig. 3.48. From Bailey et al. (1975).

avoided in the search for hydrocarbons. Seismically delineated "reefs" have often been drilled and discovered to be igneous intrusions or volcanic plugs. A quick check of the aeromagnetic map would have shown the magnetic anomaly produced by the igneous material instantly.

In recent years, closer grid spacing and improved computer power have led to a renaissance in magnetic surveying, producing what is now described as high-resolution

aeromagnetics. Computer software programs have been devised that process the data quickly and display the results in attractive polychromatic displays (Plate 3.2). High-resolution aeromagnetics becomes still more effective when integrated with other geophysical surveying methods, such as gravity and seismic.

In conclusion, magnetic surveys are a quick and cost-effective way of defining broad-basin architecture. Although they can seldom be used to locate drillable petroleum prospects, they can sometimes differentiate genuine from phoney prospects.

3.3.2 Gravity Surveying

3.3.2.1 Methodology

According to Newton's law of gravitation,

$$F = \frac{GM_1M_2}{d^2},$$

where F is the gravitational force between two point masses, M_1 and M_2 ; d is the distance between M_1 and M_2 ; G is the universal gravitational constant, usually taken as $6.670 \times 10^{-11} \text{ m}^3/(\text{kg})(\text{s}^2)$ or 6.670×10^{-8} in centimeter–gram–second units.

According to Newton's second law of motion, the acceleration a when a point, mass M_1 , is attracted to another point, mass M_2 , may be expressed as

$$a = \frac{F}{M_1} = \frac{GM_2}{r^2}.$$

If M_2 is considered to be the mass of the earth and r its radius, then a is the gravitational acceleration on the earth's surface. Were the earth a true sphere of uniform density, then a would be a constant anywhere on the earth's surface. The value of a , however, varies from place to place across the earth. This variation is due to the effect of latitude, altitude, topography, and geology. These first three variations must be removed before the last residual can be detected.

The earth is not a true sphere, but is compressed at the poles such that the polar radius is 21 km less than the equatorial radius. Thus, the force of gravity increases with increasing latitude. Further, gravity is affected by the speed of the earth's rotation, which increases the effect of latitudinal variation.

The correction for latitude is generally calculated using the international gravity formula of 1967, which supersedes an earlier version of 1930:

$$G = 978031.8[1/(0.0053024 \sin^2 y - 0.0000058 \sin^2 2y)],$$

where y is the latitude. The acceleration due to gravity is measured in gals (from Galileo): 1 gal is an acceleration of 1 cm/s^2 . For practical purposes, the milligal (mgal), which is 1 thousandth of 1 gal, or the gravity unit (gu), which equals 0.00001 gal, is generally used.

When allowance has been made for variations in G due to latitude, the gravity value still varies from place to place. This variation occurs because the force of gravity is also affected by local variations in the altitude of the measuring station and topography. Gravity decreases with elevation, that is, distance from the center of the earth, at a rate of 0.3086 mgal/m. Thus, a free-air correction must be made to compensate for this effect. A second correction

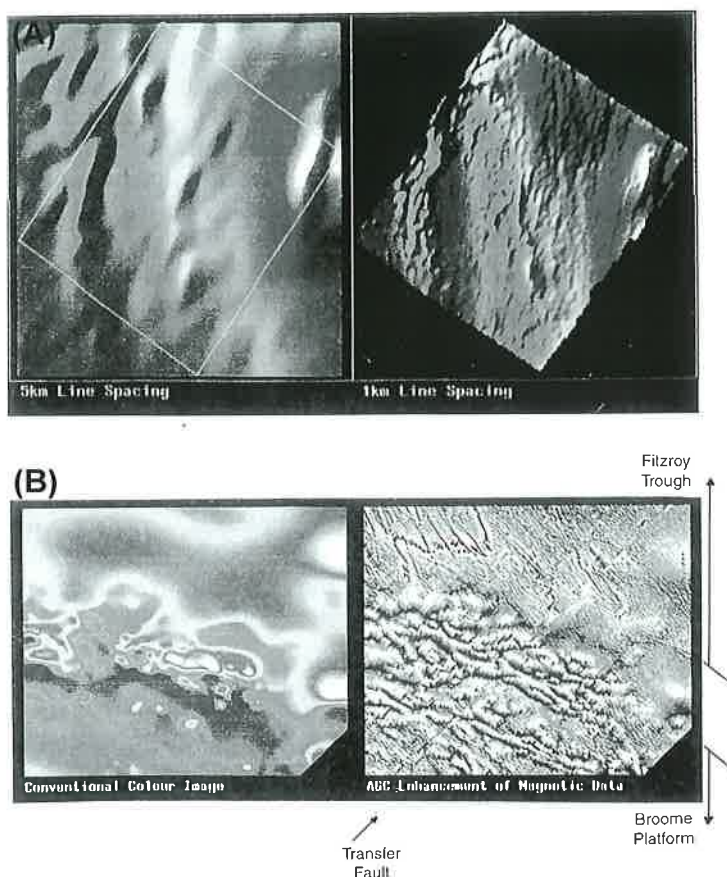


PLATE 3.2 Examples of aeromagnetic maps. Note how the increase in line spacing enhances resolution (A), and how data can be manipulated for further resolution enhancement (B) (See the color plate). *Courtesy of World Geoscience.*

must be made to compensate for the force due to the mass of rock between the survey station and a reference datum, generally taken as sea level. This difference, the Bouguer anomaly, is $0.04191 d$ mgal/m, where d is the density of the rock.

The free-air and Bouguer effects (E) can be removed simultaneously:

$$E = (0.3086 - 0.4191d)h,$$

where d is the density of rock and h is the height in meters above reference datum.

In mountainous terrain, a further correction is necessary to compensate for the gravitational pull exerted by adjacent cliffs or mountains. When the free-air, Bouguer, and terrain corrections have been made for the readings at each station in a gravity survey, they can be plotted on a map and contoured in milligals (Fig. 3.53).

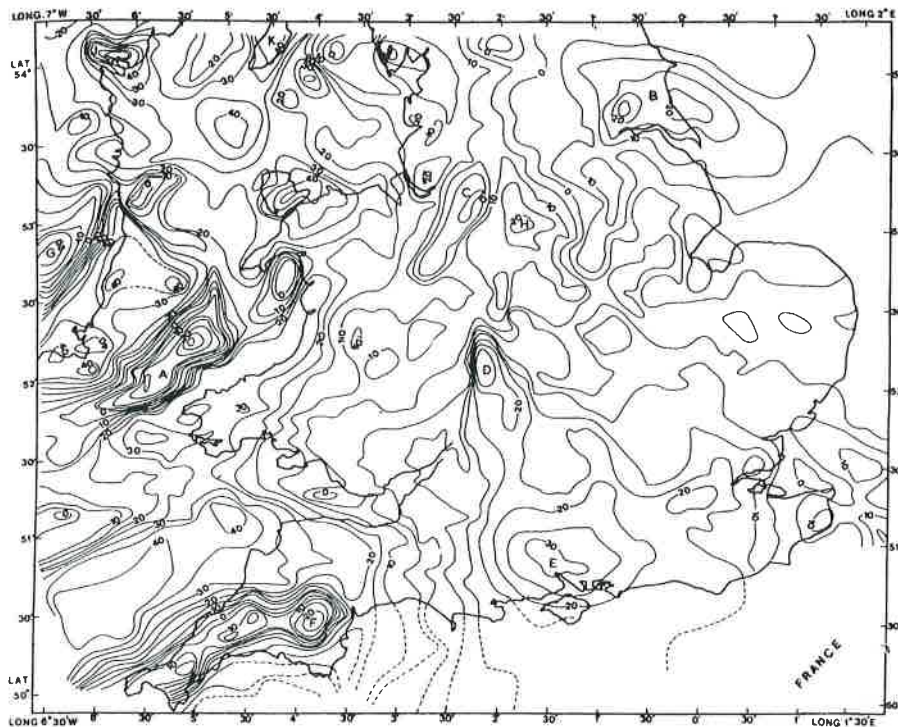


FIGURE 3.53 Bouguer anomaly map of southern Great Britain. Contours in milligals. From Maroof (1974).

Gravity surveys can be carried out on land and at sea, both on the sea floor and aboard a ship. In the latter case, corrections must be made for the motion of the ship and for the density and depth of the seawater. Airborne gravity surveys are also now feasible.

3.3.2.2 Interpretation

The interpretation of gravity maps presents many problems, the simplest of which are caused by different subsurface bodies producing the same anomaly on the surface. For example, distinguishing between a small sphere of large density and a large sphere of low density at similar depths is impossible.

The precise cause of an individual anomaly can be tested by a series of models, each model being posited on various depths, densities, or geometries for the body. Gravity maps are seldom used for such detailed interpretation, however, because seismic surveys are generally more useful for small areas. Like magnetic maps, gravity maps are more useful for showing the broad architecture of a sedimentary basin. In general, terms depocenters of low-density sediment appear as negative anomalies, and ridges of dense basement rock show up as positive anomalies (Fig. 3.54).

In some circumstances, gravity maps may indicate drillable prospects by locating salt domes and reefs. Salt is markedly less dense than most sediments and, because of this lower

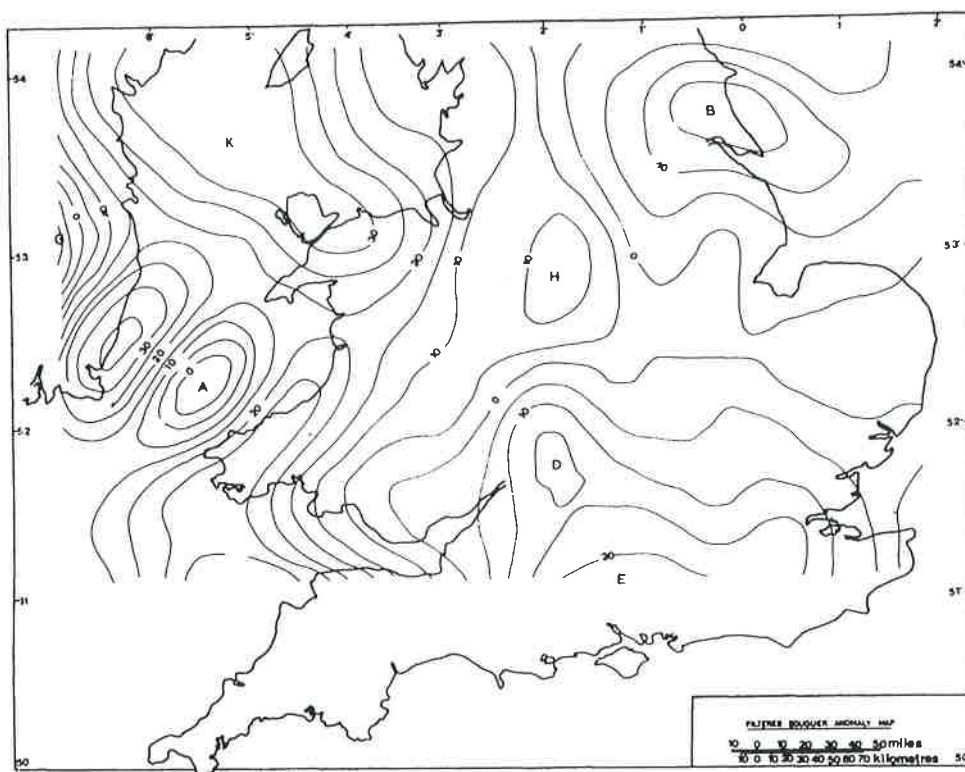


FIGURE 3.54 Filtered Bouguer anomaly map of southern Great Britain computed from the raw data shown in Fig. 3.53. From Maroof (1974).

density, often flows up in domes. These salt domes can generate hydrocarbon traps in petroliferous provinces. Because of their low-density, salt domes may often be located from gravity maps. Likewise, reefs may trap hydrocarbons, and they may also show up as gravity anomalies because of the density contrast between the reef limestone and its adjacent sediments (Ferris, 1972).

3.3.3 Magnetic and Gravity Surveys: Summary

Magnetic and gravity surveys are seldom sufficiently responsive to small-scale geological variations so that they can be used to locate individual petroleum prospects. Although gravity surveys can sometimes locate reef and salt dome traps, aeromagnetic surveys can identify igneous bodies (Fig. 3.55).

Both magnetic and gravity surveys are, however, cost-effective methods of reconnoitering large areas of the earth's surface onshore and offshore before lease acquisition. Their main use is in defining the limits and scale of sedimentary basins and the internal distribution of structural highs and lows. When used in combination, a far more accurate basement map can be prepared than when they are interpreted separately. Aeromagnetic and gravity surveys can

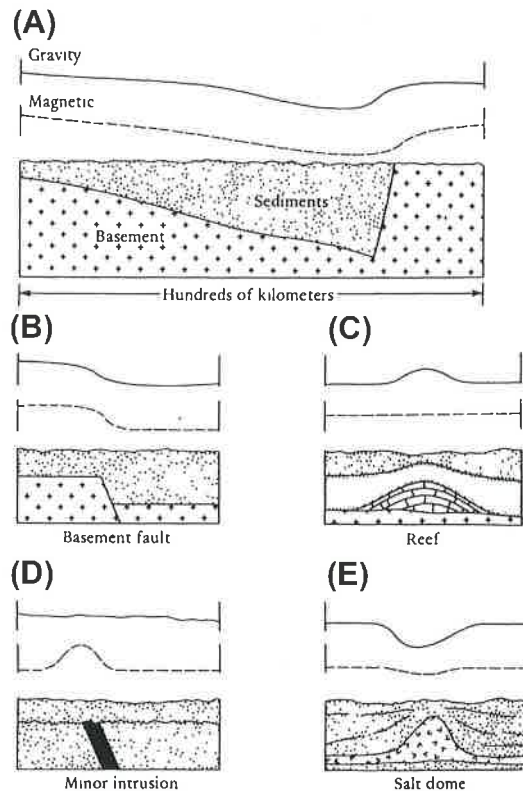


FIGURE 3.55 Gravity and magnetic responses for various geological features. (A) Regional responses across a sedimentary basin. (B)–(E) Local anomalies that may be present on a scale of a few kilometers.

be integrated with one another, or with seismic surveys. Once well control becomes available, the true depth to basin is known. Then, the surveys can be accurately calibrated and more reliable depth-to-basement maps redrawn.

Both magnetic and gravity surveys are undergoing a renaissance in 2014 for several reasons. Magnetic and gravity surveys are now being run concurrently with offshore seismic surveys. Ever-improving computing power, coupled with extremely accurate satellite navigation systems, enables integrated geophysical studies to be carried out that lead to much improved imaging of the geological structure. The sum is greater than the individual parts (George, 1993).

3.3.4 Seismic Surveying

3.3.4.1 Basic Principles

Seismic surveying is the most important of the three main types of geophysical prospecting. To understand the method, a review of the physical principles that govern the movement of acoustic or shock waves through layered media is necessary.

Consider a source of acoustic energy at a point on the earth's surface. Three types of waves emanate from the surface and travel through the adjacent layers, which have acoustic velocities and densities $v_1\rho_1$ and $v_2\rho_2$. *Surface*, or *longitudinal*, waves move along the surface. The two other types of waves termed *body waves* move radially from the energy source: *P* (push) waves impart a radial movement to the wave front; *S* (shake) waves impart a tangential movement. *P* waves move faster than *S* waves. Surface waves are of limited significance in seismic prospecting. They move along the ground at a slower velocity than do body waves. The surface disturbance is termed *ground roll* and may include Rayleigh and other vertical and horizontal modes of propagation.

Seismic surveying is largely concerned with the primary *P* waves. When a wave emanating from the surface reaches a boundary between two media that have different acoustic impedance (the product of density and velocity), some of the energy is reflected back into the upper medium. Depending on the angle of incidence, some of the energy may be refracted along the interface between the two media or may be refracted into the lower medium.

The laws of refraction and reflection that govern the transmission of light also pertain to sound waves. Thus, it is convenient to consider the movement of waves in terms of their ray paths. A ray path is a line that is perpendicular to successive wave fronts as an acoustic pulse moves outward from the source. Figure 3.56 shows the ray paths for the three types of wave just described.

The fundamental principle of seismic surveying is to initiate a seismic pulse at or near the earth's surface and record the amplitudes and travel times of waves returning to the surface after being reflected or refracted from the interface or interfaces of one or more layers of rock. Seismic surveying is more concerned with reflected ray paths than refracted ones.

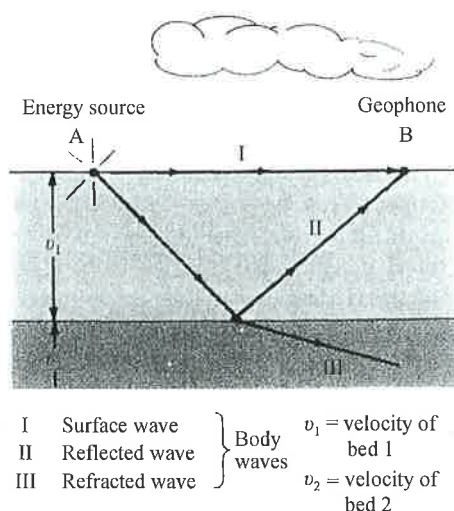


FIGURE 3.56 Cross-section illustrating various seismic wave paths.

If the average acoustic velocity of the rock is known, then it is possible to calculate the depth D to the interface:

$$D = \frac{vt}{2},$$

where v is the acoustic velocity and t is the two-way (i.e., there and back) travel time.

The acoustic velocity of a rock varies according to its elastic constants and density. As sediments compact during burial, their density (and hence their acoustic velocities) generally increases with depth. Theoretically, the velocity of a P wave can be calculated as follows:

$$v = \sqrt{\left(k + \frac{4}{3}h\right)/p},$$

where k is the bulk modulus, h is the shear modulus, and p is the density. The relationships between the velocity and density of common sedimentary rocks are shown in Fig. 3.57. The product of the velocity and density of a rock is termed the *acoustic impedance*. The ratio of the amplitudes of the reflected and incident waves is termed the *reflectivity* or *reflection coefficient*:

$$\begin{aligned} \text{Reflection coefficient} &= \frac{\text{amplitude of reflected wave}}{\text{amplitude of incident wave}} \\ &= \frac{\text{change in acoustic impedance}}{2 \times \text{mean acoustic impedance}} \\ &= \frac{P_2 v_2 - p_1 v_1}{p_2 v_2 + p_1 v_1}, \end{aligned}$$

where p_1 is the density of the upper rock; P_2 is the density of the lower rock; v_1 is the acoustic velocity of the upper rock; and v_2 is the acoustic velocity of the lower rock.

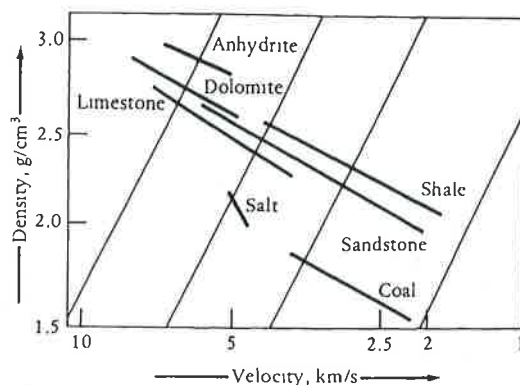


FIGURE 3.57 The velocity–density relationships for sedimentary rocks. Note how velocity increases with density for most rocks except salt. Diagonals are lines of equal acoustic impedance. After Gardner et al. (1974).

Because velocity and density generally increase with depth, the reflection coefficient is usually positive. Negative coefficients occur where there is a downward decrease in velocity and density, for example, at the top of an overpressured shale diapir. A reflection coefficient that is positive for a downgoing wave is negative for an upgoing wave and, of course, vice versa.

Velocity and density generally increase with depth for a homogenous lithology, but at the boundary between two units we can, and usually will, get a lithological contrast. Therefore, the positive and negative reflection coefficients tend to appear with approximately equal frequency (taking the case of a downgoing wave only). Seismic processing is often based on the assumption that the earth's reflection coefficient series is random, which is empirically true. This assumption would not be the case if most reflection coefficients were positive. Negative coefficients occur where there is a decrease in acoustic impedance across the reflecting interface. Reflection coefficients have a maximum range limited by +1 and -1. Values of +0.2 or -0.2 would occur for very strong reflectors. In practice, most reflection coefficients lie between -0.1 and +0.1. The boundary between a porous sand and a dense, tight limestone will have a high reflection coefficient and show up as a prominent reflecting surface. By contrast, the interface between two shale formations of similar impedance will have a negligible reflection coefficient and will reflect little energy.

It is now appropriate to see how these general principles are used in seismic surveying. Traditionally, seismic exploration involves three steps: data acquisition, data processing, and interpretation.

3.3.4.2 Data Acquisition

Seismic surveys are carried out on land and at sea in different ways. On land, the energy source may be provided by detonating explosives buried in shot holes, by dropping a heavy weight off the back of a lorry (the thumper technique is actually a rather sophisticated procedure), or by vibrating a metal plate on the ground (Vibroseis). The returning acoustic waves are recorded on geophones arranged in groups. The signals are transmitted from the geophones along cables to the recording truck. Equipment in this truck controls the firing of the energy source and records the incoming signals from the geophones on magnetic tapes.

The shot points and the receiving geophones may be arranged in many ways. Many groups of geophones are commonly on line with shot points at the end or in the middle of the geophone spread. Today, common depth point, or CDP, coverage is widely used. In this method the shot points are gradually moved along a line of geophones. In this way, up to 48 signals may be reflected at different angles for a common depth point.

In Arctic conditions, a different technique is employed. Bundles of geophones are rowed on a cable, termed a *streamer*, behind a snowmobile that contains the recording gear. The energy source is detonating cord laid on top of the snow ahead of the snowmobile. Care is taken to ensure that explosions occur before the arrival of the recording vehicle. Used carefully, this technique can acquire a large amount of information quickly. It is faster than conventional onshore seismic because it does not require jug hustlers to lay and pick up geophones (Rygg et al., 1992). In wetlands, such as the swamps of Louisiana, hovercraft are used for seismic surveys.

The basic method of acquiring seismic data offshore is much the same as that of onshore, but it is simpler, faster, and, therefore, cheaper. A seismic boat replaces a truck as the controller and recorder of the survey. This boat trails an energy source and a cable of

hydrophones, again termed a *streamer* (Fig. 3.58). It is possible for one boat to operate several energy sources, but experience has shown that, in this instance, more bangs is not necessarily the best. Streamer lengths can extend for up to 6000 m to the annoyance of fisher folk. Currently, survey vessels, such as the *Ramform Explorer*, can operate up to three energy sources whose signals are received by hydrophones on 8–12 streamers, up to 3000 m in length, with a total survey width of 800 m.

In marine surveys, dynamite is seldom used as an energy source. For shallow, high-resolution surveys, including sparker and transducer surveys, high-frequency waves are used. In sparker surveys, an electric spark is generated between electrodes in a sonde towed behind the boat. Every time a spark is generated, it implodes after a few milliseconds. This implosion creates shock waves, which pass through the sea down into the strata. Transducers alternately transmit and receive sound waves. These high-resolution techniques generally only penetrate up to 1.0-s two-way time. They are useful for shallow geological surveys (e.g., to aid production platform and pipeline construction) and can sometimes indicate shallow gas accumulations and gas seepages (Fig. 3.59).

For deep exploration, the air gun is a widely used energy source. In this method, a bubble of compressed air is discharged into the sea; usually a number of energy pulses are triggered simultaneously from several air guns. The air guns can emit energy sufficient to generate signals at between 5- and 6-s two-way travel time. Depending on interval velocities, these signals may penetrate to >5 km.

The reflected signals are recorded by hydrophones on a cable towed behind the ship. The cable runs several meters below sea level and may be up to 6 km in length. As with land surveys, the CDP method is employed, and many recorders may be used. The reflected signals are transmitted electronically from groups of hydrophones along the cable to the recording unit on the survey ship. Other vital equipment on the ship includes a fathometer and position fixing devices. The accurate location of shot points at sea is obviously far more difficult than it is on land. Formerly this was done either by radio positioning, or by getting fixes on two or more navigation beacon transmitters from the shore. Nowadays, satellite navigation systems enable pinpoint accuracy to be achieved.

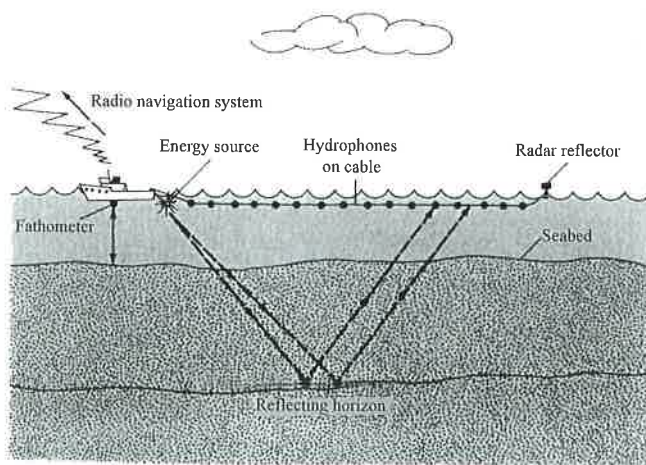


FIGURE 3.58 Sketch showing how seismic data are acquired at sea.

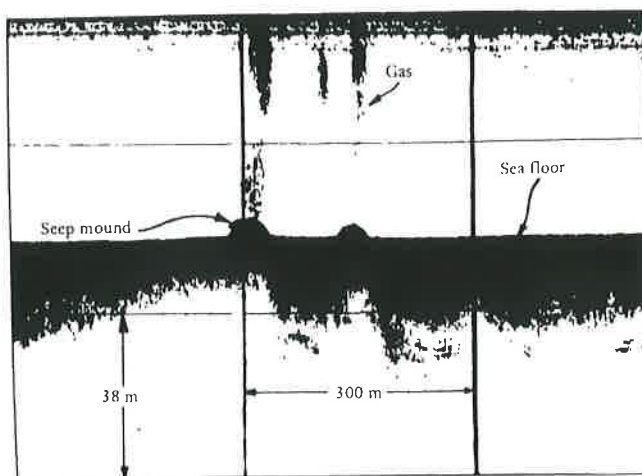


FIGURE 3.59 Transducer record showing gas seeps and mounds in offshore Texas. From H. C. Sieck and G. W. Self, namely Fig. 4, p. 358 in *AAPG Memoir Series No. 26*, © 1977; Analysis of High-Resolution Seismic Data.

3.3.4.3 Data Processing

Once seismic data have been acquired, they must be processed into a format suitable for geological interpretation. This process involves the statistical manipulation of vast numbers of data using mathematical techniques far beyond the comprehension of geologists. Seismic data processors include mathematicians, physicists, electronic engineers, and computer programmers.

Consider the signals of three receivers arranged in a straight line from a shot point. The times taken for a wave to be reflected from a particular layer will appear as a wiggle on the receiver trace. The arrival times will increase with the distance of receivers from the shot point. Thus, a time–distance graph may be constructed as shown in Fig. 3.60. When time squared is plotted against distance squared, a straight line can be drawn through the arrival times of the signal. Velocity of the wave through the medium is

$$\text{Velocity} = \sqrt{\frac{1}{\text{slope of the line}}}$$

The depth from the surface can then be calculated as follows:

$$\text{Depth} = \text{velocity} \times \text{time (one way)}.$$

But since the travel time recorded is two way (there and back),

$$\text{Depth} = \text{velocity} \times \frac{\text{time (one way)}}{2}.$$

With common depth point shooting (discussed previously), reflections from the same subsurface points are recorded with a number of different combinations of surface source and receiver positions, and the signals are combined, or stacked. Thus, wave–time graphs can

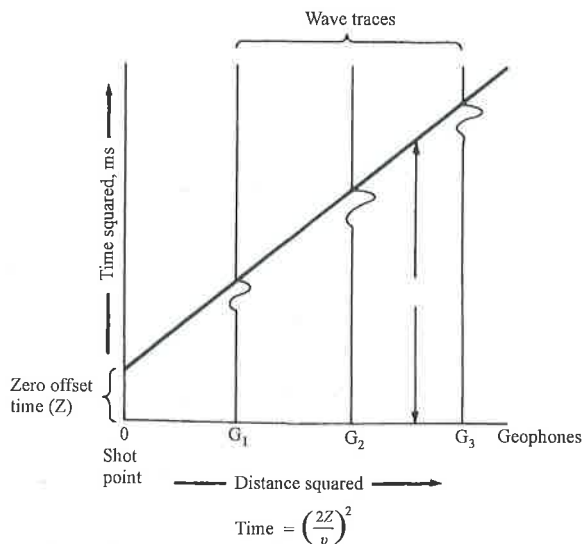


FIGURE 3.60 Travel-time graph showing how velocity may be calculated by measuring the length of time taken for a wave to travel from a shot point to geophones placed known distances away.

be displayed in a continuous seismic section, and a single seismic reflecting horizon can be traced across it. Wave traces are displayed in several ways. They may be shown as a straight-forward graph or wiggle trace. Reflectors show up better on a variable area display in which deviations in one direction (positive or negative polarity) are shown in black (Fig. 3.61). This type of display is the basis for the conventional seismic section used today.

Four main steps are involved in the processing of raw seismic data before the production of the final seismic section:

1. Conversion of field magnetic tape data into a state suitable for processing
2. Analysis of data to select optimum processing parameters (e.g., weathering correction and seawater velocity)
3. Processing to remove multiple reflectors and enhance primary reflectors
4. Conversion of data from digital to analog form and printout on a graphic display (i.e., final seismic line)

During processing, many unwanted effects must be filtered out. All seismic records contain both the genuine signal from the rocks and the background "noise" due to many extraneous events, which may range from a microseism to a passing bus. The signal-to-noise ratio is a measure of the quality of a particular survey. Noise should obviously be filtered out. The frequency and amplitude of the signal are the result of many variables, including the type of energy source used and its resultant wave amplitude, frequency, and shape, and the parameters of the various rocks passed through. Deconvolution is the reverse filtering that counteracts the effects of earlier undesirable filters (Fig. 3.62).

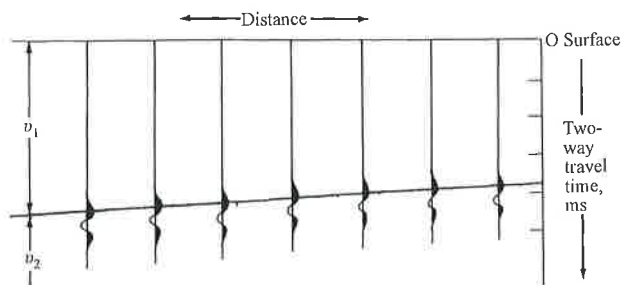


FIGURE 3.61 Distance-time graph showing common depth point wave traces for a series of geophones recording a signal reflected from the boundary between rocks with velocities v_1 and v_2 . The wave traces are shaded in the variable area format. This is the basis for the conventional seismic section.

One particularly important aspect of processing is wave migration. When beds dip steeply, the wave returns from the reflector from a point not immediately beneath the surface location midway between the shot point and each individual geophone but from a point up-dip from this position (Fig. 3.63). During processing, the data must be migrated to correct this effect. This migration causes several important modifications in the resultant seismic section. Anticlines become sharper, synclines gentler, and faults more conspicuous.

The preceding discussion briefly covered some aspects of seismic processing. The main point to note is that digitally recorded seismic data can be processed time and time again, either by using new, improved computer programs or by tuning the signal to bring out aspects of particular geological significance.

3.3.4.4 3D Seismic Surveying

In the old days, seismic surveys were shot on loose grids several kilometers wide. Increased computer power, however, has made it possible to handle ever larger amounts of data faster and cheaper. If seismic surveys are shot on a grid of only 50 m or so, then a three-dimensional matrix of data is acquired that enables seismic displays to be produced, not only along the survey lines shot but also in any other orientation. This is called 3D seismic, naturally. The 3D seismic is very appealing because horizontal displays, or time slices, can be produced (Plate 3.3). Not only can these reveal structural features, such as faults and salt domes, but also stratigraphic ones, such as reefs and channels (Brown, 1991, 2004).

3.3.5 Interpretation of Seismic Data

3.3.5.1 First Principles

Geologists looking at seismic lines and maps inevitably tend to see them as representations of rock and forget that they do, in fact, represent travel time.

According to Tucker and Yorston (1973), three main groups of pitfalls in seismic interpretation are to be avoided:

1. Pitfalls due to processing
2. Pitfalls due to local velocity anomalies
3. Pitfalls due to rapid changes in geometry

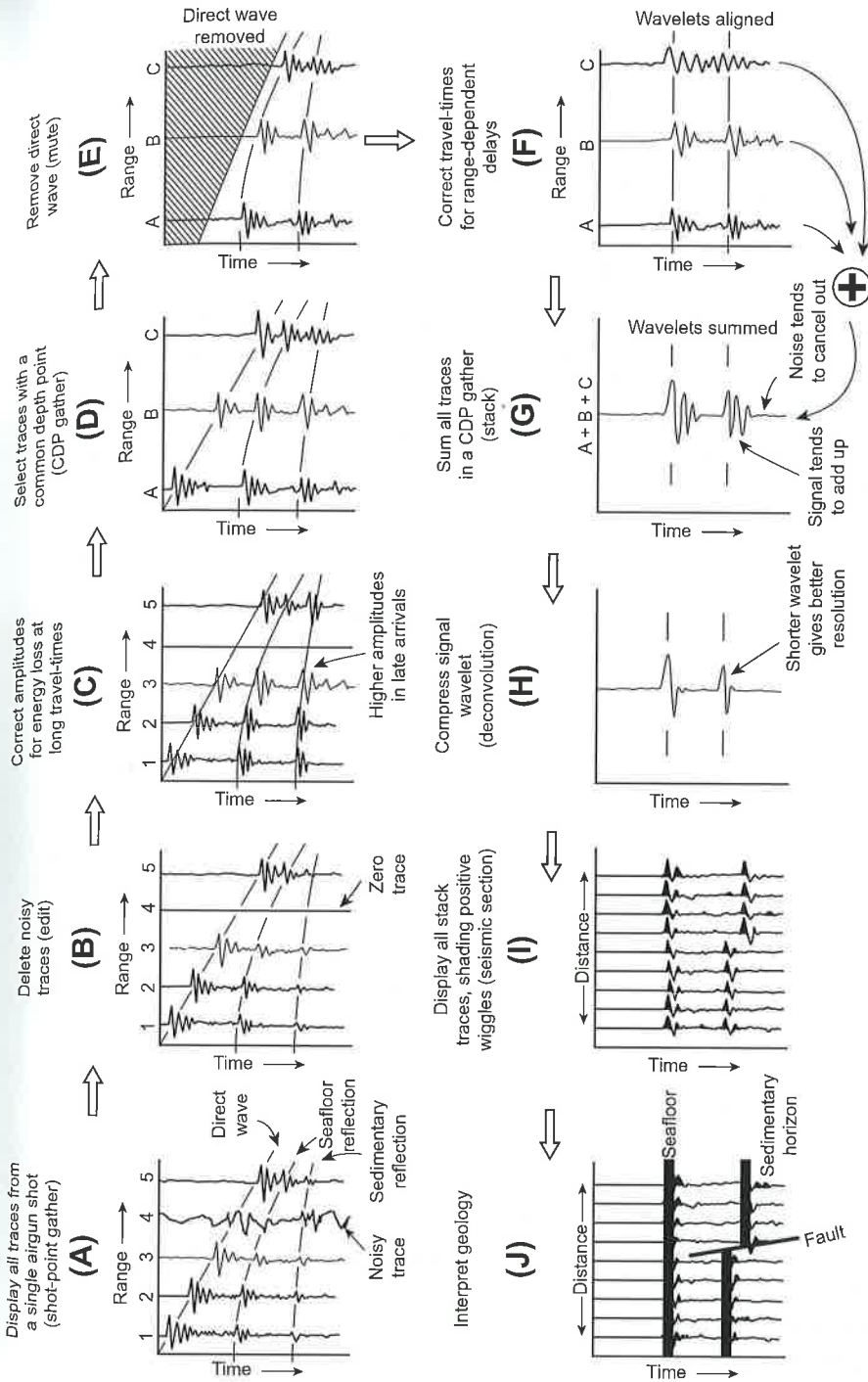


FIGURE 3.62 Simplified seismic processing sequence. The traces illustrated in part (A) result from a single shot, and were recorded by a single receiver. The direct wave (refracted wave) appears at a time proportional to the receiver distance from the shot, while the reflections lie on a hyperbolic travel-time curve. Any bad or noisy traces are deleted (B). The seismic amplitudes recorded decrease with increasing travel-time because the reflectors are further away, so the weaker amplitudes are boosted (C). Then, the traces are resorted so that all traces with an identical source-receiver midpoint are gathered together in (D), one trace each from (A), (B), and (C). The direct wave is removed (the shaded area in (E)), and then each trace is separately corrected for the time delay appropriate to its source-receiver offset (F). This is known as the *normal move-out*, or NMO, correction. The wavelets from each reflection are now lined up, as if each trace had been recorded with coincident source and receiver (i.e., without source-receiver offset delays), and all the traces in the gather can be summed up (stacked) to give the single trace in (G) with a higher signal-to-noise ratio. If the wavelet is rather reverberatory, or lengthy, then its resolution is poor, but can be shortened by a digital filtering technique called *deconvolution* (H). Finally, all the traces are displayed as a seismic section and may then be interpreted. From Klempner and Paddy (1992). © Cambridge University Press, reprinted with permission.

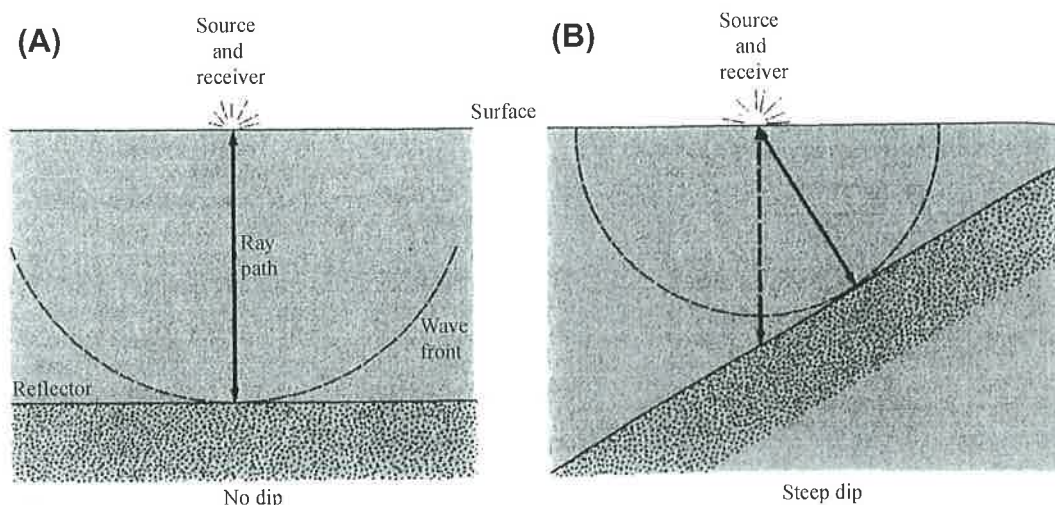


FIGURE 3.63 Diagrams showing the problem encountered when beds dip steeply. (A) The strata are horizontal. Thus, the wave fronts first strike reflectors vertically beneath the energy source and receiver. (B) In contrast, these beds are steeply dipping. Thus, signals return to the receiver from points up-dip earlier, and thus apparently shallower, than from the true vertical depth (TVD). This phenomenon may be corrected by using a mathematical process termed *migration*.

Pitfalls due to processing are the most difficult for geologists to avoid. One of the most common processing pitfalls is multiple reflections—a series of parallel reflections caused by the reverberation between two reflectors. The most prevalent variety is the seabed multiple, which, as its name states, is caused by reverberation between the sea surface and the sea floor (Fig. 3.64(A)). Harder to detect are multiples caused by events within the sediments themselves. These events generally occur where there is a formation with high reflection coefficients above and below. Multiples can be removed by deconvolution and filtering during processing.

Rapid local variations in formation velocity cause many pitfalls. Two of the best-known examples of these variations are produced by salt domes and reefs. Evaporites have faster travel times than do most other sediments. Thus, the presalt reflector may appear on the seismic section as an apparent anticline, when it is, in fact, a velocity pull-up (Fig. 3.64(B)). A number of salt domes were drilled in the quest for such fictitious anticlines until the method of undershooting them was developed as an effective aid to mapping presalt structure. This was first developed for the sub-Zechstein Rotliegende gas play of the North Sea (Krey and Marschall, 1975). The discovery of a major subsalt petroleum play in the Gulf of Mexico in recent years has led to further improvements in the methods of acquiring and processing subsalt seismic data (see George, 1996; Ratcliff, 1993; respectively).

Other velocity pitfalls are associated with carbonate *build-ups* or *reefs*. Porous reefs may be acoustically slower than the surrounding sediments. This may engender a *velocity pull-down* beneath the reef. Thus, the seismic survey may not only identify a drillable prospect but also indicate that it has porosity. The Intisar, formerly Idris, reefs of Libya are celebrated examples

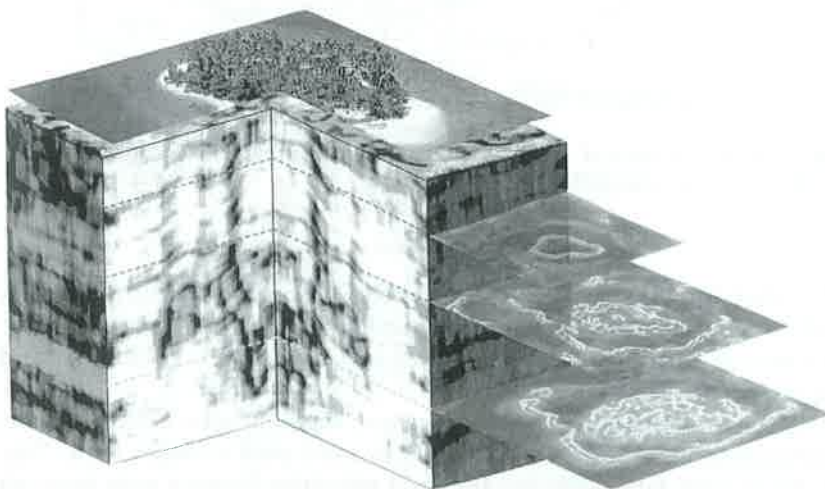
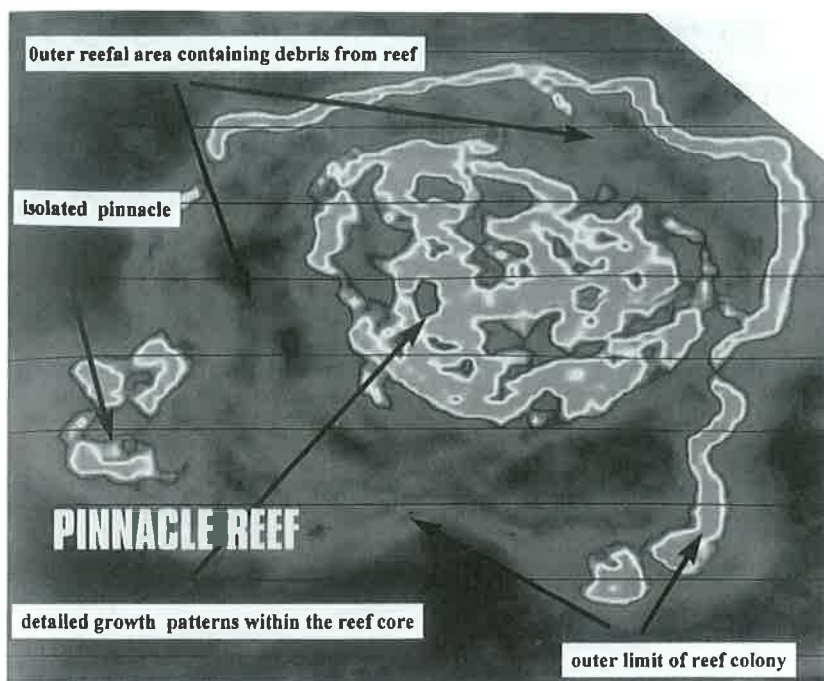


PLATE 3.3 A limestone reef imaged by 3D seismic, with accompanying geophantasmogram. Note how not only horizontal time slices, but any orientation may be selected for display from 3D seismic data. These images were produced by Coherence Cube technology (See the color plate). *Courtesy of GMG Europe Ltd.*

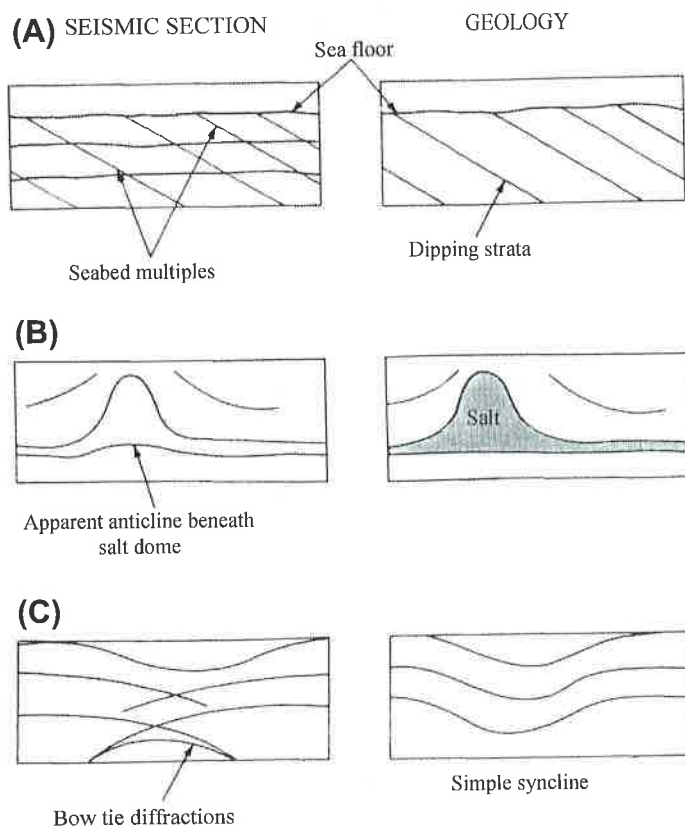


FIGURE 3.64 Examples of each of the three main pitfalls in seismic interpretation: (A) processing pitfall, (B) velocity pitfall, and (C) geometry pitfall.

of this phenomenon (Brady et al., 1980). Conversely low-porosity, tightly cemented reefs may be acoustically much faster than the enclosing sediments. The seismic section may show the apparent existence of an anticline beneath the reef. Such prospects should not be drilled since the reef is tight and the anticline nonexistent.

A further velocity pitfall may be encountered on a regional scale. Seismically mapped units sometimes apparently thin with increasing depth from shelf to basin floor. The formations may, in fact, have a constant thickness, but their velocities increase with increasing compaction. Thus, the time taken for seismic waves to cross each interval decreases basinward.

The third group of pitfalls in seismic interpretation occurs because of the departure of rock geometry from a simple layered model. This pitfall may cause reflectors to dip steeply, as in tight folds and diapirs, or even to terminate adjacent to faults and diapirs. The former can give rise to distorted reflections, such as the "bow tie" effect produced by synclines (Fig. 3.61(C)). Reflector terminations cause diffractions, which crosscut the reflectors on the seismic line.

When the seismic data have been correctly interpreted, avoiding the pitfalls just discussed, the various reflecting horizons can be mapped. In the old days, reflectors were mapped from hard copy prints using brightly colored pencils. Today, computers loaded with appropriate software packages enable reflectors to be mapped on monitors with a mouse. Since seismic lines are generally shot on an intersecting grid, reflectors can be tied from line to line. For large surveys, reflectors can be traced from line to line and tied in a loop to check that the reflector has been correctly picked and that the interpreter has not jumped a reflecting horizon, colloquially referred to as a *leg*, in the process.

The times for the reflectors for each shot point may then be tabulated. Contour maps may then be drawn for each horizon (red, blue, green, etc.). Note that these are time maps, not depth maps. They show isochrons (lines of equal two-way travel time), not structure contours. Figure 3.65 shows, in a very simple way, how reflectors may be picked on two intersecting seismic lines and used to construct isochron maps.

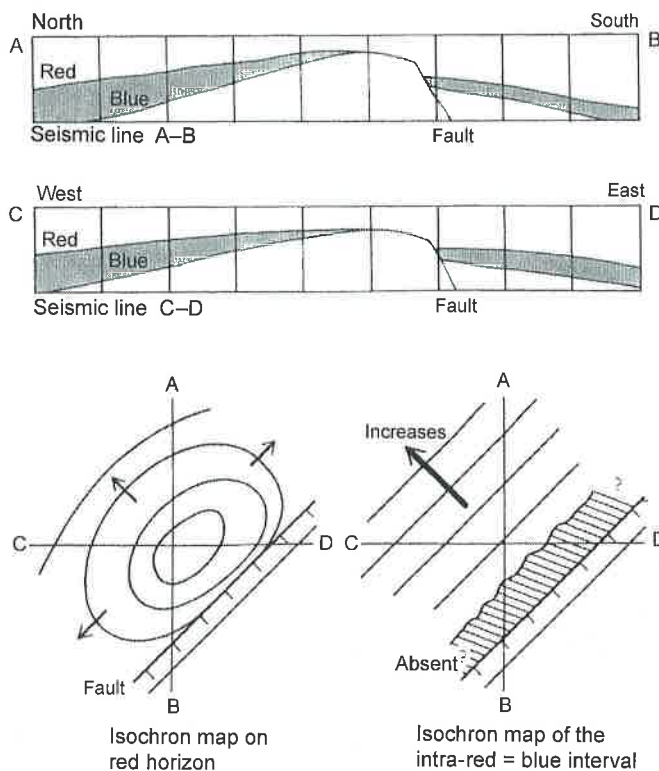


FIGURE 3.65 Simplified sketch showing how reflectors may be picked on two intersecting seismic lines (A-B) and (C-D), and used to construct isochron maps of an individual reflector (bottom left), or the interval between two reflectors (bottom right).

3.3.5.2 Geological Application

Seismic surveying is an essential part of the whole cycle of petroleum exploration and production. It is applied in six main ways: regional mapping, prospect mapping, reservoir delineation, seismic modeling, direct hydrocarbon detection, and the monitoring of petroleum production. Pacht et al. (1993) have proposed a threefold hierarchy of seismic interpretation, in terms of the parameter that is analyzed, and the interpretations that may be drawn from the analysis; these are seismic sequence analysis, seismic facies analysis, and seismic attribute analysis (Table 3.2).

3.3.5.2.1 SEISMIC SEQUENCE ANALYSIS

In the early stages of reconnaissance mapping of a new sedimentary basin, a broad seismic grid will be shot and integrated with magnetic and gravity surveys, as discussed earlier. The advent of high-quality offshore seismic data in the 1960s and 1970s led to a whole new way of looking at sedimentary sequences, termed *sequence stratigraphy* (Vail et al., 1977). This is now a very important and integral part of petroleum exploration. It is briefly expounded here. For further details, see Neidell and Poggiali (1977), Payton (1977), Vail et al. (1991), Van Wagoner et al. (1988), Weimer (1992), Neal et al. (1993), and Steel et al. (1995). Seismic sequence stratigraphic analysis is carried out in a logical series of steps (Fig. 3.66).

The fundamental unit of sequence stratigraphy is the depositional sequence. This is defined as "a stratigraphic unit composed of a relatively conformable succession of genetically related strata bounded at its top and base by unconformities or their correlative conformities" (Vail et al., 1977, p. 53). The boundaries of depositional sequences may be associated with onlap, toplap, downlap, or truncation (Fig. 3.63, step 1). Two types of sequence boundaries are recognized:

Type 1: Sequence boundary—subaerial only and characterized by channeling

Type 2: Sequence boundary—subaerial and submarine

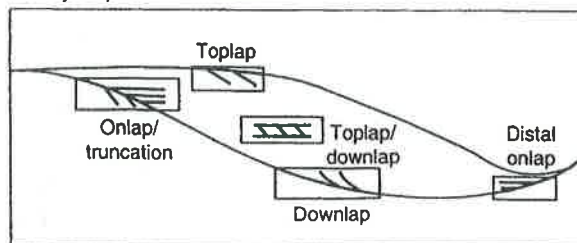
The age and lithology of a seismic sequence may not be directly apparent without well control, but they are, nonetheless, mappable units (Figs 3.67 and 3.68). Vail and colleagues argue for the existence of a worldwide stratigraphy in which a regular sequence of characteristic seismic sequences can be related to global fluctuations in sea level (Fig. 3.69). These are old ideas that few experienced geologists would dispute. The broad global changes of sea

TABLE 3.2 Summary of the Parameters Examined and Interpretations Made for the Threefold Hierarchy of Seismic Data Analysis

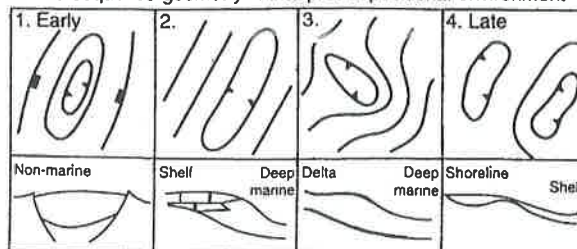
Seismic analysis	Parameter studied	Interpretation
Sequence analysis	Sequences defined and mapped; nature of sequence contacts recorded	Sequences correlated with global sea level changes (if possible) and time calibrated
Facies analysis	Description of sequence-defined seismic character	Identification of vertical mounded and pelagic sediments
Attribute analysis	Analysis of wave shape, amplitude, polarity, and continuity	Identification of vertical changes in rock properties, including grain-size profiles and direct hydrocarbon indicators (DHIs)

STEP 1.

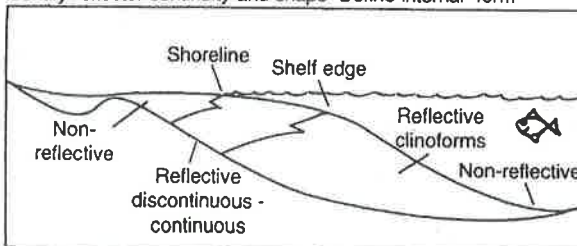
Identify sequence boundaries

**STEP 2.**

Define sequence geometry & interpret depositional environment

**STEP 3.**

Identify reflector continuity and shape Define internal form

**STEP 4.**

Identify reflector shapes and amplitude

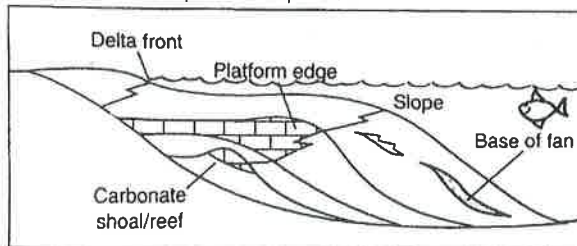


FIGURE 3.66 Illustration to show the terminology of reflection conjunctions (step I) and the subsequent steps to be taken in seismic sequence analysis. Based on Hubbard et al. (1985).

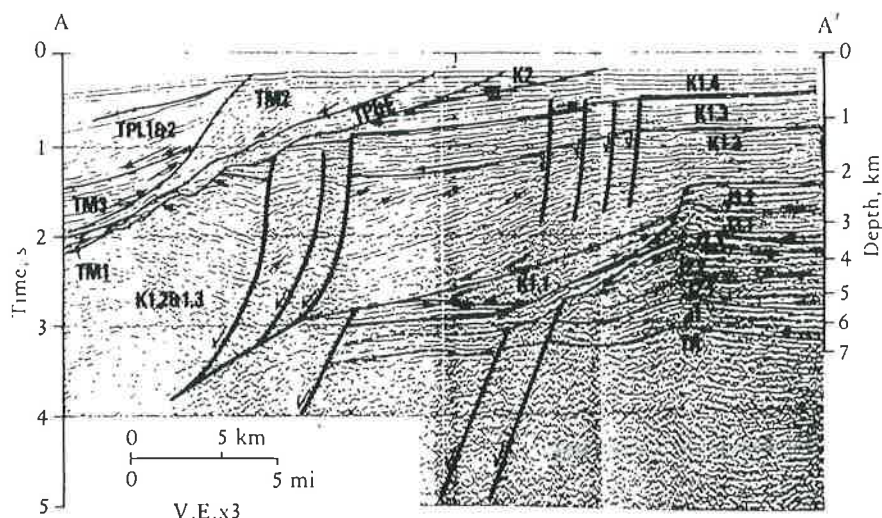


FIGURE 3.67 Seismic line of offshore west Africa showing sequence boundaries, ranging in age from Tertiary (T) to Cretaceous (K), Jurassic (J), and Triassic (Tr). For location, see Fig. 6.66. From R. M. Mitchum, Jr., and P. R. Vail, namely Fig. 1, p. 137 in *AAPG Memoir Series No. 26*, © 1977; *Seismic Stratigraphy and Global Changes of Sea Level*, Part 7.

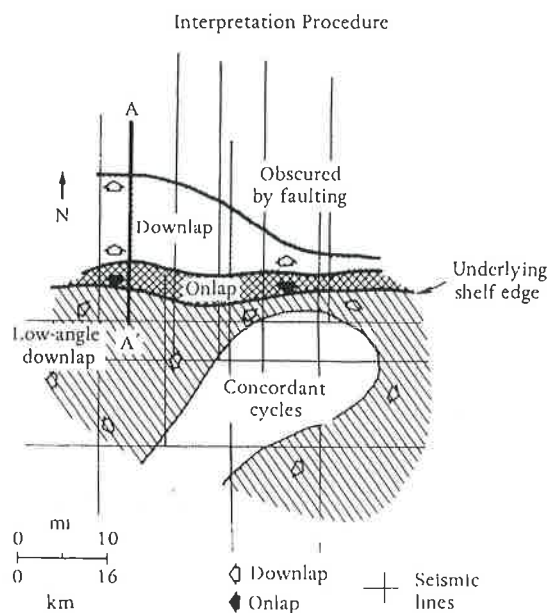


FIGURE 3.68 Map showing reflection patterns at lower surface of Lower Cretaceous sequence, offshore west Africa. A—A' is the seismic line shown in Fig. 3.64. From R. M. Mitchum, Jr., and P. R. Vail, namely, Fig. 1, p. 137 in *AAPG Memoir Series No. 26*, © 1977, *Seismic Stratigraphy and Global Changes of Sea Level*, Part 7.

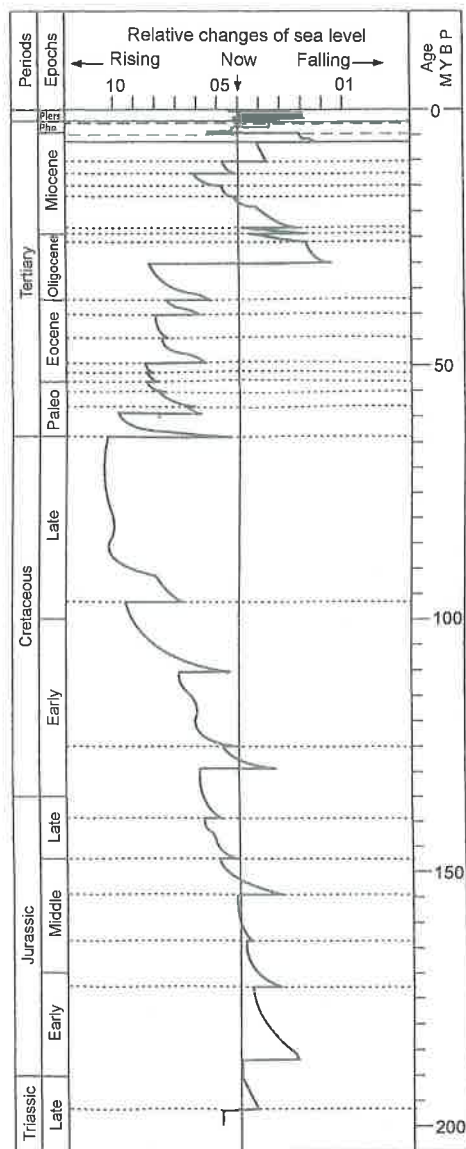


FIGURE 3.69 A global sea level curve for the last 200 million years, or so. For sources, see Vail *et al.* (1977) and Haq *et al.* (1988).

level were remarked by Stille (1924), and the remarkable uniformity of sedimentary facies by Ager (1973, 1993). Vail and colleagues further argue, however, that seismic surveys can now be used to erect a sequence stratigraphy with a hierarchy of cycles on four different scales. These cycles can be correlated universally because seismic reflectors are chronostratigraphic

horizons. It is in this fine detail that many geologists become nervous about seismically defined sequence stratigraphy.

The first-order cycles are believed to have spans of at least 50 my, and to be driven by the break-up of continental plates. The second-order cycles, with spans of 3–50 my are also believed to be driven by plate movements. The third-order cycles are deemed to be on a scale of 500,000 years to 3 my and are believed to be driven by long-term tectonic processes, and shorter-term climatic changes. These are the sequence cycles. It is argued that each third-order sequence cycle begins with a drop in sea level. The land becomes emergent and incised by channels, to ultimately become a type 1 unconformity. At the same time, sand is transported off the emergent shelf and deposited in submarine fans on the basin floor (Plate 3.4(A)). When sea level has reached its nadir sedimentation slows down to deposit a condensed sequence. As sea level begins to rise, submarine fan deposition encroaches up

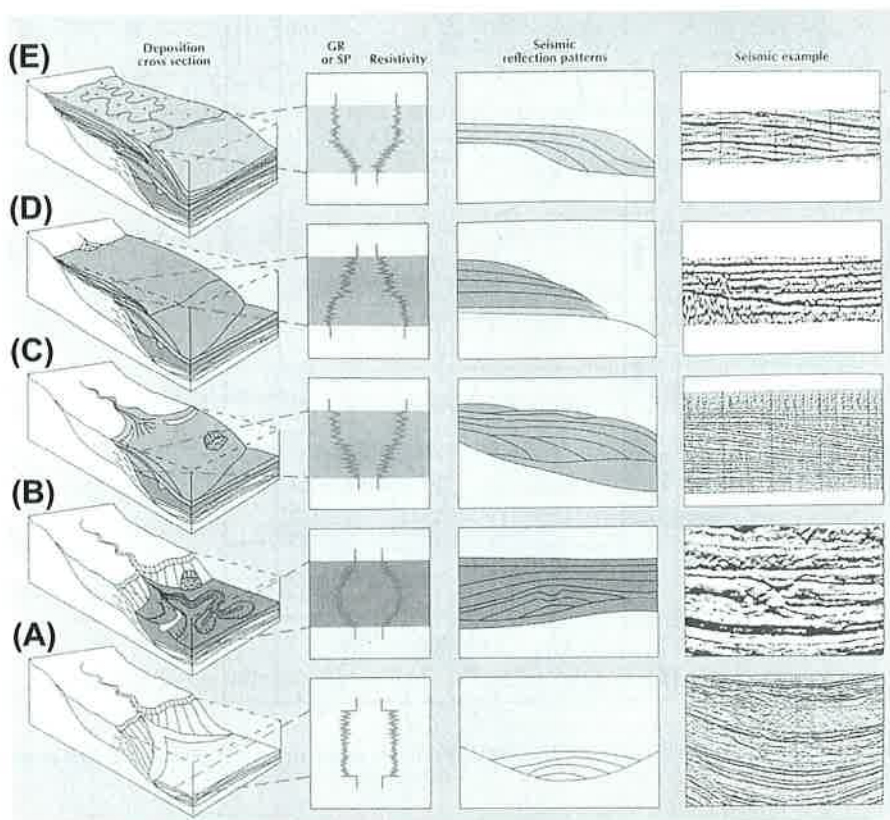


PLATE 3.4 Geophantomograms, log motifs, seismic reflection patterns, and examples to illustrate a third-order stratigraphic sequence. A = Low stand sea level. B = Rising sea level floods the continental slope. C = Sea floods shelf providing accommodation space for prograding deltas. D = Rapid flooding of the shelf permits deposition of a transgressive systems tract. E = Slow rising sea level permits the slow basinward progradation of thin high stand system tracts (See the color plate). From Neal et al. (1993); courtesy of Schlumberger oil field review.

onto the slope (Plate 3.4(B)). A continually rising sea level favors the progradation of clastic wedges out into the basin (Plate 3.4(C)). As sea level continues to rise, it will brim over the continental shelf edge rapidly flooding the continental shelf itself. The horizon at which the shelf is drowned is termed the *main* or *maximum flooding surface*. This may then be succeeded by a thin sequence of reworked shallow marine sands (Plate 3.4(D)). As the rate of rise of sea level begins to slow down toward the end of the cycle a second episode of progradation may occur, but this is thinner than the earlier basinfill phase, and is restricted to the shelf itself (Plate 3.4(E)). Note how each stage in the cycle has a characteristic wireline log motif, and a characteristic seismic reflection pattern. The sediments deposited during the cycle are termed *systems tracts*, qualified by transgressive, high stand, shelf edge, and low stand, as appropriate (Fig. 3.70).

The fourth-order cycles, termed *parasequences*, are believed to span 10,000–50,000 years and are supposed to be driven by climatic cyclic events. Parasequences are what used to be termed *genetic increments*, and *parasequence sets* are what used to be called genetic sequences (Busch, 1971).

While many geologists have happily pedaled the cycles of sequence stratigraphy, some have viewed the underlying tenets of sequence stratigraphy critically. The two main areas of concern are the recognition of the hierarchy of cycles, and the dogma that seismic reflectors are of chronostratigraphic significance. These are now considered in turn.

Geologists are trained in pattern recognition. We see what we want to see. This was demonstrated in a rotten trick played on geologists by Zeller (1964). He generated an artificial sequence of coal measure sediments using random numbers taken from the last digit of the telephone directory of Lawrence, Kansas (i.e., 1 = coal, 2 = sandstone, 3 = siltstone, etc.). He gave these artificially generated stratigraphic sequences to geologists, who had no difficulty

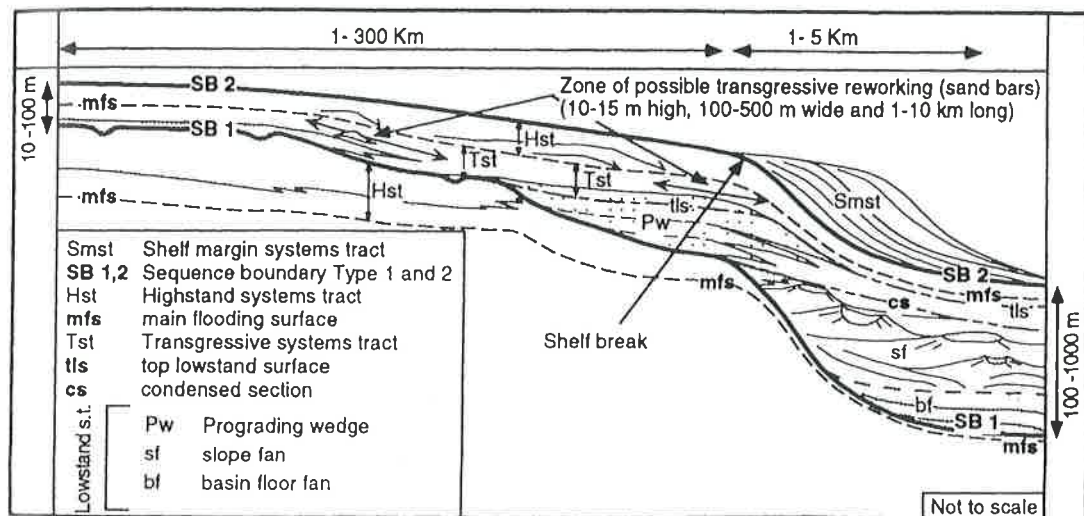


FIGURE 3.70 Sketch to show the terminology of sequence boundaries and systems tracts for a third-order cycle on a clastic continental shelf. Reprinted from *Marine and Petroleum Geology*, Vol. 13, Raymond and Stempl, pp. 41–60. Copyright 1996, with kind permission from Elsevier Science Ltd.

in correlating coal measure cyclothem from section to section. More recently, and more relevant to the present discussion, both Embry (1995) and Miall (1992) have queried the validity of the events on the Exxon sea level curve, arguing that they are too subjective, and based on circular arguments. Miall (1992) generated several artificial sequences, with random events. He then tested the statistical significance of these with the event boundaries on the Exxon sea level chart. A minimum of 77% successful correlations of random events with the Exxon curve was achieved (Fig. 3.71).

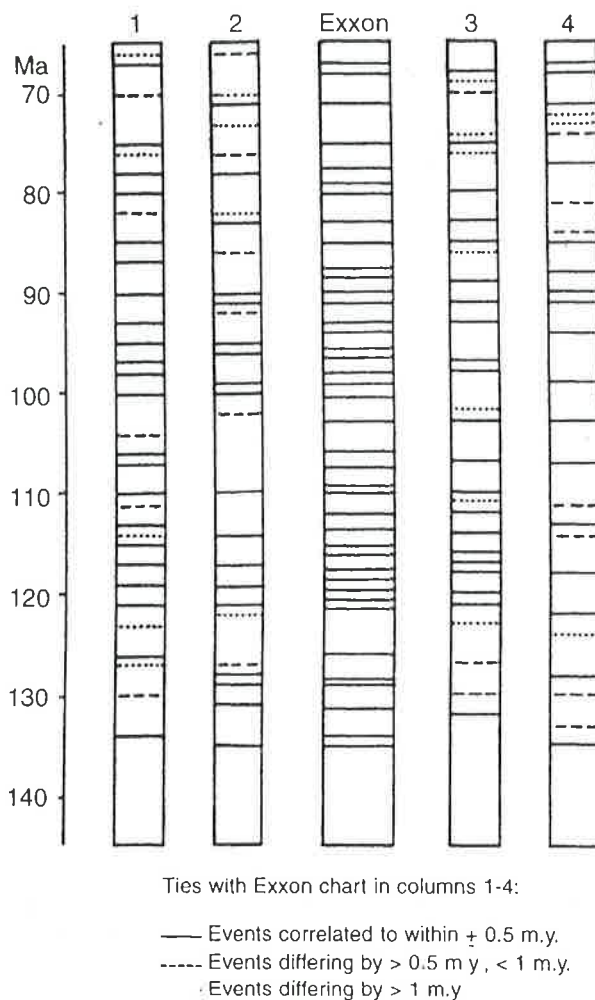


FIGURE 3.71 (Middle column) Event boundaries in the Exxon global cycle chart (Haq et al., 1988). Adjacent columns show events generated randomly. In the worst example in column 3, a 77% successful correlation of random events was achieved for intervals ± 1 my from an Exxon event. *From Geology. Miall. Reproduced with permission of the publisher, The Geological Society of America, Boulder, Colorado USA. Copyright © 1992.*

Some geologists find it hard to accept that sea level changes are global and therefore can be correlated. Geologists know that the advances or retreat of a coastline may be caused by three processes. It may indeed be related to eustatic changes caused by fluctuations of the earth's temperature. It may also, however, be due to local tectonic processes, or even to changes in the rate and locus of deposition. Neotectonics shows how rapid and localized tectonic uplift and subsidence may be on a geological timescale. Today, for instance, the eastern coast of England is subject to severe coastal erosion and encroachment by the North Sea, while the western coasts show evidence of uplift. Synchronous advance and retreat of coastlines within a few kilometers of one another have been described from Spitzbergen (Martinsen, 1995), from New Zealand (Leckie, 1994), and are particularly well known in Louisiana. The modern Mississippi delta advances into the Gulf of Mexico, depositing a low stand systems tract. At the same time, however, only a few kilometers to the north, the sea advances across the subsiding older St Bernard delta, depositing a transgressive systems tract (Coleman and Gagliano, 1964). In some published sequence stratigraphic studies, which shall remain nameless, authors admit that the third-order cycles are not ubiquitous, and that they are identified in different wells by different criteria and are below the limits of seismic resolution.

The second tenet of sequence stratigraphy that makes geologists uneasy is that seismic reflectors are time horizons. Hubbard et al. (1985) have demonstrated that this is false when horizons are traced on a basinwide scale. On a smaller scale, Thorne (1992) and Tipper (1993) have demonstrated that this is erroneous on a smaller scale. Essentially, seismic waves are reflected from tangible changes in lithology, not from intangible time lines. The diachronous nature of formation boundaries is too well known to geologists for it is to be believed that lithological boundaries are time horizons. Tipper modeled the seismic responses for sand-shale bodies of different thickness, and for different seismic wavelength. He showed how seismic reflectors may clearly crosscut time lines (Fig. 3.72).

Thus, some of the fundamental assumptions of sequence stratigraphy are open to question, notably the tetracyclic nature of global transgressions and regressions, and the synchronicity of seismic reflectors. Nonetheless, sequence stratigraphy has made geologists question some of the fundamental assumptions about sedimentary processes. The main contribution of sequence stratigraphy to petroleum exploration has been that it has drawn attention to the fact that high stands of the sea favor the deposition of source rocks, for reasons discussed in Chapter 5. Conversely, a drop in sea level leads to the transport of sand off the continental shelf, to be deposited as submarine fans on adjacent basin floors (Shanmugam and Moiola, 1988).

3.3.5.2.2 SEISMIC FACIES ANALYSIS

Seismic facies analysis is the description and geological interpretation of seismic reflectors between sequence boundaries (Sieck and Self, 1977). It includes the analysis of parameters such as the configuration, continuity, amplitude, phase, frequency, and interval velocity. These variables give an indication of the lithology and sedimentary environment of the facies. Large-scale sedimentary features that may be recognized by the configuration of seismic reflectors include prograding deltas, carbonate shelf margins, and submarine fans (Sheriff, 1976). There are also characteristic features of reflectors that correlate with geophysical log motifs in the different systems tracts. Plate 3.4 illustrates examples of some of these.

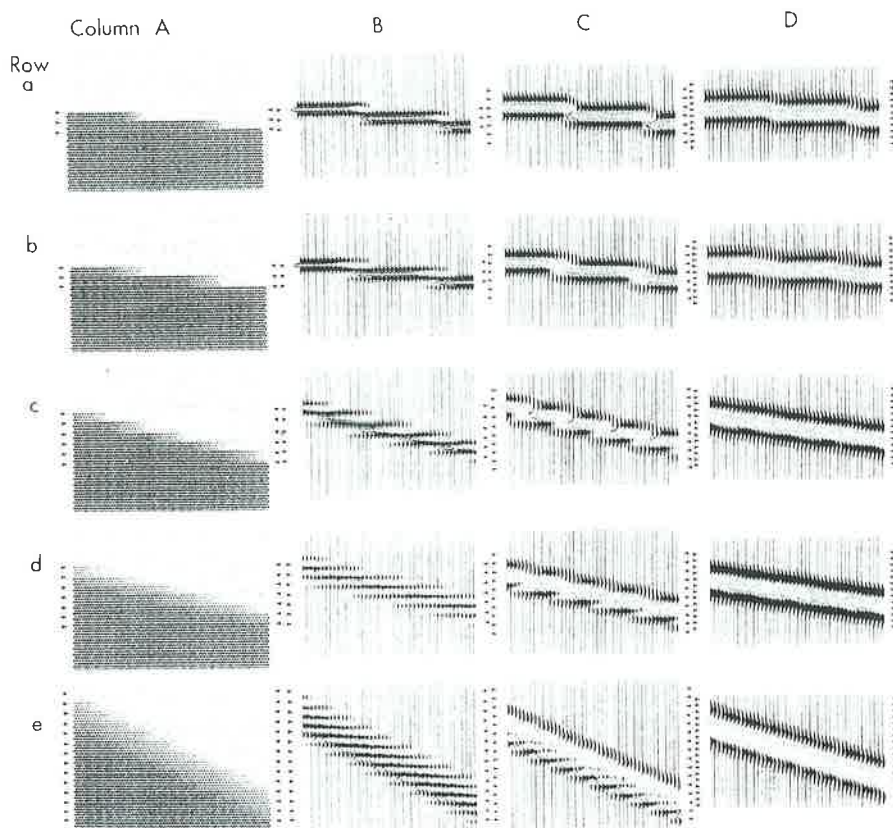


FIGURE 3.72 Synthetic seismic models for different sand:shale bodies using different wavelengths. Column A shows different shale (light tone) on sand (dark tone) transitions for uniform sedimentation, so that horizontal surfaces are synchronous. Rows a–e are for lithological transition belt width to lateral shift ratios of 1:4, 1:2, 1:1, 2:1, and 4:1, respectively. Columns B–D model these situations for different wavelength/bed thickness ratios of 1/2, 1/4, and 1/8, respectively. They have been depth converted, so that vertical intervals equal time. This study clearly shows instances where seismic reflections of lithological boundaries cross horizontal time surfaces. Some instances image the episodic nature of the lithological shift, but this is by no means ubiquitous. *From Tipper (1993). © Cambridge University Press, reprinted with permission.*

3.3.5.2.3 SEISMIC ATTRIBUTE ANALYSIS

The third and final stage of the hierarchy of seismic interpretation is seismic attribute analysis (Taner and Sheriff, 1977). This is concerned with study of wave shape, polarity, continuity, dip, frequency, phase, and amplitude. Seismic attribute analysis provides information related to structure, stratigraphy, and reservoir properties. Such analysis may give an indication of the thickness and of the nature of the upper and lower contacts of a sand bed. Comparison of observed seismic waves with synthetic traces computed from a geological model may give some insight into the depositional environment of the sand, and hence help to predict its geometry and internal reservoir characteristics (Fig. 3.73). Because of the advances

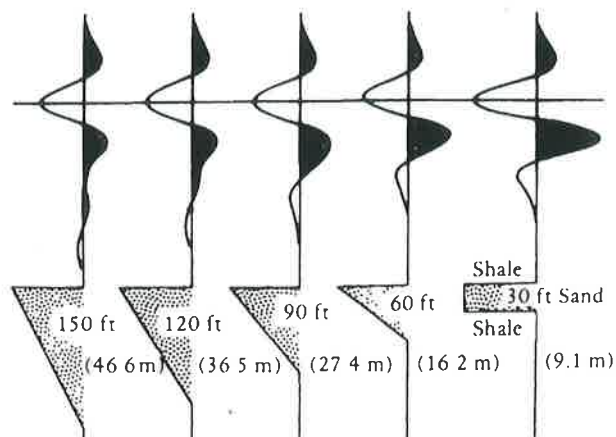


FIGURE 3.73 Seismic responses for different types of sand-shale sequences. These signals may give some indication of the depositional environment of a sand body. Those signals to the left suggest progradational deposition. The right-hand example is more typical of some channels. From N. S. Neidell and E. Poggiagliomi, namely Fig. 17, p. 404 in AAPG Memoir Series No. 26, © 1977; Stratigraphic Modeling and Interpretation—Geophysical Principles and Techniques.

made in 3D seismic methods, illustrated earlier, this type of application is of less use than heretofore.

The extraction of seismic attributes, such as amplitude, dip, curvature, and azimuth can produce remarkable 3D images of rock formations (e.g., Rijks and Jauffred, 1991). Refer again to Plate 3.3.

The simplest attribute is seismic amplitude generally reported as maximum (positive or negative) amplitude along a horizon picked. Amplitude in many cases corresponds directly to the porosity or saturation of the formation picked (oil/water vs gas).

Time/horizon attributes include coherence, dip, azimuth, and curvature. Coherence measures trace-to-trace similarity of the seismic waveform within a small analysis window. It is used to image faults, channels, and other discontinuous events. Dip and azimuth measure the direction of trace offset for maximum similarity. Curvature is a measure of how bent a surface is at a particular point and is closely related to the second derivative of a curve defining a surface.

Frequency attributes commonly separate seismic events based on their frequency content. The application of this attribute is called spectral decomposition. This attribute can be used to help determine bed thickness, presence of hydrocarbons, and fracture zones.

One application of attribute analysis that is particularly important; however, is in the direct recognition of hydrocarbons. Sometimes a single reflector cross cuts many parallel dipping reflectors. This is termed a *flat spot* (Backus and Chen, 1975). Flat spots are commonly discovered to be reflectors generated from petroleum/water contacts. Normally, they are produced by gas/water contacts, rather than by oil/water contacts, because of the greater impedance of the former. Figure 3.74 illustrates a celebrated flat spot produced by the gas/liquid contact of the Frigg field in the North Sea.

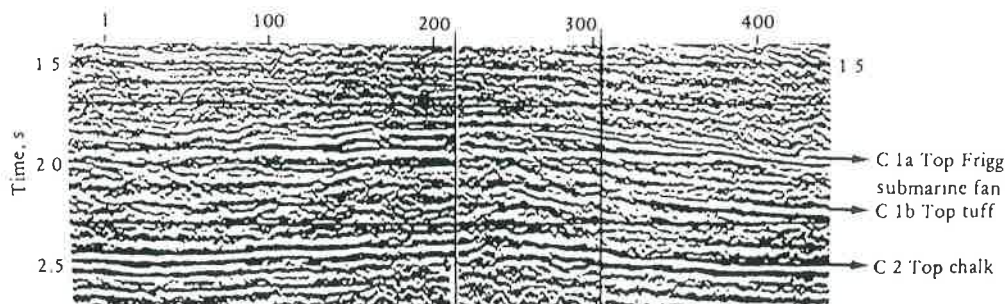


FIGURE 3.74 Seismic line through the Frigg field of the northern North Sea showing a famous example of a flat spot, a particular type of direct hydrocarbon indicator (DHI). The reservoir is a submarine fan, whose arched paleotopography is clearly visible. Within the fan, a flat reflector marks the gas: water contact. From Héritier et al. (1979). Reprinted with permission.

Occasionally, however, structures exhibiting flat spots fail to reveal the presence of hydrocarbons. A possible explanation for these disappointments is that these are “ghosts” of old fluid contacts in traps that have leaked. As discussed in Chapter 6, petroleum inhibits cementation, but cementation of a reservoir commonly continues in the water zone beneath a hydrocarbon accumulation. Thus, if the petroleum leaks out of a trap, there may be a sufficient velocity contrast at the old fluid contact between cemented and uncemented sand to generate a reflecting horizon.

A flat spot is normally the result of a rapid increase in velocity caused by a seismic wave crossing from acoustically slow gas-saturated sand to faster water-saturated sand. Given the conventional display, whereby a downward increase in velocity generates a strong deflection of the seismic trace to the right, a flat spot appears as a black high amplitude reflector termed a *bright spot*. By contrast, the reflecting horizon over the crest of a gas sand may show a reversal of polarity, as the wave passes from faster to slower rock, the reverse of the normal situation (Fig. 3.75).

Thus, they calculate out as

$$A = \frac{(3,200 \times 2.15) - (2,300 \times 2.2)}{(3,200 \times 2.15) + (2,300 \times 2.2)} = +0.152,$$

$$B = \frac{(1,900 \times 2.1) - (2,300 \times 2.2)}{(1,900 \times 2.1) + (2,300 \times 2.2)} = -0.118,$$

$$C = \frac{(3,200 \times 2.15) - (1,900 \times 2.1)}{(3,200 \times 2.15) + (1,900 \times 2.1)}$$

The reverse of a bright spot is termed a *dim spot*. This is where a positive reflector locally reverses polarity. This might be seen, for example, over the crest of a limestone reef, and could be interpreted as indicating that the limestone becomes acoustically slower due to increased porosity, over the crest of the reef. This would obviously be an important indicator of improved reservoir characteristics due to solution or fracture-generated porosity.

One particular technique of verifying whether a bright spot is really a gas anomaly has been the analysis of the amplitude variation with offset (colloquially referred to as AVO

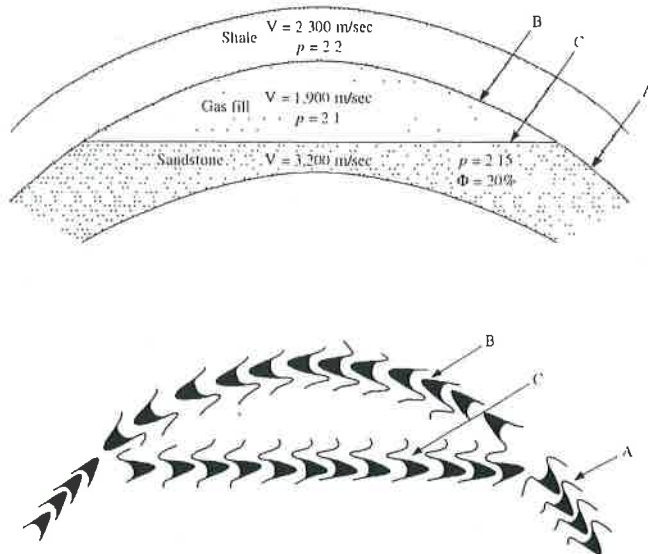


FIGURE 3.75 Illustration demonstrating the theory behind the formation of flat spots, and the reversal of polarity over a gas-saturated sand (After Stone, 1977). A = reflection coefficient of shale on water-saturated sand, B = reflection coefficient of shale on gas-saturated sand, and C = reflection coefficient of gas-saturated sand on water-saturated sand. The reflection coefficient, described earlier in the text is $p_2v_2 - p_1v/p_1v_1 + p_2v_2$.

analysis). AVO analysis is a particular type of attribute analysis that measures variations in the Poisson ratio of different rock formations (D'Angelo, 1994). It consists of examining the amplitude of a reflection at increasing source–receiver distances. Gas sands commonly have a low Poisson ratio (0.1–0.2) compared with other lithologies such as shale (0.3–0.35). A large difference between the Poisson ratio of gas sands and shales produces a dramatic anomalous pattern of amplitudes versus offset (Fig. 3.76). These AVO sections are also referred to as *lithostratigraphic sections* (Hilterman and Sherwood, 1996).

Modern 3D seismic and inversion algorithms can yield information concerning rock strength parameters such as Young's modulus and Poisson's ratio. Principal stresses, vertical, maximum horizontal, and minimum horizontal, can also be analyzed.

Shale reservoir characterization is also the focus of 3D seismic interpretation. Thickness, fracture permeability, brittleness, organic richness, pore pressure, and more can be determined from seismic data (Chopra et al., 2014). Thickness can be determined by seismic stratigraphic interpretation and conversion from time data to depth. Fracture permeability can be determined from seismic discontinuity attributes (coherence and curvature). Fractures are correlated to areas of high strain as measured by coherence and curvature on poststack seismic data. Brittleness is exhibited by areas of high Young's modulus and low Poisson's ratio. Organic richness can be determined with the use of simultaneous inversion. Variations in Young's modulus and Poisson's ratio are expected due to variations in lithology, porosity, fluid content, and cementation. The density attribute helps with total organic carbon (TOC) characterization. Low densities imply high TOC.

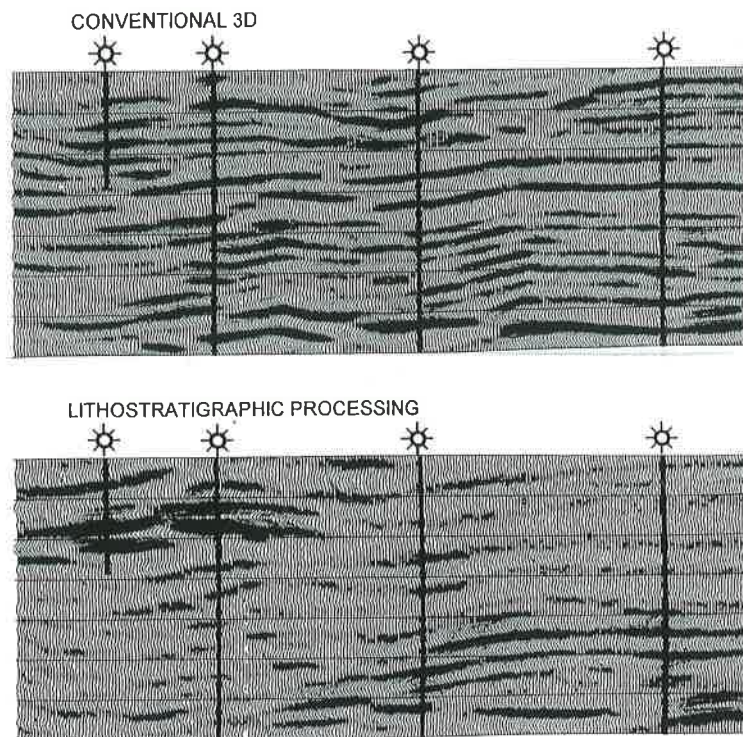


FIGURE 3.76 Comparison of conventional 3D and amplitude versus offset attribute lithostratigraphic processing. The latter highlights gas sands in the shallower parts of the two left-hand wells, and in the lower part of the two right-hand wells. Courtesy of F. Hiltebert and Geophysical Development Corporation.

3.4 BOREHOLE GEOPHYSICS AND 4D SEISMIC

The early part of this chapter discussed the one-dimensional imaging of the subsurface using boreholes and geophysical well logs. The last section described the two- and three-dimensional imaging of the subsurface using seismic surveying. This section integrates geophysical logs with seismic surveys in what is now generally referred to as *borehole geophysics*. The integration of these two technologies opens up the feasibility of imaging petroleum in four dimensions, the fourth dimension being time.

3.4.1 The Vertical Seismic Profile

Earlier, it was shown how the sonic log could be used to calibrate seismic reflectors with the rock boundaries penetrated by a borehole. This is the starting point for an evolutionary sequence of techniques termed *vertical seismic profiles* (colloquially VSPs).

For more than half a century, it has been standard practice to place receivers at strategic depths in a borehole, and to record the time taken for sound to travel from an energy source

at the surface. These velocity check shots are more reliable than counting the pips on a sonic log. In VSPs, the downhole geophones are more closely spaced than for the earlier check shots. Indeed the recovered data are sufficiently abundant that a simulated seismic section of the strata adjacent to the borehole can be generated (Fitch, 1987).

The simplest instance of this technique is the zero-offset VSP in which there is a single energy source at the surface located immediately adjacent to the borehole (Fig. 3.77). Over the years, however, this has been superseded by a spectrum of improvements (Christie et al., 1995). These include the offset VSP, in which the energy source is removed some distance from the well. For theoretical reasons, this will provide a maximum distance of coverage of half the offset distance. Next comes the walkaway VSP in which there is a series of surface energy sources. These can be arranged in a straight line away from the borehole, or may be arranged in radial patterns like the spokes of an umbrella. Walkaway VSPs can thus produce a 3D image of the strata adjacent to the borehole that can be calibrated with conventional 2D and 3D surveys. Further, not only can they image geology away from the side of the borehole but they can also image geology below the bottom of the borehole. Walkaway VSPs make it possible to image geological discontinuities, such as faults, the margins of salt domes and reefs. When run over deviated wells these surveys are referred to as walk-above VSPs.

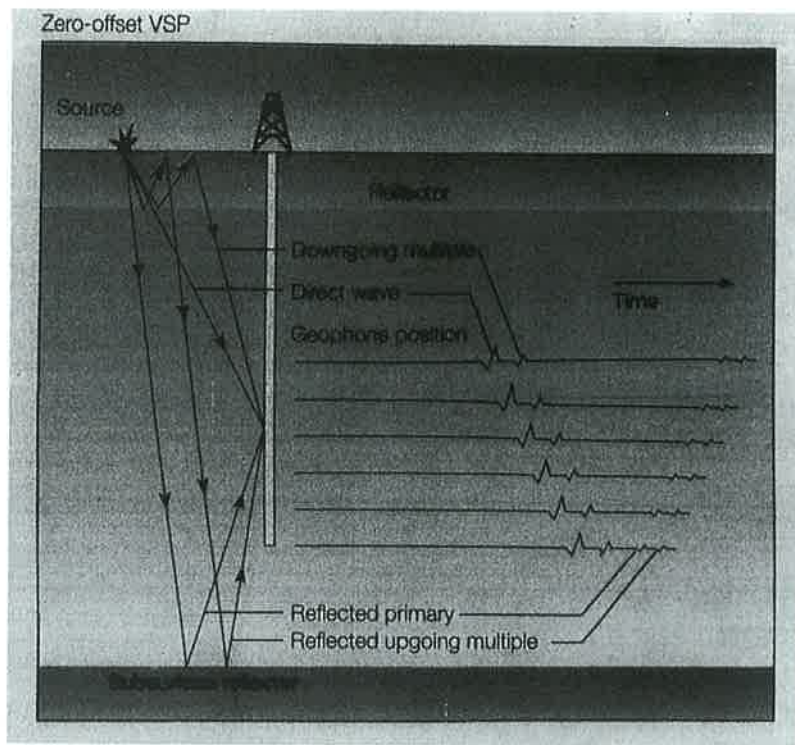


FIGURE 3.77 Illustration of the arrangement for a zero-offset vertical seismic profile (VSP). Courtesy of Schlumberger oil field review.

Specialized variants of the walkaway VSP have been developed for imaging salt domes, for measuring shear waves, and for listening to drilling noise (Fig. 3.78).

Traditionally, VSP surveys were run after a well was drilled. Now, however, they are run during the actual drilling of a borehole. Because VSP surveys record data adjacent to and below a borehole, it is possible to recalibrate continually estimates of the depth to geological horizons ahead of the drill bit (Borland et al., 1996). Data can be acquired by using a conventional energy source to generate a signal and also by using the noise generated by the drill bit, a technique termed the reverse VSP. The latter produces a continuous signal, and is of course cheaper than a conventional VSP. This technique has important implications, not only for predicting the depth to petroleum reservoirs but also more importantly for the depth of potentially perilous intervals of formation overpressure (Fig. 3.79). Thus, the acronym LWD is joined by seismic while drilling.

3.4.2 4D Seismic

Now, to add the fourth dimension, time, it is possible to shoot both 3D seismic and VSP surveys at regular intervals during the lifetime of a producing field. In fields where petroleum/water contacts may be imaged it thus becomes possible to produce what is, in effect, a time lapse film recording the movement of fluids during the life of a field (Archer et al., 1993). This is extremely useful for the reservoir engineers, because they cannot only monitor the movement of petroleum within the reservoir but also the movement of fluids that may have been injected into the field as part of an enhanced recovery scheme (as described in Chapter 6). Figure 3.80 illustrates the theory, showing computer-generated seismic sections before and after simulated fluid production, and the difference in signal extracted from the "before" and "after" surveys. Figure 3.81 illustrates a VSP shot for a well in the Frigg field some years after it was discovered and production commenced. Plate 3.5 shows VSPs over a field shot some 18 months apart. These last two examples both clearly demonstrate the upward migration of the gas/liquid contact. 3D examples of time lapse 4D surveys have been published by Anderson et al. (1996).

Once an offshore field has been discovered, it is now becoming common practice to permanently position geophones on the seabed. Then, seismic surveys are shot before production begins and throughout the life of the field. Thus, a preproduction image of the fluid boundaries of the field may be mapped, and deviations from the primary model can be used to

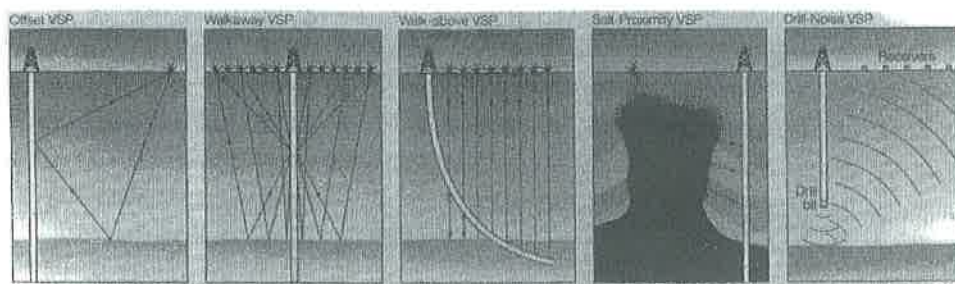


FIGURE 3.78 Illustration of the arrangement for the various types of vertical seismic profile (VSP). *Courtesy of Schlumberger oil field review.*

Drill-Bit Seismic Depth Image Upgrade

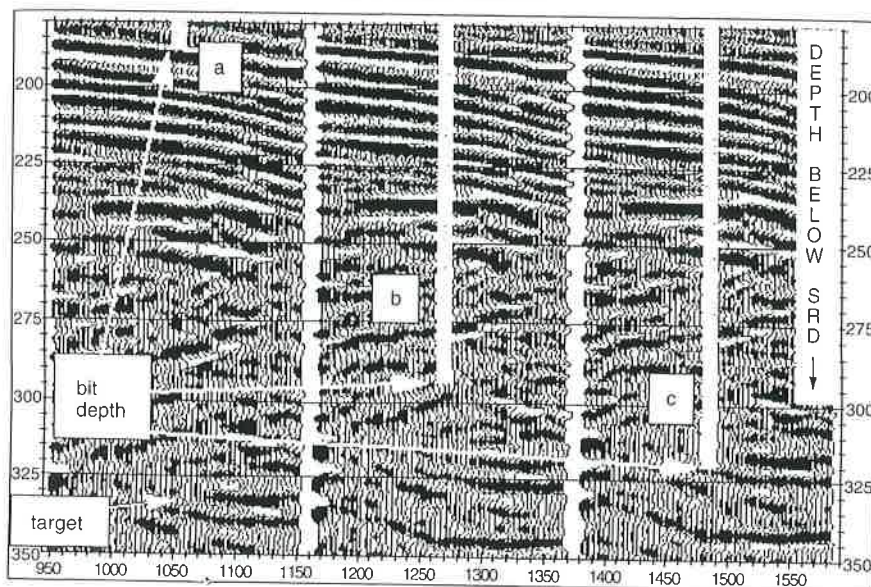


FIGURE 3.79 An example of how vertical seismic profiles (VSPs) shot at three times during the drilling of a well (A, B, and C) produce increasingly accurate predictions of a reflector marking the top of a zone of overpressure. *From Borland et al. (1996); courtesy of Schlumberger.*

interpret changes in the rock properties and fluid geometries during the life of the field. Examples of this practice from fields in the North Sea and West Shetlands are cited in Berteussen (1994) and George (1995) respectively.

3.5 SUBSURFACE GEOLOGY

Successful petroleum exploration involves the integration of the wireline logs and geophysical surveys, described earlier in this chapter, with geological data and concepts. This section is concerned with the manipulation and presentation of subsurface geological information. It is written on the assumption that the reader is familiar with the basic principles of stratigraphy, correlation, and contour mapping. Many of the methods to be discussed are not, of course, peculiar to petroleum exploration, but have wider geological applications. Essentially, the two methods of representing geological data are cross-sections and maps. These methods are discussed in the following sections.

3.5.1 Geological Cross-Sections

Vertical cross-sections are extremely important in presenting geological data. This account begins with small-scale sections and well correlations and proceeds to regional sections.

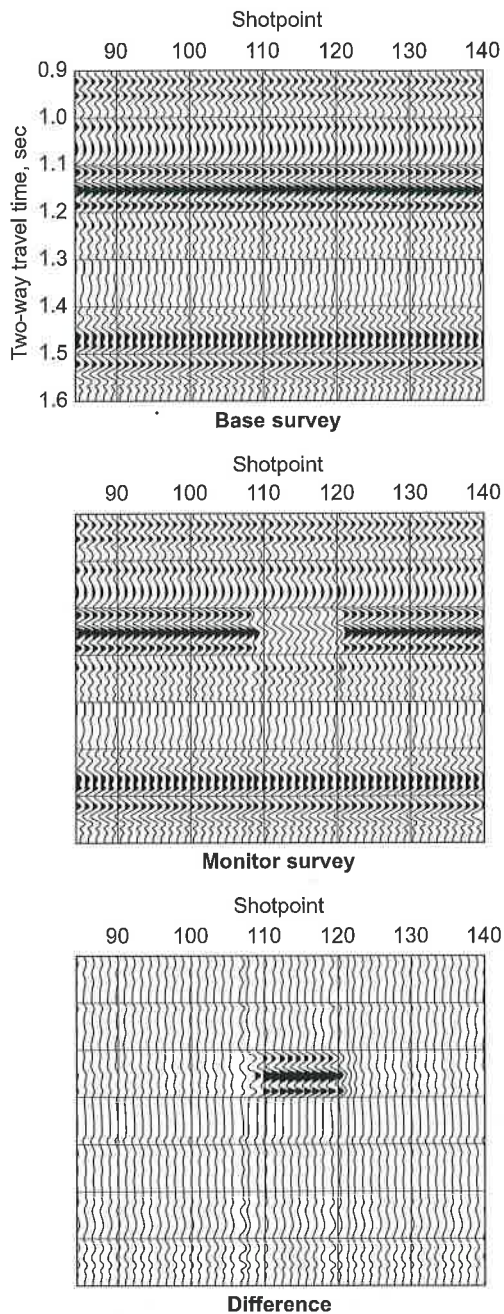


FIGURE 3.80 Computer-modeled seismic lines to show the response produced by the simulated production of petroleum from a reservoir horizon. From Albright et al. (1994); courtesy of Schlumberger oil field review.

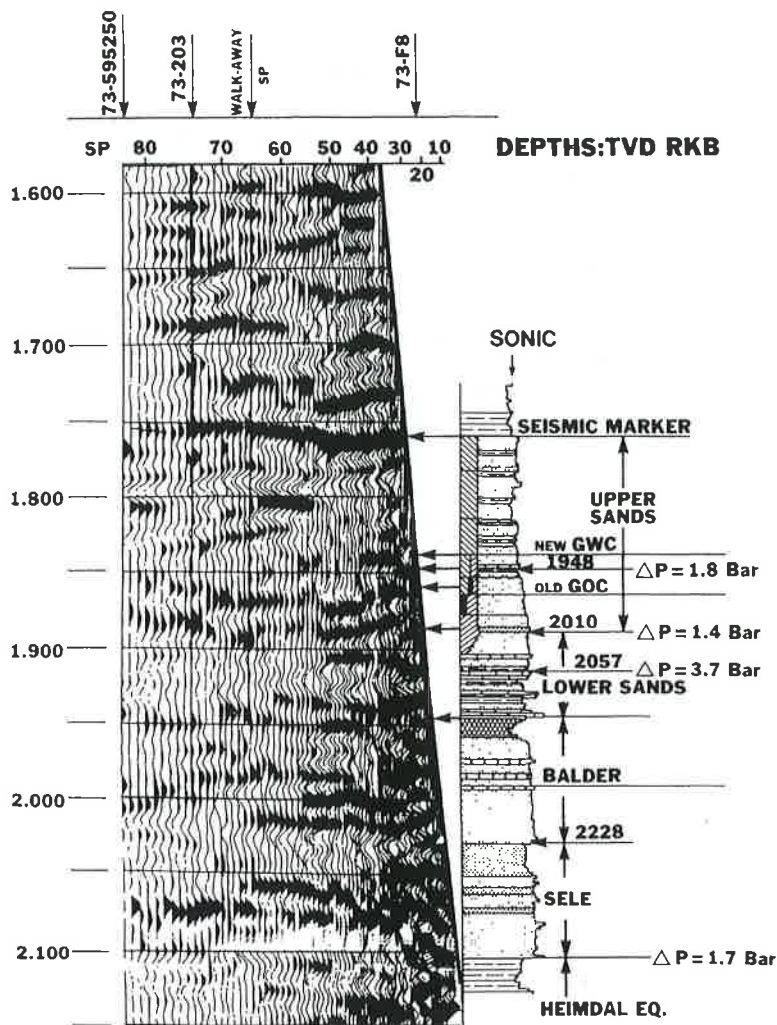


FIGURE 3.81 Vertical seismic profile (VSP) of a well in the Frigg gas field, Norwegian North Sea, whose flat spot was illustrated in Fig. 3.71. Note how the signal of the gas:liquid contact has moved up during the productive life of the field. A reflection at the original gas:liquid contact may be due to a diagenetic effect, as discussed in the text. From Brewster and Jeaneot (1987); courtesy of the Norwegian Institute of Technology.

3.5.1.1 Well Correlation

The starting point for detailed cross-section construction, as for example within a field, is consideration of well correlation. When a well has been drilled and logged, a composite log is prepared. This log correlates the geological data gathered from the well cuttings with that of the wireline logs. The formation tops then have to be picked, which is not always an easy task. The geologist, the paleontologist, and the geophysicist may all pick the top of the

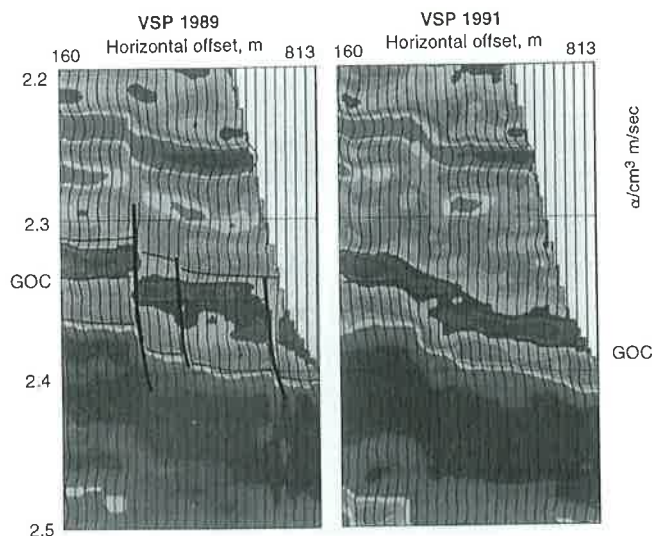


PLATE 3.5 An example of 4D seismic showing the downward movement of a gas:oil contact over a 22-month period during the productive life of a field (See the color plate). *Courtesy of Schlumberger oil field review.*

Cretaceous section, for example, at a different depth. The geologist may pick the top at, say, the first sand bed; the paleontologist, at the first record of a particular microfossil (which may not have thrived in the environment of the sediments in question); and the geophysicist, at a velocity break in the shales, which is a prominent reflecting horizon.

When the formation tops have been selected, correlation with adjacent wells can be made. This correlation is an art in which basic principles are combined with experience. First, the most useful geophysical logs to use must be determined. In the early days of well correlation, the induction electrical survey (IES) array was the most widely used for composite logs. Now, the gamma-sonic is often more popular, especially where the SP curve is ineffective. The gamma, sonic, and resistivity curves all tend to share the high amplitudes necessary for effective correlation. As a general guide, coal beds and thin limestones often make useful markers: they are both thin and also give dramatic kicks on resistivity and porosity logs. Figure 3.82 illustrates a difficult series of logs to correlate. The correlation has been achieved by using the coals to the best advantage, but it allows them to be locally absent because of nondeposition or erosion by channels.

Sometimes, when correlating wells, significant intervals of section may be missing. This phenomenon may be caused by depositional thinning, erosion, or normal faulting (Fig. 3.83). Examination of the appropriate seismic lines will generally reveal which of these three possibilities is the most likely. Repetition of sections may sometimes be noted. Repetition may be caused by reverse faulting, but this possibility should only be considered in regions known to have been subjected to compressional tectonics. An alternative explanation is that sedimentation is cyclic, causing the repetition of log motifs.

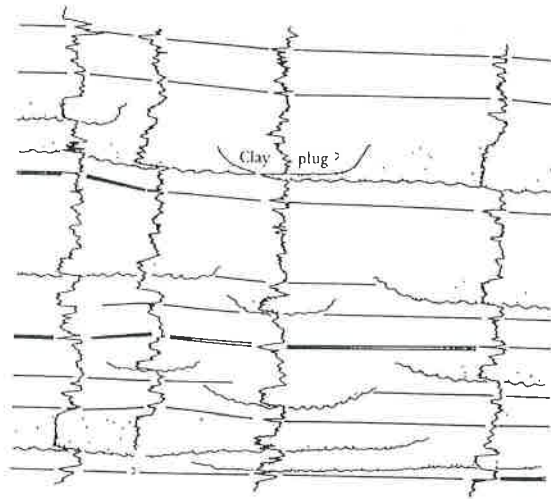


FIGURE 3.82 Correlation of wells in a complex deltaic reservoir. Note that the coals provide the best markers. They have been identified not only from the gamma logs shown here but also from porosity logs that are not illustrated in this figure. *After Rider and Laurier (1979).*

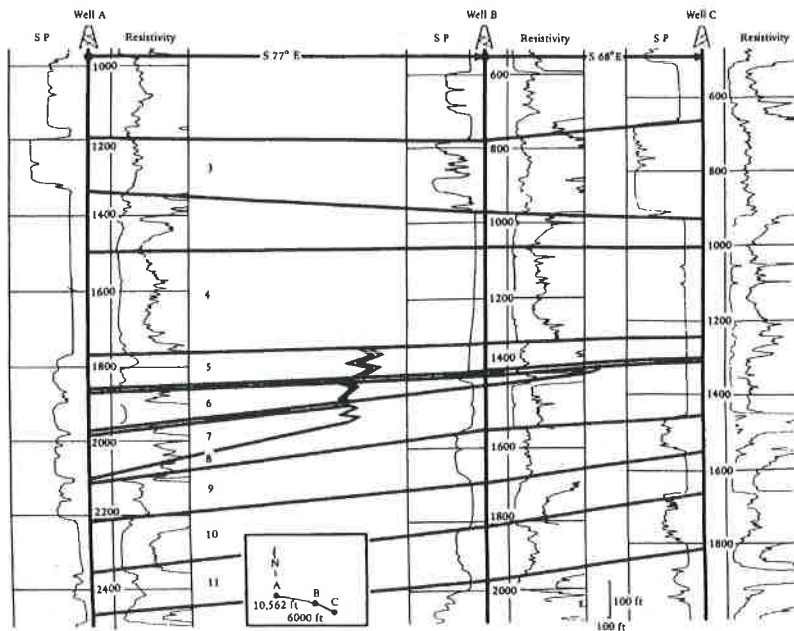


FIGURE 3.83 Correlation of three wells in the Niger delta showing lateral thinning and facies change. *Courtesy of Schlumberger.*

3.5.1.2 Constructing Cross-Sections

Once wells have had their formation tops picked and they have been correlated, they may be hung on a cross-section. This procedure is done with a datum, which may be sea level, a fluid contact, or a particular geological marker horizon. When sea level is used, the elevation of the log must be adjusted. Log depths are generally measured below the rotary table or kelly bushing. The elevation of whichever one of these was used is given on the log heading. The elevation above sea level is subtracted from each formation top to find its altitude or depth. This procedure is relatively simple for vertical wells, but less so for deviated and horizontal wells, such as those drilled from a marine production platform. For these types of wells the TVD must be determined, which requires a detailed and accurate knowledge of the path of the borehole.

When a cross-section is drawn to a horizontal datum, be it sea level or a petroleum:water contact, the result is a structural cross-section (Fig. 3.84). Alternatively, a cross-section can be constructed using a geological horizon as a datum (Fig. 3.85). The purpose of the cross-section should be considered before the datum is selected. In Fig. 3.82, the purpose is to show the truncation of horizons below the Cimmerian unconformity.

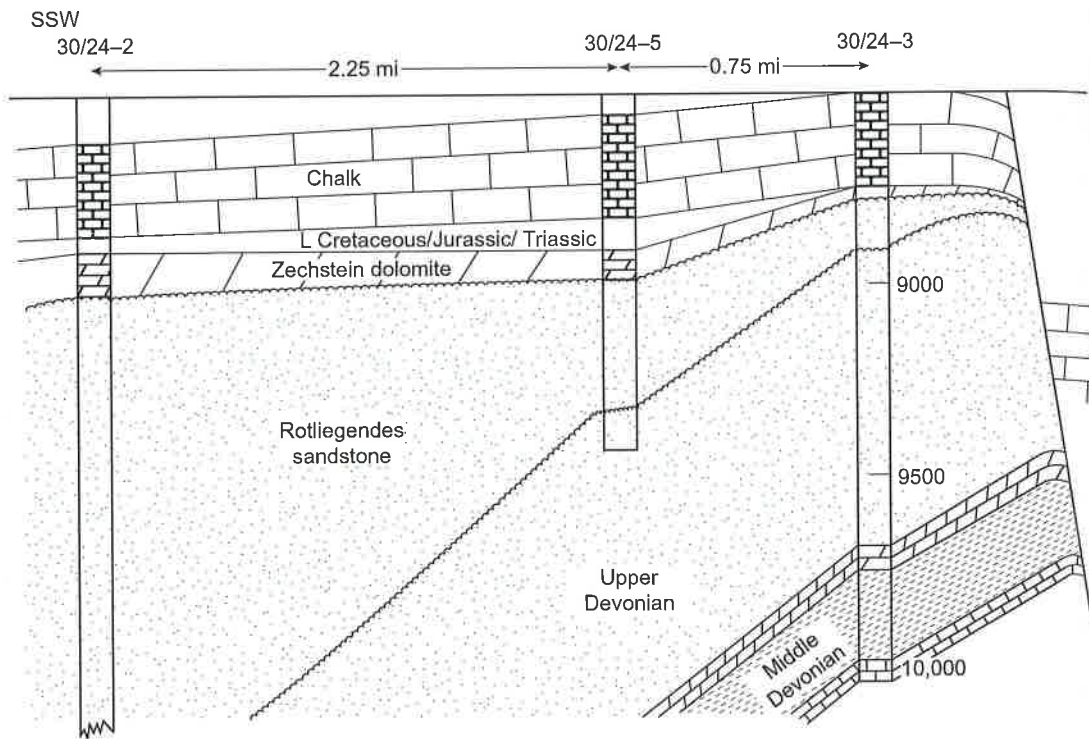


FIGURE 3.84 Structural cross-section through the Argyll field, North Sea. After Pennington (1975).

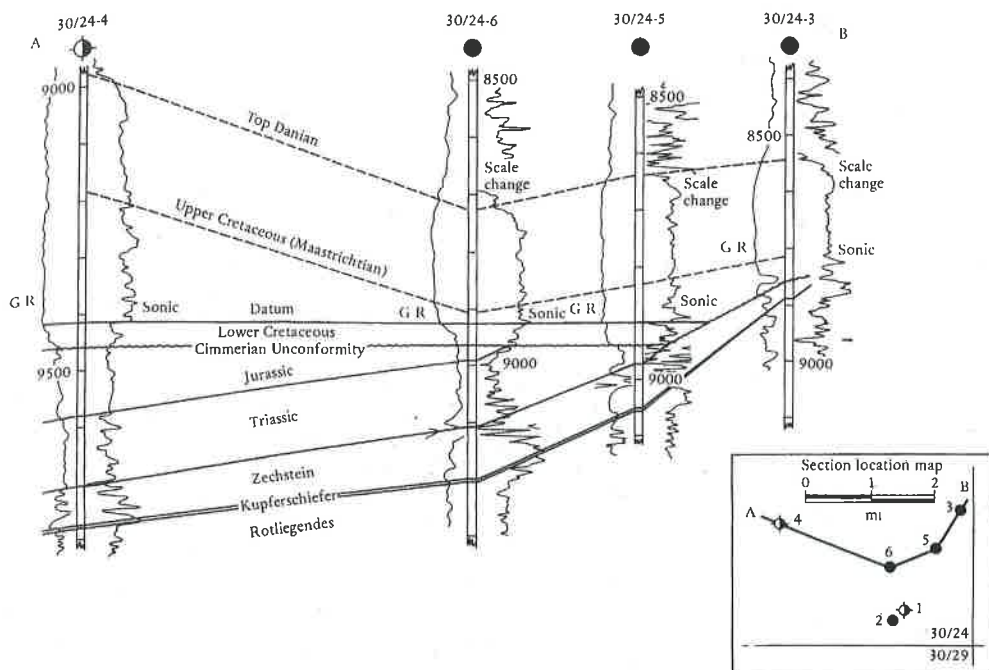


FIGURE 3.85 Cross-section of wells through the Argyll field of the North Sea, using the Cimmerian unconformity as a datum. This figure usefully demonstrates the pre-Lower Cretaceous truncation of strata. *After Pennington (1975).*

Cross-sections of fields are generally based on well control. For regional studies, a combination of seismic and well data is used. A development of the single cross-section is a series drawn using a sequence of different data horizons. Where these data horizons are selected to span a number of markers up to the present day, they can be used to document the evolution of a basin or an individual structural feature (Fig. 3.86). More accurate, but complex, reconstructions can be made by decompacting the shale formations (selecting an appropriate decompaction formula), and adding in water depth across the line of section. This technique of "backstripping" cross-sections is used for basin modeling (Chapter 8).

Although in olden days cross-sections were constructed by geologists leaning over drawing tables with well logs, tracing paper, rulers, pencils, and erasers, nowadays, it is all done by computer (Fang et al., 1992).

3.5.2 Subsurface Geological Maps

Many different types of subsurface geological maps are used in oil exploration. Only a few of the more important kinds are reviewed in this section. The simplest, and probably most

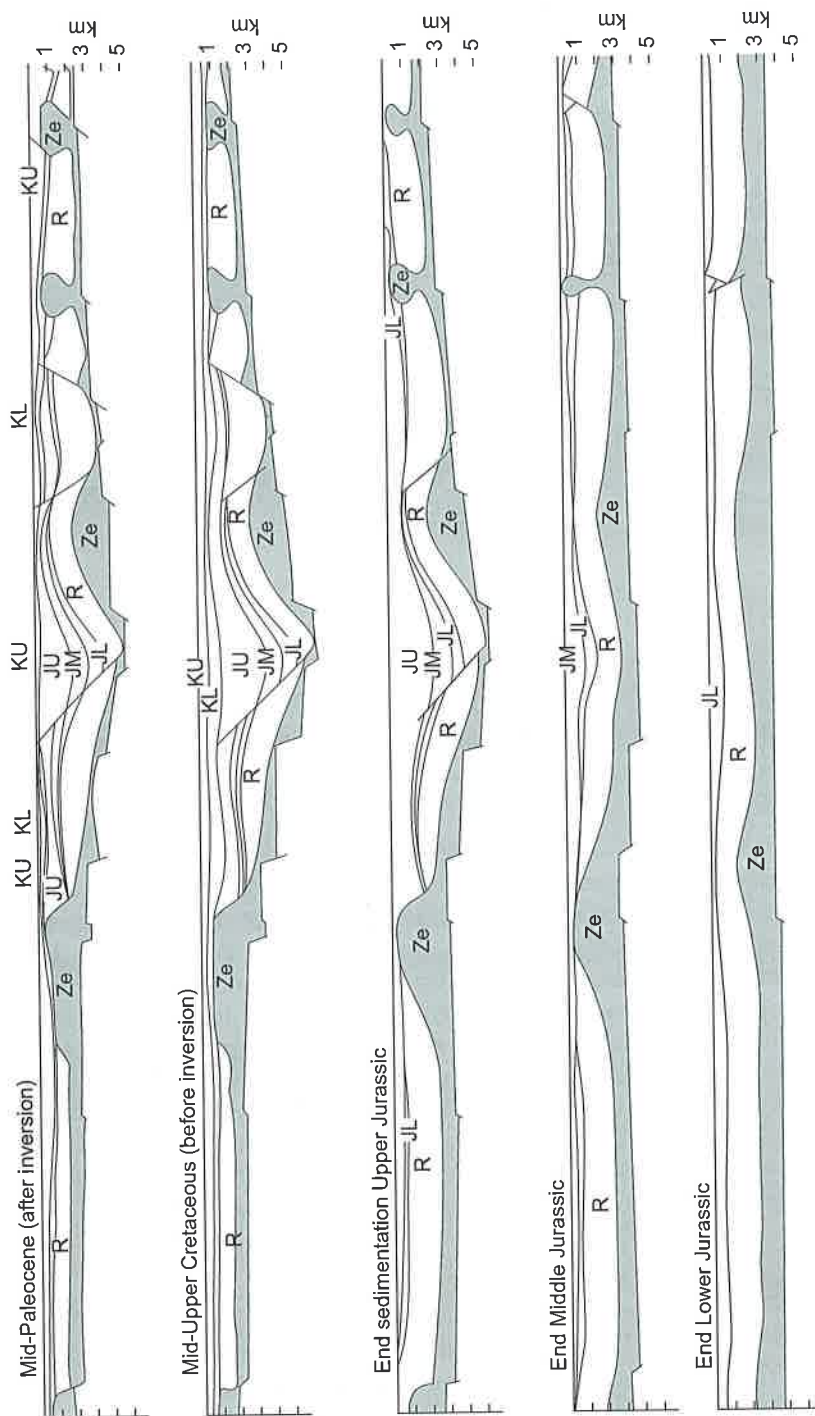


FIGURE 3.86 Regional cross-sections showing the structural evolution of the southern part of the central North Sea graben. After Heybrook (1975).

important, subsurface map is the structure contour map. This map shows the configuration of a particular horizon with respect to a particular datum, generally sea level. Structure contour maps may be regional or local, indicating the morphology of basins and traps, respectively. This information may be based on seismic data, well control, or, most effectively, a combination of both. Structure contour maps delineate traps and are essential for reserve calculations.

Next in importance are isopach maps, which record the thickness of formations. As with structural maps, they may be regional or local and tend to be most reliable when seismic and well data are integrated. Care must be taken when interpreting isopach maps. There is a natural tendency to think that thickness increases with basin subsidence, which is not necessarily so. Both terrigenous and carbonate sedimentation rates are often at a maximum a short way into a basin. Beds thin toward the shore, because of erosion, and basinward because of nondeposition or slow sedimentation rates. Likewise, local or regional truncation may result in formation thickness being unrelated to synde-positional basin morphology.

An isochore map is a particular type of isopach map that indicates the thickness of the interval between the oil:water contact and the cap rock of a trap. A related type of subsurface geological map is the net pay map, which contours the ratio of gross pay to net pay within a reservoir. Sand:shale ratio maps can be drawn, which are very useful both on a local and a regional scale, because they may indicate the source of sand and, therefore, areas where good reservoirs may be found. Net sand and net pay maps are essential for detailed evaluation of oil and gas fields. Field development also requires maps that contour porosity and permeability across a field in percent and millidarcies, respectively. These maps are generally based on well information, but, as seismic data improve, net sand and porosity maps can be constructed without well control. Obviously, their accuracy is enhanced when they can be calibrated with log information. Figure 3.87 illustrates the various types of maps just discussed for the Lower Permian (Rotliegendes) of the southern North Sea basin.

Net sand maps may often be combined with paleogeographic maps. Paleogeographic maps should be based on seismic and well data from which the depositional environment has been interpreted. These data may then be used to delineate the paleogeography of the area during the deposition of the sediments studied. Such maps can be used to predict the extent and quality of source rocks and reservoirs across a basin (Fig. 3.88).

Another useful type of map is the subcrop, or preunconformity map, which can be constructed from seismic and well data (Fig. 3.89). Regional subcrop maps are useful for showing where reservoirs are overlain by source rocks and vice versa. On a local scale, subcrop maps may be combined with isopach maps to delineate truncated reservoirs. Subcrop maps also give some indication of the structural deformation imposed on the underlying strata.

Finally, maps for all of the types previously discussed may be used in combination to delineate plays and prospects. A play map shows the probable geographic extent of oil or gas fields of a particular genetic type (i.e., a reef play, a rollover-anticline play, etc.). Figure 3.90 shows the extent of the Permian gas play of the southern North Sea. It selectively overlays several of the maps previously illustrated. Subject to a structure being present, the parameters that define this play include subcropping Carboniferous coal beds (the source rock), Lower Permian Rotliegendes of eolian type (the other facies lack adequate porosity and permeability), and capping Upper Permian Zechstein evaporites to prevent the gas from escaping. Prospect maps are also based on a judiciously selected combination of the

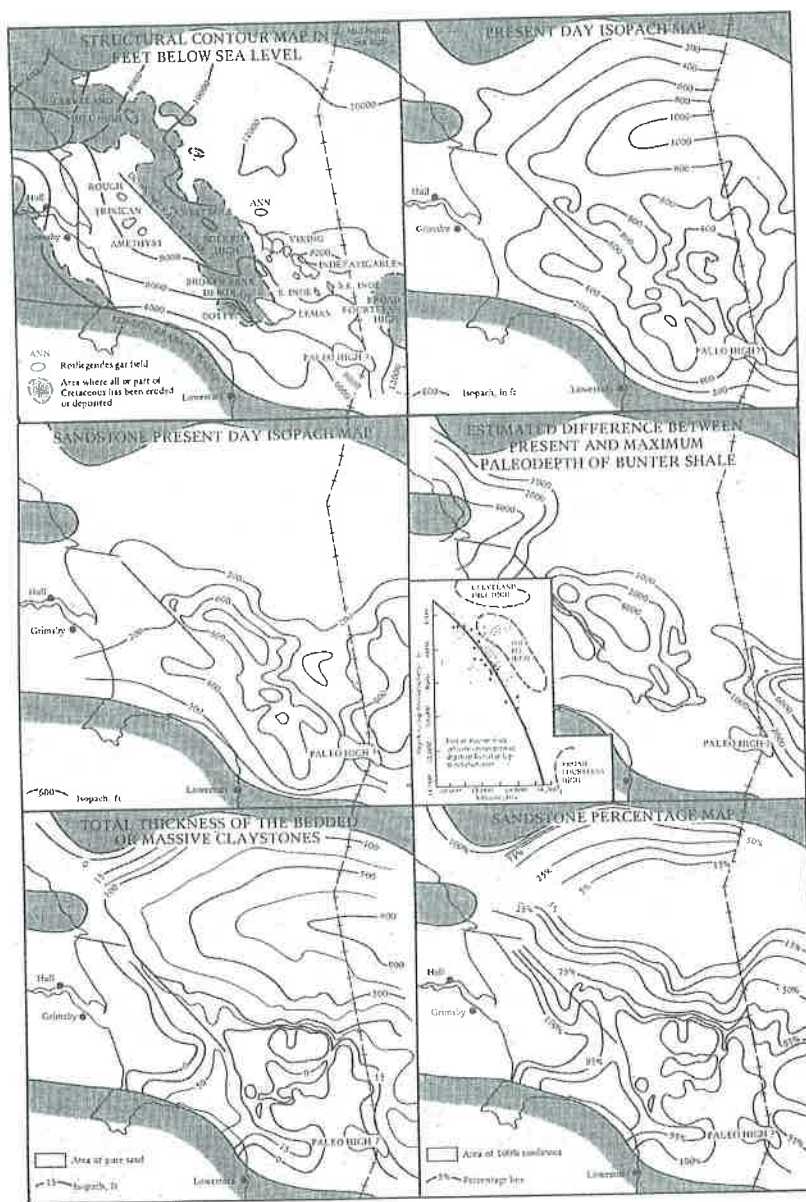


FIGURE 3.87 Maps of the Lower Permian (Rotliegendes) all constructed from the same basic data set. After Marie (1975).

previously discussed types of maps, but will, of necessity, contain a structure contour map to define the prospect in question.

The preceding review shows some of the subsurface geological maps that may be constructed and some of the problems of making and interpreting them. Examples of these maps are used throughout the following chapters.

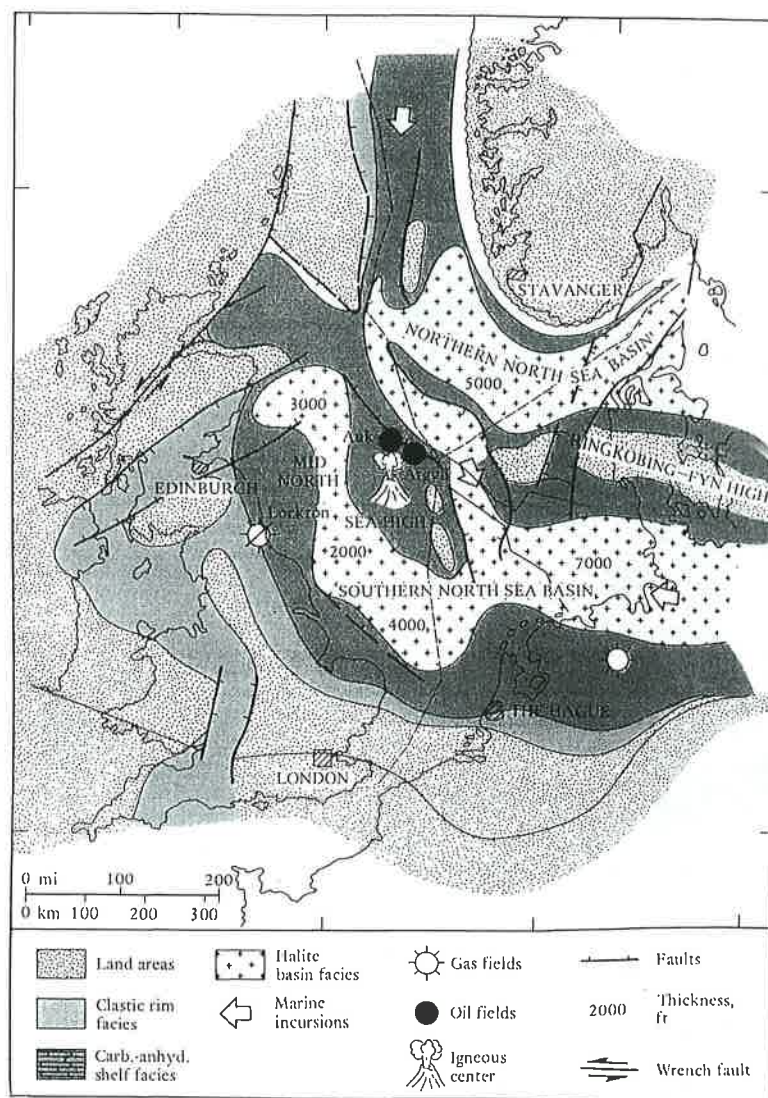


FIGURE 3.88 Paleogeographic map for the Zechstein (Upper Permian) of the North Sea. After Ziegler (1975).

3.6 REMOTE SENSING

Remote sensing is the collection of data without actual contact with the object being studied. Thus, in terms of geology, remote sensing includes aeromagnetic and gravity geophysical surveys, which have already been described. This section is concerned only with remote sensing using electromagnetic waves.

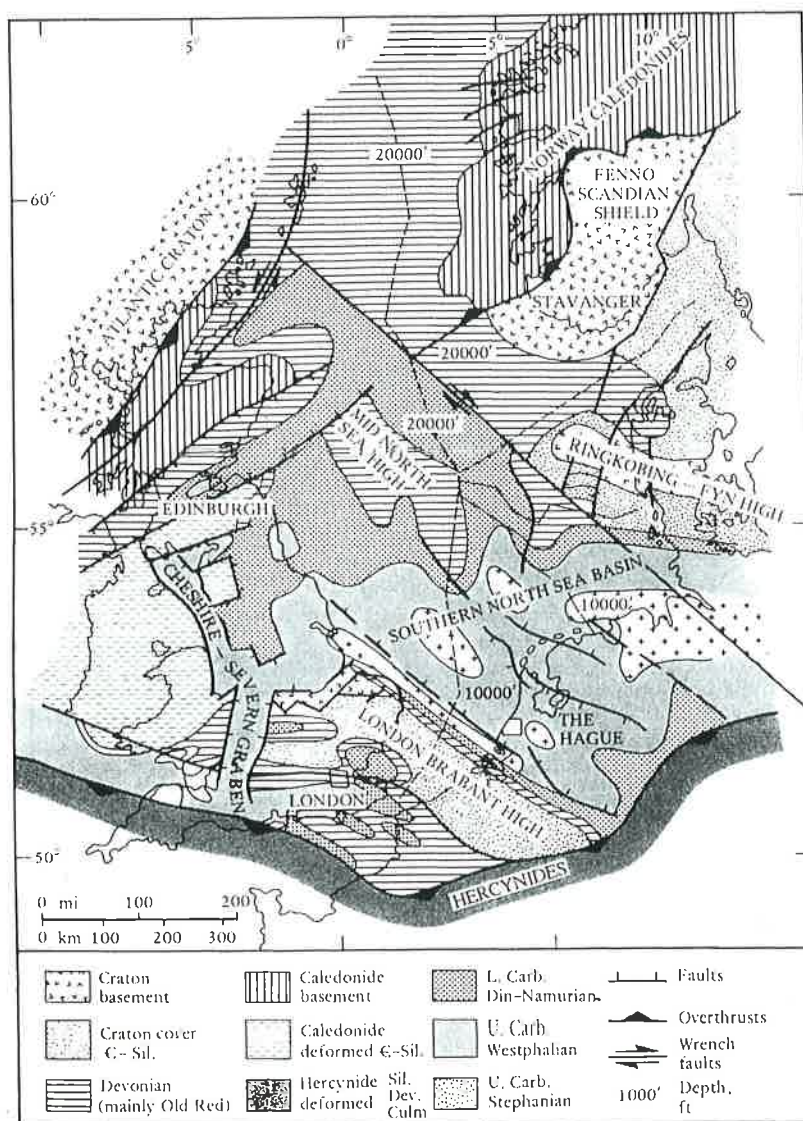


FIGURE 3.89 Pre-Permian subcrop map of the North Sea showing the nature and extent of pre-Permian structural deformation and erosion. It also indicates the extent of the Upper Carboniferous coal measures, which are the source for gas trapped in overlying Permian sands. After Ziegler (1975).

The electromagnetic spectrum includes visible light, but ranges from cosmic radiation to radiowaves (Fig. 3.91). Remote sensing can be carried out from various elevations, ranging from treetop height to satellites in the upper atmosphere. Thus, the two crucial parameters to remote sensing using electromagnetic waves are elevation and the wavelength analyzed. However, these techniques contain many common factors. An energy source is essential; it

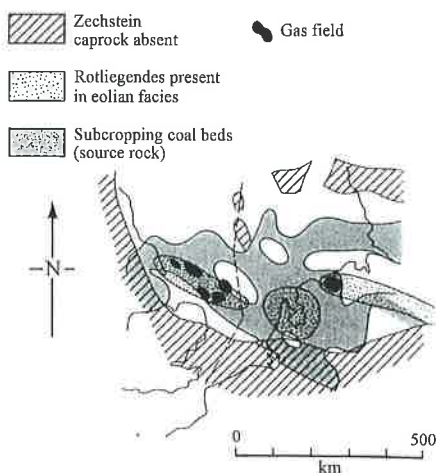


FIGURE 3.90 Play map showing the factors that control the habitat of the Permian Rotliegende gas fields of the southern North Sea.

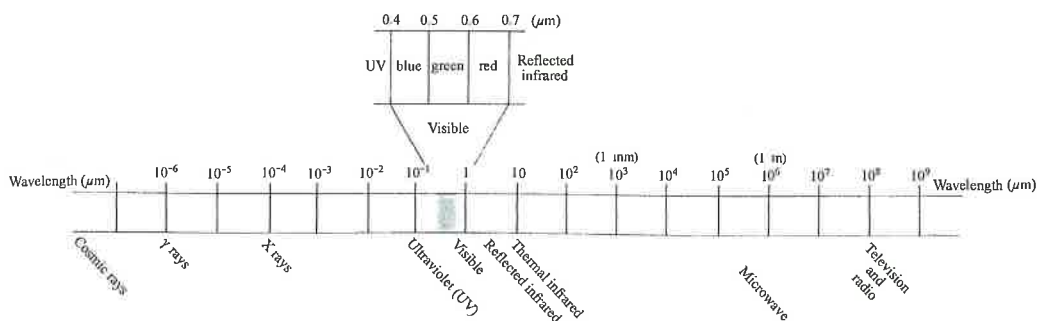


FIGURE 3.91 The electromagnetic spectrum. After Lillesand and Kiefer (1994). Remote Sensing and Image Interpretation, © John Wiley & Sons, Inc.

may be induced (as with microwave radiation used in radar) or natural (as with solar radiation). The sun's electromagnetic waves are filtered through the atmosphere and either absorbed by or reflected from the earth's surface. Reflected waves are modified by surface features of the earth. Some types of wave vary according to thermal variance of the surface, vegetation cover, geology, and so on. These wave variations can be measured photographically or numerically. They are then analyzed, either visually and subjectively or by more sophisticated computer processing. The results may then be interpreted (Fig. 3.92).

The field of remote sensing is large and rapidly expanding. Many new techniques are evolving and are being applied not only to petroleum exploration but to other geological surveys and the study of many other aspects of the earth's surface. The main remote sensing

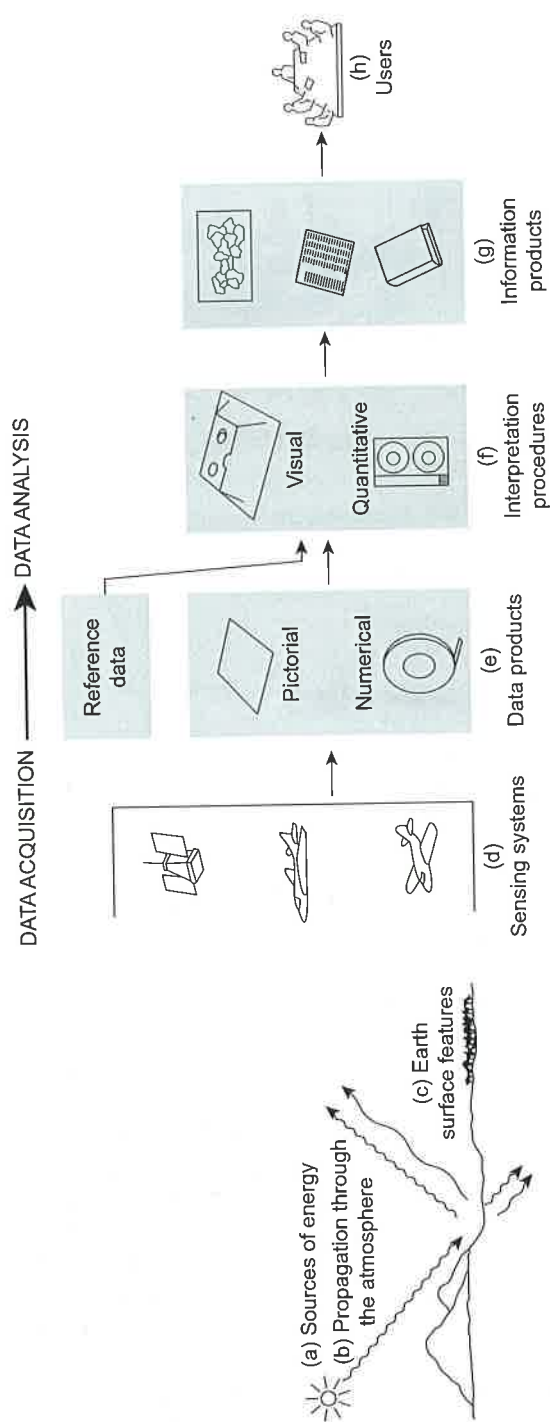


FIGURE 3.92 Electromagnetic sensing of earth resources. After Lillesand and Keifer (1994). Remote Sensing and Image Interpretation, © John Wiley & Sons, Inc.

techniques applied to petroleum exploration are visual, radar, and multispectral. These techniques are described in the following sections. For further details, see Lillesand and Kiefer (1994) and Sabins (1996).

3.6.1 Visual Remote Sensing

Conventional aerial photography is one of the oldest applications of remote sensing to petroleum exploration. The first aerial photographs were taken from balloons in the late nineteenth century. In the early part of the twentieth century, photographs were taken from planes, mainly as isolated snapshots used for map making. The discipline of aerial photography advanced rapidly for military purposes during the Second World War. By this time, a basic technique was established by which specially designed cameras took a sequence of photos at regular intervals along a plane's carefully controlled flight path, which must be accurately mapped. Photographs are taken at a sufficiently close interval to produce a 50–60% overlap (endlap within a line and sidelap between adjacent lines).

The photographs may be used in two ways. In one method, they can be fitted together in a mosaic, with the unwanted overlapping photograph carefully removed. The resultant mosaic may then be rephotographed for ease of reproduction. Air photograph mosaics may be used as a base for both topographic and geological surveys. Before a final map is prepared, however, the mosaic requires a number of corrections. The actual scale of the mosaic must be calibrated by reference to locations whose separation has been measured on the ground. The scale may not be constant over the mosaic if altitude has altered during the flight or if the elevation of the land surface varies. The terrain elevation is generally made with reference to sea level. The exact orientation and location of the mosaic on the earth's surface must also be determined. This task may be done by making astrofixes of ground locations, which can be clearly identified on the photograph.

A second technique widely employed in aerial photography is to use the overlap of adjacent photographs. Two overlaps can be viewed side by side stereoscopically (Fig. 3.93). Thus, the topography can actually be seen in three dimensions. In the early days of aerial photography, the photographs were viewed with a simple binocular stereoscope. In 2014, far more sophisticated viewers are available. Accurately measuring ground elevation with respect to a datum is now possible. Thus, spot heights may be digitized and located on a base map, or contours can be drawn straight from the photographs. Therefore, extremely accurate topographic and geological maps can be prepared.

Since topography is closely related to geology, aerial photographs can also be used in geological mapping. The boundaries of various rock units may be delineated, but, more importantly, the actual dip and strike of strata can be measured from air photographs, so the regional structure can be mapped. Further, linear features show up from the air far better than on the ground. Major structural lineaments, invisible on the ground, can be seen and traced for hundreds of kilometers using air photographs. At the other extreme of the scale, fracture systems may be detected from air photographs and their orientation and frequency numerically analyzed.

The preceding account pertains to the interpretation of air photographs shot from planes at elevations of only a few kilometers. Satellite photographs are useful in a rather different way.

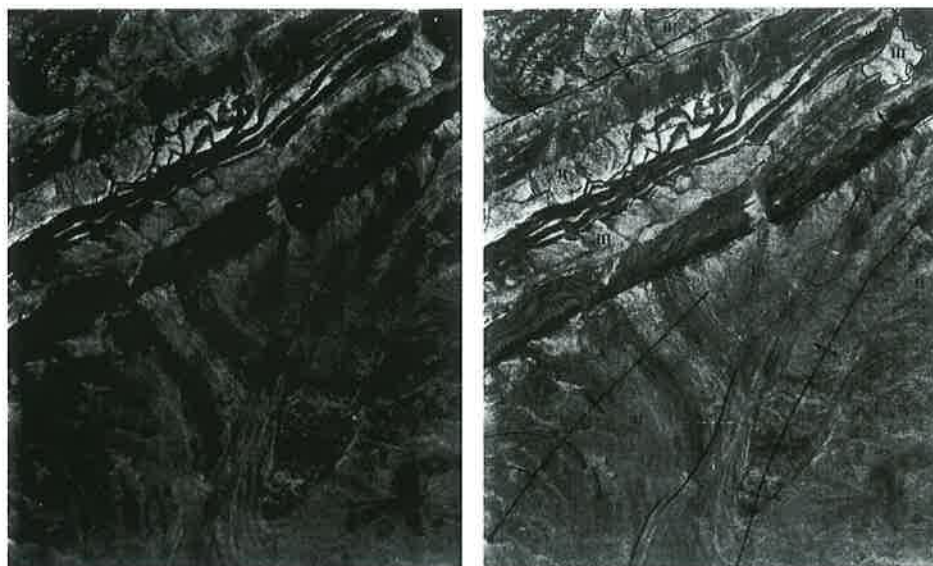


FIGURE 3.93 Stereo pair off air photographs with interpretation (right-hand photograph). The scale is approximately 1:30,000. I represents the oldest unit exposed, and consists of well-bedded limestones. II consists of sands and shales, and III represents superficial deposits. Several folds and faults can be mapped. *Courtesy of Huntings Geology and Geophysics Ltd.*

Because of the great height, stereoscopic mapping is not feasible. On the other hand, satellite photographs may show the presence of major lineations invisible from the ground or from the lower elevations of aircraft. Similarly, because of the large area covered, whole sedimentary basins may be seen in a single photograph, complete with concentric centripetally dipping strata.

3.6.2 Radar

Another method of remote sensing is provided by radar (an acronym for RAdio Detection And Ranging). Although aerial photography records light reflected from the sun, radar uses an energy source on the plane or satellite that emits microwave radiation. The returning radiation is recorded and displayed in a format similar to an aerial photograph.

Radar has several advantages over light photographs. Microwaves penetrate cloud cover and haze and can be used at night as well as during the day. Thus, radar surveys can be carried out with fewer operational constraints than can photographic surveys. A second advantage is that radar records data continuously, rather than in a series of separate photographs, so many of the problems of overlap and matching are eliminated. The spatial resolution of radar imagery is largely related to the diameter of the antenna. The larger the antenna, the better the resolution for a given wavelength. Because of the difficulty in mounting a rotating antenna on a plane, it is generally mounted underneath and pointed out to the

side. Thus, most radar systems are side-looking airborne radar, referred to as SLAR or, more simply, SLR.

Radar images can, of course, not only be recorded from planes but also from satellites (Radarsat). The recent development of synthetic aperture radar imaging is now being deployed in satellites to produce maps for use in petroleum exploration surveys (Tack, 1996).

3.6.3 Multispectral Scanning

A conventional aerial photograph measures reflected light. Measuring the thermal radiation of the earth's surface using a thermal sensor is also possible. Multispectral scanning extends these concepts, measuring several different energy wavelengths simultaneously. Instead of recording light on film via an optic lens, the data are recorded electronically. This type of recording has the great advantage of eliminating the need to have the information transported to the ground in a film that has to be processed. Multispectral scanning can be carried out from planes, and is also extensively employed in satellites, notably the LANDSAT and SEASAT systems. The data can be transmitted back to a receiver on earth by radio-waves. The information can then be displayed visually in false-color photographs, which show variations not of light, but of whatever wavelength was selected for recording and analysis. Although light photographs show wavelengths of 0.3–0.9 μm , multispectral scanning can extend this value to some 14 μm .

Because the information is recorded electronically rather than optically, it can be processed by computers in many ways. Three principal steps are used in processing before the data can be interpreted. First, the image must be restored as closely as possible to the original. Image defects and the effects of haze are corrected. The location of the image with respect to the earth's surface must be exactly fixed, and adjacent images fitted into a mosaic. In the second stage of processing, the image is improved by enhancing the edges of different types of surface by central stretching, density slicing, and selecting colors for various spectral bands. In the third and final stage of processing, the information is extracted and displayed in hard copy form using false colors.

Multispectral scanning provides far more data than a conventional photograph does. Because such a wide range of spectra can be recorded and because the data can be processed in so many ways, the information is open to a great diversity of interpretation. Thus, it is possible to identify petroleum seeps from space by remote sensing (Plate 3.6).

3.6.4 Conclusion

Remote sensing is an invaluable technique in petroleum exploration. Indirectly, it is useful for topographic mapping; more directly, aerial photography has been widely used in geological mapping, especially in desert areas, where the effect of vegetation is minimal. The application of multispectral sensing from satellites requires great care to be taken in its interpretation. Thus, Halbouty (1980) showed how 15 giant oil and gas fields around the world are not revealed by LANDSAT imagery. Nonetheless, as Plate 3.8 shows, when appropriately processed, it may identify surface petroleum



PLATE 3.6 A remotely sensed image of northwest Iraq from Landsat thematic mapper. False-color display. Fold structures can be seen crosscutting the central area from the northwest to the southeast. Petroleum-related sulfur springs are visible in blue (See the color plate). *Courtesy of World Geoscience Ltd.*

seepages. As with all exploration tools, multispectral sensing is open to abuse and misinterpretation when used on its own. When used in conjunction with other techniques, such as gravity and magnetics, it may delineate anomalies that deserve further attention on the ground.

References

- Ager, D.V., 1973. *The Nature of the Stratigraphical Record*, first ed. Wiley, Chichester.
- Ager, D.V., 1993. *The Nature of the Stratigraphical Record*, third ed. Wiley, Chichester.
- Albright, J., Cassell, B., Dangerfield, J., Deflandre, J.P., Johnstad, S., Withers, W., January 1994. Seismic surveillance for monitoring reservoir changes. *Schlumberger Oilfield Rev.* 6, 4–14.
- Anderson, R.N., Boulanger, A., He, Wei, Sun, Y.F., Xu, Liqing, Sibley, D., Austin, J., Woodhams, R.R., Andre, R., Rinehart, N.K., May 20 1996. Gulf of Mexico reservoir management. *Oil & Gas J.* 41–46.
- Archer, S.H., King, G.A., Seymour, R.H., Uden, R.C., 1993. Seismic reservoir modelling—the potential. *First Break* 11, 391–397.
- Archie, G.F., 1942. The electrical resistivity log as an aid in determining some reservoir characteristics. *J. Pet. Technol.* 5. Tech. Pap. No. 1422.
- Backus, M.M., Chen, R.L., 1975. Flat spot exploration. *Geophys. Prospect* 23, 533–577.
- Bailey, R.J., Buckley, J.S., Kielmas, M.M., 1975. Geomagnetic reconnaissance on the continental margin of the British Isles between 54° and 57° N. *J. Geol. Soc. London* 131, 275–282.